DISS. ETH NO. 22192

SAGA ensures the mutual accumulation of non-centromeric DNAs and nuclear pores during aging

A thesis submitted to attain the degree of
DOCTOR OF SCIENCE OF ETH ZURICH
(Dr. sc. ETH Zurich)

presented by
ANNINA DENOTH LIPPUNER
Dipl. Biol. ETH Zurich

born on 29.4.1982
citizen of Valsot, GR, Switzerland

accepted on the recommendation of
Prof. Yves Barral, examiner
Prof. Ulrike Kutay, co-examiner
Prof. Françoise Stutz, co-examiner
Prof. Claudio Sunkel, co-examiner

2014

Parts of this thesis have been published in:

Denoth Lippuner, A., Julou, T., and Barral, Y. (2014). Budding yeast as a model organism to study the effects of age. FEMS Microbiol Rev.

Parts of this thesis are in a manuscript currently under revision at eLIFE:

Denoth Lippuner, A., Krzyzanowski, M.K., Stober, C., Barral, Y. Role of SAGA in the asymmetric segregation of DNA circles during yeast aging

Contributions:

All experiments presented in this thesis were performed by Annina Denoth Lippuner, except the microfluidic experiments (Fig. 2.9 and 2.10), which were run by Marek Konrad Krzyzanowski and analyzed and quantified by Annina Denoth Lippuner and the chromatin immuno precipitation experiments (ChIP; Fig. 2.3), which were performed by Catherine Stober and analyzed and quantified by herself.

Table of Contents

Abstract

Every human individual experiences the process of aging and even unicellular organisms, such as *Saccharomyces cerevisiae*, are subjected to the aging process. Budding yeast cells divide asymmetrically: even though the mother cell divides a limited number of times, meanwhile ages and eventually dies, each produced daughter cell is born young. Thus, all generated aging factors have to be kept in the aging mother cell. One such aging factor are extrachromosomal rDNA circles (ERCs). ERCs are formed by homologous recombination within the rDNA repeats and, once formed, they replicate during S-phase but are strictly retained in the mother cell. Therefore, they accumulate exponentially and contribute to aging. However, how yeast cells ensure the retention of ERCs in the mother cell during cell division and why ERC accumulation becomes toxic to the cells is still poorly understood.

Here, we found that the SAGA complex, a complex previously described for its role in transcription, mediates the attachment of ERCs and other non-centromeric DNA molecules to nuclear pore complexes (NPCs) and thereby ensures their asymmetric segregation. Thus, we propose a novel role for SAGA as a key player in the process of recognizing non-centromeric DNA molecules and thereby preventing their spreading in a population.

The attachment of circles to nuclear pores reduces their mobility and thereby hinders them to pass a previously described diffusion barrier at the bud neck. Thereby, the retention of ERCs concomitantly mediates the retention of NPCs, leading to a tremendous accumulation of NPCs as the cells age. We propose that aging is, at least in part, the consequence of altering nuclear organization and NPC number. Accordingly, uncoupling ERCs from NPCs in SAGA deficient cells prolongs their replicative lifespan.

Finally, we investigated the fate of acentric DNAs in mammalian cells. Non-centromeric DNA circles transfected into HeLa cells accumulated into mainly one focus, thereby ensuring their asymmetric segregation during mitosis. However, in contrast to yeast cells, the accumulated plasmids were excluded from the nucleus, presumably during nuclear envelope breakdown. Afterwards, they remained in a micronucleus containing Lap2-β but no NPCs. Thus, we propose that mammalian cells not only segregate DNA circles asymmetrically, but even exclude them from the nucleus, owing to open mitosis.

Zusammenfassung

Jeder Mensch altert und sogar einzellige Organismen wie die Bäckerhefe unterliegen dem Prozess des Älterwerdens. Zellen der Bäckerhefe teilen sich asymmetrisch: Die Mutterzelle altert mit jeder Teilung und stirbt schliesslich, während jede dadurch produzierte Tochterzelle jung geboren wird. Daraus schliessen wir, dass alle Altersfaktoren in der Mutterzelle zurückgehalten werden. Ein solcher Alterungsfaktor sind die sogenannten extrachromosomalen rDNS-Ringe (ERRs). ERRs entstehen durch homologe Rekombination zwischen repetitiven rDNS-Sequenzen und replizieren sich während der S-Phase, werden jedoch strikt in der Mutterzelle zurückgehalten. Dadurch akkumulieren sie exponentiell und tragen zum Alterungsprozess der Zelle bei. Es ist jedoch wenig darüber bekannt, wie ERRs in der Mutterzelle zurückgehalten werden und weshalb ihre Akkumulation der Zelle schadet.

Dass der SAGA-Komplex bei der Transkription von Genen eine Rolle spielt ist bekannt. In der vorliegenden Studie zeigen wir, dass der SAGA-Komplex ERRs und andere DNS-Moleküle, die kein Zentromer enthalten, an Kernporen bindet und dadurch ihre asymmetrische Verteilung sicherstellt. Wir gehen deshalb davon aus, dass SAGA eine zentrale Rolle beim Erkennen von zentromerlosen DNS-Molekülen spielt und ihre Ausbreitung in einer Population verhindert.

Das Anhängen der DNS-Ringe an die Kernporen verlangsamt diese und verhindert deren Überquerung der bereits früher beschriebenen Diffusionsbarriere am Knospenhals. Daher führt das Zurückhalten der ERRs gleichzeitig zu einem Zurückhalten von Kernporen, was in einer enormen Anhäufung von Kernporen während dem Alterungsprozess resultierte. Aus diesem Grund nehmen wir an, dass der Alterungsprozess zumindest teilweise durch die Veränderung der nukleären Organisation und der Anzahl an Kernporen hervorgerufen wird. Entsprechend leben Zellen ohne SAGA, in welchen die ERRs nicht mehr an die Kernporen binden, länger.

Des Weiteren haben wir das Verhalten von zentromerloser DNS in Säugetierzellen untersucht. So akkumulieren die zentromerlosen DNS-Ringe nach deren Transfektion in HeLa-Zellen mehrheitlich zu einem einzigen Punkt, wodurch deren asymmetrische Verteilung während der Zellteilung sichergestellt wird. Im Gegensatz zu den Bäckerhefezellen werden die akkumulierten DNS-Ringe aus dem Nukleus ausgeschlossen, höchstwahrscheinlich während der Auflösung der Kernhülle.

Danach bleiben sie in einem Mikronukleus, umhüllt von Lamina assoziierten Proteinen, aber ohne Kernporen. Wir vermuten deshalb, dass Säugetierzellen DNS-Ringe nicht nur asymmetrisch verteilen, sondern diese, dank der Auflösung der Kernhülle während der Zellteilung, sogar aus dem Nukleus ausschliessen können.

1. Introduction

1.1 Aging in *Saccharomyces cerevisiae*

Every human being experiences the effects of getting older, a process called aging, and every grey hair, senile lentigo or forgotten name serves as a reminder. But, although signs of age are evident in most multicellular organisms, unicellular species have long been mistaken as being immortal. For example, budding yeast can be propagated in culture indefinitely, similarly to mammalian immortalized cells. However, when A. Barton followed single "mother" yeast cells, systematically removing every daughter cell produced, he discovered that single cells eventually die (Barton, 1950). The analysis of cell cohorts indicates that mortality increases during the life, a hallmark of aging (Mortimer and Johnston, 1959). Furthermore, cultures inoculated with the first or last daughters of the same mother cell are both able to grow (Barton, 1950). These early experiments demonstrated that, although yeast cells are mortal, their offspring do not inherit what kills their mother cells and are therefore born with a reset lifespan. This also speaks for the finite lifespan of yeast cells being the product of an aging process, rather than of some cellular disease. Because budding yeast has been characterized in great detail at the molecular level and powerful tools are readily available to alter and monitor cellular processes, this organism has emerged as an unexpected model species for studying aging.

In yeast, aging is studied using two main approaches. Replicative lifespan is defined as the number of buds produced before death. In practice, the replicative lifespan is measured by counting the number of divisions achieved by a cell whose buds are removed one by one by microdissection (Fig. 1.1A). Alternatively, instead of focusing on divisions, the chronological lifespan is measured as the time a cell survives in a non-dividing state, with survival being defined as cell wall integrity or as ability to form a colony. Aging is then characterized based on the distribution of chronological lifespans, obtained by measuring the decrease of survival with time in a stationary phase culture. Yeast replicative aging is thought to be comparable to aging phenomena observed in asymmetrically dividing cells of higher eukaryotes, such as stem cells. Yeast chronological aging is akin to the aging of non-dividing cells such as neurons (Longo et al., 2012). Finally, a third type of aging is observed in certain mutant strains that cannot be propagated eternally, a phenomenon called clonal senescence, which resembles the senescence process in telomerase deficient

mammalian cells (Lundblad and Szostak, 1989; Singer and Gottschling, 1994). In this project, we focused only on replicative aging.

Preparing large amount of cells that have undergone multiple divisions is intrinsically difficult, since old cells are diluted in their progeny during exponential growth; hence replicative aging has been studied primarily by manual microdissection. However, this technique is both tedious and unsuitable for high-throughput studies. In the past years, new methods have been developed that overcome this limitation. In this study we used three different methods. First, classical microdissection was used to determine the lifespan of different strains, whereas every produced daughter cell is manually removed from the mother cell using a dissection needle (Fig. 1.1.A). The Mother Enrichment Program (MEP) was used to obtain old cells for ERC detection using Southern blotting (Lindstrom and Gottschling, 2009). The MEP strain contains two essential genes flanked by lox sites and the Cre recombinase fused to the estradiol binding domain under the control of a daughter specific promoter. Upon addition of estradiol, the Cre excises the essential genes specifically in the newly born daughter cells preventing them from dividing. This leads to a linear dilution (rather than exponential) of mothers in a population of arrested daughters, and greatly facilitates the biotin-based purification of old mother cells using streptavidin coated beads (Fig. 1.1B). And finally, microfluidic devices were used to study the segregation of nuclear pores in old cells. In a microfluidic chamber the cells are trapped and the new born daughter cells are removed based on their smaller size by a constant flow of medium within the device (Lee et al., 2012; Xie et al., 2012). The advantage of this method is the possibility to monitor cells throughout their entire lifespan using transmission and fluorescence imaging and therefore allows the study of cellular events over the lifespan with unprecedented accuracy (Fig. 1.1C).

In general, aging is defined as “any age-specific decline in variables associated with individual fitness, specifically mortality, reproduction and physiological performance” (Reznick et al., 2004). All these three components of aging are observed during replicative aging in budding yeast. Two classes of hypotheses on the origin of aging were proposed: it either follows a program selected by evolution and leading to cell death after a given time, or it results from the accumulation of damage during life. Since any program-based explanation is unlikely to be general from an evolutionary point of view (Kirkwood and Melov, 2011), most attention has been given to damage accumulation. In particular, aging has been proposed early on to result from features selected for advantages they provide to the individual early in its life, but become

deleterious later. Because of the unique insights we have into molecular mechanisms in yeast, this species may allow us to test how this hypothesis translates into molecular and cellular terms.

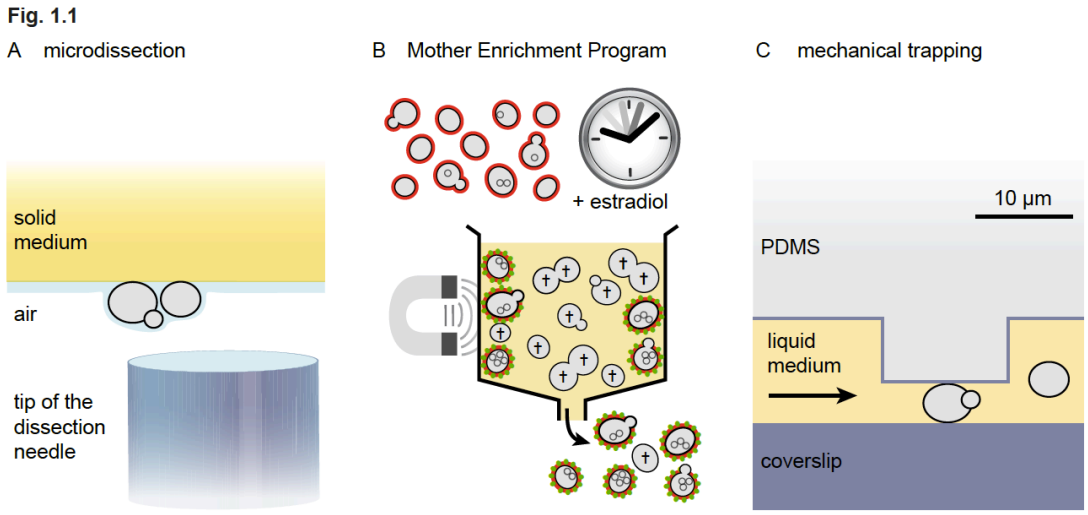

Fig. 1.1 Different techniques to investigate old yeast cells used in this study.

(A) Microdissection, the traditional life-long monitoring method, consists in manual usage of a microscopic needle to remove all buds produced by a newborn cell. (B) In the MEP, the excision of two essential genes prevents daughter cells to divide upon addition of estradiol, leading to linear rather than exponential growth of the population. Old cells are purified using Streptavidin-based sorting. (C) Newly designed microfluidic devices based on size-dependent trapping allow the life-long monitoring of dividing cells and to quantify the intensity of fluorescent reporters during the lifespan.

Rejuvenation restores the bud lifespan potential

How do populations composed of aging individuals maintain viability over time? Under the simplistic assumptions that aging occurs and that the two individuals produced at mitosis are identical, one would expect that the progeny have an increased age at birth, which would ultimately lead to the extinction of a population. However, yeast cells divide highly asymmetrically with the daughter cells being born with a full replicative lifespan potential, independent of the age of their mothers. Such a rejuvenation mechanism allows the maintenance of a lineage with full lifespan potential. This observation has been instrumental in characterizing the causes of aging in yeast: early studies showed that the last bud born to a specific mother is able to divide, which ruled out the possibility that genomic mutations play a causal role in aging (Johnston, 1966). Remarkably, rejuvenation becomes less effective as the mother ages: buds produced in the first third of the life of their mother live, on

average, as long as their mothers. Buds born later display a progressively reduced lifespan (10-15% shorter for buds born at the middle of the life of their mother, ca 60% for the last daughters) (Kennedy et al., 1994). This indicates that rejuvenation occurs throughout the whole lifespan, although it is only partially complete later in life (Fig. 1.2). Accordingly, the replicative lifespan distributions of buds born at the 8th and 12th divisions are identical to that of their mothers, although at the individual level, the bud lifespan is little influenced by that of its mother (Shcheprova et al., 2008). Here as well, rejuvenation does not always fully reset age, and this effect is stochastic. This highlights that rejuvenation, like aging itself, is best described at the population level, but highly stochastic at the level of the individual cell.

Fig. 1.2

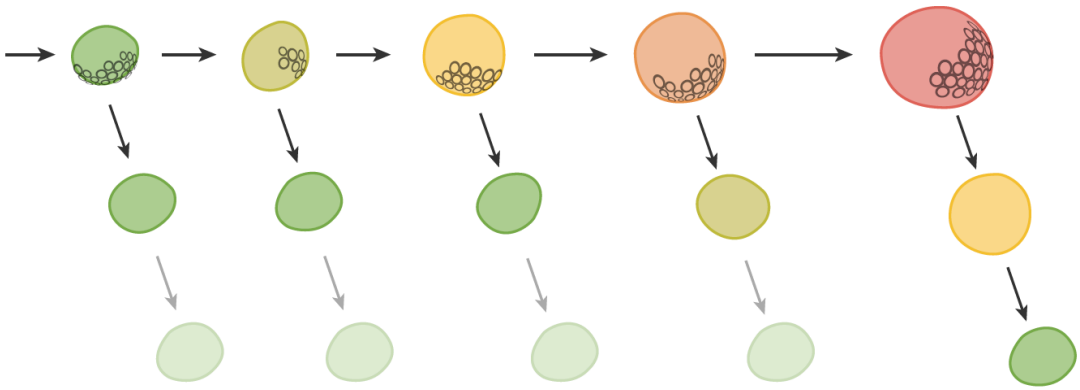

Fig. 1.2 Age is distributed asymmetrically to the mother cell

Rejuvenation ensures a complete reset of the replicative lifespan potential during most of the lifespan (depicted by the color). Only daughter cells of very old mother cells have a shorter lifespan. However, this decrease is not passed on to the next generations.

Whole-cell phenotypes indicate the existence of aging factors

The impaired rejuvenation of late born buds suggests that old mothers start “passing age” to their daughters, leading to the hypothesis that aging occurs through the progressive accumulation of aging factors. This view is supported by the observation that when cells of different ages are mated, the zygote replicative lifespan is set by the age of the older haploid cell, indicating that age is a dominant phenotype (Muller, 1985). Under this hypothesis, rejuvenation corresponds to the retention of such aging factors in the mother at division, passively or actively. The decreased rejuvenation of

daughters produced by very old mothers could reflect age-induced defects of the molecular machinery involved in retention or titration of the retention machinery by large amounts of the aging factors. Interestingly, while the replicative lifespan of the last bud is decreased, its first daughter and granddaughter show a gradual restoration of a normal lifespan (Fig. 1.2; (Kennedy et al., 1994)), suggesting that one or more factors must be diluted in order to achieve full rejuvenation. Together, these observations have led to the general paradigm that aging is caused by the accumulation of aging factors.

Aging factors must fulfill four basic requirements (Henderson and Gottschling, 2008). First, these factors must accumulate with age. Second, during mitosis, they must segregate asymmetrically to the older cell. These two first requirements are shared between aging factors and any marker of aging that has no impact on the aging process. A third requirement, specific for *bona fide* aging factors, is that preventing or reducing the presence of an aging factor should lead to lifespan extension. Fourth, conditions that increase the levels of an aging factor should decrease lifespan. This definition places aging factors in the category of toxic damage that cells are unable to repair or eliminate. However, this definition does not explain why these factors are toxic, how they cause cell death, or whether their toxicity is dependent on environmental conditions. To investigate potential aging factors, their molecular composition, their contribution to aging and their segregation during mitosis, the following parts will summarize the current knowledge of contributing factors grouped by organelles. However, even trying to discuss the most relevant findings, this summary will be far from being complete. The summary includes the nucleus, mitochondria, vacuoles, the cytoplasm and endoplasmatic reticulum (ER).

1.2 Nucleus

Human diseases leading to premature aging phenotypes, including Hutchinson-Gilford progeria syndrome (HGPS) and Werner syndrome, provide important insights into the mechanisms of normal aging, since these diseases cause premature aging-associated phenotypes in several tissues (Martin and Oshima, 2000). HGPS is caused by a silent point mutation in the lamin A encoding gene, leading to an alternatively spliced variant of lamin A termed “progerin”. Lamin A is a component of the nuclear lamina, and cells from HGPS patients show altered nuclear structure, thickening of the lamina and loss of peripheral heterochromatin (Dechat et al., 2008). Werner syndrome results from a mutation in a helicase called WRN (Sgs1 in budding yeast), which is important for DNA integrity. Loss of function of WRN leads to defects in DNA double-strand break repair and increased aberrations at telomeres (Burtner and Kennedy, 2010). Together, these phenotypes suggest that loss of nuclear integrity leads to premature aging in humans, which might reflect a role of nuclear dysfunction in normal aging. However, still very little is known about the mechanisms of how defects in those proteins lead to accelerated aging. Studying the yeast homologs and their role in nuclear integrity during aging is a fist step towards understanding laminopathic diseases.

Chromosomal DNA

As described above, genomic DNA mutations cannot explain the aging process and the aging phenotypes, since daughter and granddaughter cells of old mother cells have a restored lifespan potential. However, epigenetic changes of the genomic DNA were observed. As yeast cells age, acetylation of histone H4 at lysine 16 (H4K16) increases. This increase has been observed mostly at subtelomeric regions and is accompanied by the loss of histones and decreased transcriptional silencing (Dang et al., 2009). The authors simultaneously observed a decrease in protein levels of Sir2, the deacetylase of H4K16 (the role of Sir2 in aging is further discussed below). Together, this suggests that age-dependent decrease of Sir2 levels leads to increased histone acetylation and therefore to loss of histones at certain chromosomal loci, which might contribute to the aging process. Supporting this hypothesis, overexpression of histone H3 and H4 prolongs lifespan (Feser et al., 2010). Therefore, the level of histones that can be incorporated into nucleosomes

decreases with age and might reach a critical level in some old cells, impairing their viability.

Telomeres attracted the attention of aging researchers very early on: in mammalian cells that do not express telomerase, like fibroblasts, telomeres shorten with every cell cycle, leading to cellular senescence, whereas artificial expression of telomerase rescues their division potential (Bodnar et al., 1998). These findings led to the hypothesis that the length of telomeres sets a clock for every cell. Although telomere length seems to be critical for a normal lifespan in mice, it is unclear whether telomere shortening is directly involved in the aging process since telomerase deficient mice showed a normal survival curve and only their 6^{th} generation progeny showed a shortened lifespan (Hornsby, 2007; Rudolph et al., 1999). This suggests that the function of telomerase is rather important in gametes than in normal aging. In budding yeast, telomerase is constantly active, comparable to stem cells. Therefore, telomere length is unaffected during replicative aging and telomere shortening cannot account for aging phenotypes in yeast (D'Mello and Jazwinski, 1991). Nevertheless, mutations in the telomerase encoding *EST* genes (ever shorter telomeres) or *TLC1*, the template RNA, lead to progressive telomere shortening and limit the propagation potential of the entire population over time. This process is distinct from cellular aging and is called clonal senescence (Lundblad and Szostak, 1989; Singer and Gottschling, 1994).

Extrachromosomal DNA circles

Sinclair *et al.* discovered that yeast cells lacking Sgs1 (WRN) show accelerated aging phenotypes, including shortened lifespan, increased cell size, earlier sterility and an enlarged and fragmented nucleolus (Sinclair et al., 1997). The latter observation prompted them to examine the rDNA locus more carefully, which lead to the discovery that extrachromosomal rDNA circles (ERCs) play an important role in the aging process (Larionov et al., 1980; Sinclair and Guarente, 1997).

ERCs fulfill all four requirements for an aging factor: they accumulate in old mother cells, they segregate highly asymmetrically towards the mother cell at mitosis, artificial introduction of ERCs into young cells shortens their replicative lifespan and reducing their formation leads to lifespan extension (Defossez et al., 1999; Sinclair and Guarente, 1997). Once an ERC is formed, it replicates once during S-phase due to the presence of an autonomous replication sequence (ARS). The replicated copies

segregate asymmetrically, staying in the mother cell. As a consequence, ERCs accumulate exponentially in the mother cell over division cycles and thereby contribute to limiting the lifespan of the cell ((Sinclair and Guarente, 1997) Model Fig. 1.3).

ERCs are formed by homologous recombination in the rDNA array, which contains 80-150 tandem rDNA repeats. Due to the symmetry of the Holliday junction, the resolution of such a junction between two neighboring rDNA repeats leads to excision of one ERC 50% of the times. These recombination events are due to double-strand breaks. Chromosomal breakage in the rDNA is frequent during replication due to stalling of replication forks at the fork barriers that separate individual rDNA repeats (Takeuchi et al., 2003). Consistently, removal of Fob1, a protein required to stall replication forks, dramatically reduces the frequency of double-strand breaks, decreases the rate of ERC formation and extends lifespan (Defossez et al., 1999; Kobayashi and Horiuchi, 1996). Although *fob1Δ* mutant cells are longer lived compared to wild type cells, they still age. Studies of cells harvested at different ages showed that *fob1Δ* cells still produce ERCs, although later in their lifespan, and that ERCs accumulate exponentially in these cells (Lindstrom et al., 2011). Thus, it is possible that *fob1Δ* cells still age of ERC accumulation, but alternatively, they might die of defects caused by lacking replication fork barriers.

The rate of homologous recombination within the rDNA locus is lower than expected based on recombination rates of two homologous sequences elsewhere in the genome. It was proposed that Sir2, a histone deacetylase, is required for this repression (Gottlieb and Esposito, 1989; Petes and Botstein, 1977). Deletion of *SIR2* enhances intrachromosomal recombination within the rDNA and shortens lifespan, whereas moderate overexpression of Sir2 leads to lifespan extension (Gottlieb and Esposito, 1989; Kaeberlein et al., 1999). As cells age, the levels of Sir2 decline and the rate of recombination increases (Dang et al., 2009). This suggests that the rate of ERC formation increases as the cell ages. Indeed, mathematical modeling suggests that ERC formation increases quadratically with replicative age (Gillespie et al., 2004). However, the age-dependent increase in recombination within the rDNA locus is not rescued by overexpression of Sir2, suggesting that rDNA recombination may be differently controlled in old and young cells (Lindstrom et al., 2011). Nevertheless, deletion of *FOB1* rescues the short-lived phenotype of *sir2Δ* mutant cells back to wild type levels. In these cells, the levels of ERCs are lower compared to wild type,

suggesting that, in cells containing fewer ERCs, deletion of *SIR2* shortens lifespan in an ERC-independent manner (Kaeberlein et al., 1999).

Within the rDNA repeats a bidirectional RNA polymerase II promoter was discovered, called E-pro, whose transcription is repressed by Sir2. In cells lacking Sir2, less cohesin is associated with rDNA and rDNA stability is decreased (Kobayashi et al., 2004). These data led to the hypothesis that transcription of E-pro leads to increased rDNA instability. This model was tested by replacing E-pro with the *GAL1/10* promoter, which is repressed in glucose and activated in galactose containing medium (Saka et al., 2013). In support of the model, this strain shows increased rDNA stability, decreased ERC levels and increased lifespan when grown in the presence of glucose. Conversely, growth on galactose increases rDNA instability, augments ERC accumulation and shortens lifespan. Remarkably, rDNA instability and ERC formation is repressed in *sir2Δ* mutant cells when the promoter is artificially turned off. Concurrently, lifespan is no longer shortened but is prolonged to the same extent as in *fob1Δ* cells (Saka et al., 2013). This suggests that the short lived phenotype of cells lacking Sir2 is mainly caused by rDNA instability and ERC formation.

Why ERC accumulation becomes toxic and what causes old mother cells to die is unclear. It seems that the toxicity of ERCs is not caused by sequences specific of the rDNA, since every DNA circle studied so far that lacks a partitioning sequence (centromere or 2µ plasmid) accumulates in mother cells and shortens their lifespan (Falcón and Aris, 2003). Therefore, titration of proteins that bind to any non-centromeric DNA circle, including ERCs, might explain the toxicity of these molecules. It was proposed that replication or transcription factors could be the titrated proteins (Sinclair and Guarente, 1997). Alternatively, if ERCs bind to a putative receptor in the nuclear envelope, ERCs might block this receptor. However, no experiments have addressed these hypotheses so far. Ganley *et al.* proposed that ERCs themselves are not deleterious, but rather that they have a negative effect on rDNA stability (Ganley et al., 2009). Favoring this model, another study showed that increasing rDNA instability by deleting *HPR1*, a component of the RNA polymerase II complex, causes premature aging independent of ERC accumulation (Merker and Klein, 2002). However, both studies relied on mutations shortening the lifespan. Results from an ongoing project to determine the replicative lifespan of the entire deletion collection (where every non-essential ORF is deleted) indicate that 20% of all viable gene deletions shorten lifespan (Kaeberlein and Kennedy, 2005). The

authors report that most of these strains show stochastic death events, proposing that these mutations cause stress, which indirectly shortens lifespan. Therefore, shortened lifespan may occur in an aging-independent context and should be interpreted with caution.

Taken together, these studies establish ERCs as a naturally occurring factor that is incidentally formed and, once formed, accumulates in the mother cell and contributes to its aging. However, there are still many unresolved questions: Why are large amounts of ERCs toxic to the cells? Do ERCs induce rDNA instability or does increased rDNA instability induce ERC formation? Do ERCs titrate certain factors, and if so, which ones?

Fig. 1.3

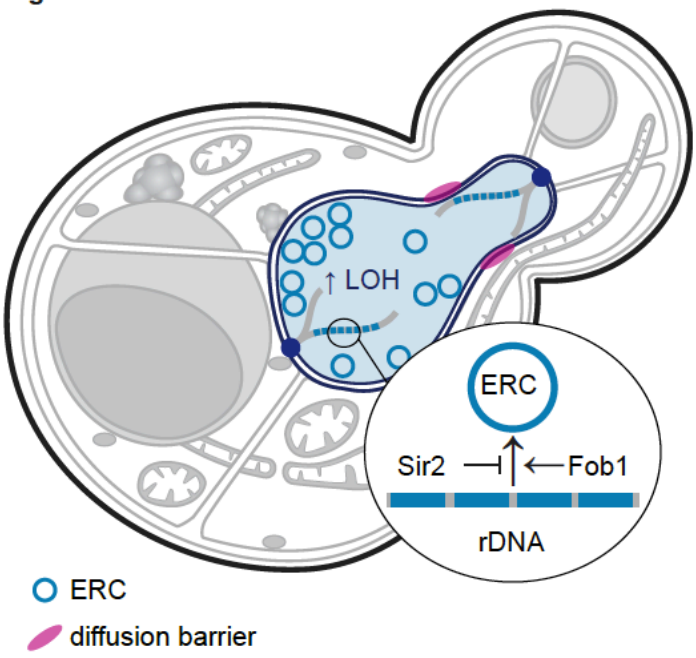

Fig. 1.3 Age-dependent changes in the nucleus

ERCs (blue circles) are formed by homologous recombination of adjacent rDNA repeats and they accumulate as the cells age. Their formation is triggered by Fob1 and repressed by Sir2 (inset) and their retention depends on a diffusion barrier in the outer nuclear membrane at the bud neck (pink). Old cells show an increase in loss of heterozygosity (LOH), especially in the rDNA array, which favors ERC formation.

Loss of heterozygosity

In diploid cells the repair of double strand breaks not only results in ERC formation but can also lead to loss of heterozygosity: the recombination of an initially heterozygous locus resulting in its homozygosity, which is a hallmark of mammalian cancer cells (Tuna et al., 2009). Interestingly, in yeast the frequency of loss of heterozygosity increases with age ((Carr and Gottschling, 2008; Lindstrom et al., 2011; McMurray and Gottschling, 2003) Model Fig. 1.3). In most old cells, this age-dependent increase originates from loss of mitochondrial DNA (mtDNA) (further discussed below). In respiration-competent cells, an age-dependent increases in loss of heterozygosity was only observed at the rDNA locus on chromosome XII (Lindstrom et al., 2011). These findings suggest that DNA stability is not globally affected but that the stability at the rDNA locus specifically decreases with age, possibly leading to the predicted increase in ERC formation with age. However, why rDNA locus stability is specifically affected during aging remains unclear.

1.3 Mitochondria

Mitochondrial integrity

A large number of studies have suggested that mitochondrial decay also contributes to aging. Remarkably, a link between the nucleus and mitochondria was established when the increased rate of loss of heterozygosity in daughters of old mother cells was found to correlated with the formation of “petite” daughter cells lacking mtDNA (also called ρ0 cells; (Veatch et al., 2009)). Even though mitochondrial function is essential for cell viability, respiration is not and yeast cells lacking mtDNA survive. These cells switch from respiration to fermentation, leading to a growth defect and their petite phenotype.

The increased loss of heterozygosity in ρ^0 cells was proposed to be triggered by defective iron-sulfur (Fe-S) cluster biogenesis in cells lacking mtDNA (Veatch et al., 2009). Fe-S clusters are synthesized in the mitochondria and act as cofactors for hundreds of proteins, many involved in DNA replication and repair (White and Dillingham, 2012). Additionally the authors found that loss of mtDNA is accompanied by a cell-cycle arrest followed by spontaneous genetic changes leading to improved growth (Veatch et al., 2009). This suggests that loss of mtDNA might be compensated by increased genetic rearrangements allowing for the survival and growth of ρ^0 cells. The observation that some old mother cells form ρ^0 daughter cells suggests that either old cells lose their mtDNA and therefore cannot pass mitochondria containing DNA to their daughters or that the DNA-containing mitochondria are retained in the old mother cell. However, little is known about the stability and partitioning of mtDNA in old yeast cells.

Upon damage, mitochondria are proposed to segregate asymmetrically depending on their integrity: Lai *et al.* studied cells with defective mitochondria, using a temperature sensitive allele of *ATP2*, a subunit of the mitochondrial F1 ATP-synthase. They found that at permissive temperature, mitochondrial potential (Ψm) decreases and mitochondrial morphology changes dramatically. This leads to accumulation of mitochondria in the mother cell and impaired segregation of active mitochondria to the daughter cell. Mother cells accumulating mitochondria fail to produce rejuvenated daughter cells (the replicative lifespan of the 7^{th} daughter cell was 7 generations shorter; (Lai et al., 2002)).

Studies using the MEP to investigate mitochondrial morphology at different time points throughout the yeast lifetime revealed that mitochondria, which are tubular in young cells, become fragmented early in the aging process (8 generation old cells) and form aggregates in older cells (17 generations), which persist for the rest of the lifespan (median of 25 generations; Model Fig. 1.4). These mitochondria have a membrane potential that decreases with age (Hughes and Gottschling, 2012). In conclusion, mitochondria change dramatically through the lifetime of yeast cells. However, why this organelle is altered early in life and how these cells maintain viability despite these dramatic changes in mitochondrial morphology remain unclear. Additionally, damaged or non-functional mitochondria appear to be retained in the mother cell, possibly to ensure the generation of rejuvenated daughter cells containing only fully functional mitochondria. It will be interesting to investigate how damaged regions of mitochondria are specifically detected and retained in the mother cell.

Reactive oxygen species (ROS)

Further studies of mitochondrial asymmetry revealed that mitochondria retained in the mother cell show a lower oxidizing redox potential and higher levels of reactive oxygen species (ROS) compared to the mitochondria inherited by the daughter cell ((McFaline-Figueroa et al., 2011) Model Fig. 1.4). Additionally, ROS levels are elevated in old cells (Xie et al., 2012). During the first 5 divisions, the mitochondrial redox potential declines in the mother cell and becomes more oxidizing, whereas the asymmetry between mother and bud is constant. Therefore, daughter cells produced from the fifth division inherit less-functional mitochondria (McFaline-Figueroa et al., 2011). This is paradoxical, since these daughter cells are fully rejuvenated. One possible explanation is that the activity of a protein implicated in detoxification of mitochondrial ROS, the catalase Ctt1, is increased in daughter cells after cytokinesis (Erjavec and Nystrom, 2007). Similarly, mitochondrial aconitase, Aco1, a protein containing an Fe-S cluster and involved in mtDNA maintenance, loses activity during normal replicative aging (Klinger et al., 2010). Intriguingly, although the amount of Aco1 is split equally between old mother and daughter cells, the daughter cell primarily receives the active form of aconitase. Therefore, if daughter cells receive less-functional mitochondria, they might repair them more efficiently than old mother cells.

Passing beneficial factors to the bud instead of retaining harmful agents in the mother is another possible way to ensure rejuvenation of the daughter cell. Such a mechanism was also proposed for the segregation of multidrug resistance proteins, transporters located at the plasma membrane that function in cellular metabolism, detoxification and stress response (Eldakak et al., 2010). It was proposed that the newly synthesized transporters are deposited into the growing daughter cell while the preexisting pool is retained in the mother cell where their function declines with time. According to a beneficial role of the transporters in the daughter cell, cells lacking them are short lived whereas their mild overexpression results in a prolonged lifespan.

In 1956, Harman postulated the so-called “Free Radical Theory of Aging”, whereby increased metabolic rate leads to increased ROS formation, which would be harmful for the cells and cause aging (Harman, 1956). Although this theory gained popularity and is supported by experiments showing that ROS levels are increased in old mother cells (Barros et al., 2004; Laun et al., 2001), other reports showed that cells containing increased ROS levels show a prolonged lifespan under certain conditions (Sharma et al., 2011). This latter finding led to the hypothesis that increased ROS levels can induce ROS-defence and stress response mechanisms which prolong lifespan (Ristow and Zarse, 2010). This theory suggests that ROS act as a signal to activate the retrograde response, a response pathway that induces the transcription of stress response genes as a defense mechanism (see next paragraph). However, whether accumulation of ROS themselves shortens or prolongs lifespan is currently under debate (Kowaltowski et al., 2009; Ristow and Schmeisser, 2011). Their effects could depend on their levels; mild ROS levels might activate stress response pathways, which lead to prolonged lifespan, but higher ROS levels might be toxic and therefore shorten lifespan.

Fig. 1.4

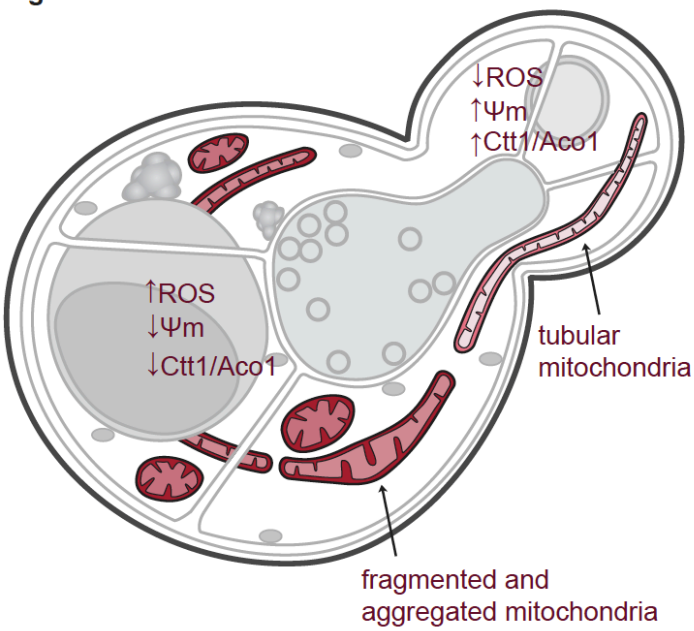

Fig. 1.4 Mitochondira in aged cells

As the cells age mitochondria become fragmented and aggregated (dark red). Concomitantly, the levels of reactive oxygen species (ROS) augment and mitochondrial membrane potential (Ψm) decreases. Additionally, daughter cells contain more active Ctt1 and Aco1, proteins involved in membrane detoxification and mtDNA maintenance. Together, this leads to the asymmetric distribution of mitochondria in respect to mitochondrial integrity.

Retrograde response

The retrograde response is a pathway that signals from the mitochondria to the nucleus and is activated upon damage or loss of mtDNA. Activation of the retrograde response in ρ^0 cells leads to transcription of a specific set of genes encoding metabolic enzymes and stress response proteins in an Rtg2-dependent manner (Butow and Avadhani, 2004; Parikh et al., 1987). The observation that the most long-lived cells in a population mainly consists of ρ^0 cells led to the hypothesis that ρ^0 cells show a prolonged lifespan. Indeed, in some strain background, loss of mtDNA leads to increased longevity. Further investigation revealed that the increased lifespan in ρ^0 cells depends on Rtg2, suggesting that activation of the retrograde response pathway leads to the lifespan extension observed in these cell (Kirchman et al., 1999).

However, another aspect of the interplay between the nucleus and mitochondria is the fact that activation of the retrograde response also enhances ERC accumulation.

At a first glance it seems paradoxical that on one hand this pathway activates longevity genes and on the other hand increases the accumulation of life-shortening ERCs (Borghouts et al., 2004). The reason for this might be the dual role of Rtg2: it is both involved in transcriptional activation of retrograde-response-induced genes and suppresses ERC accumulation. It has been proposed that activation of the retrograde response by loss of mtDNA might require more Rtg2 for the transduction of the retrograde response signaling, leading to less repression of ERC formation (Jazwinski, 2005). In addition it was proposed that ERCs signal back to the mitochondria via Tar1, a protein that is encoded on the antisense strand of the rDNA repeat and localizes to the mitochondria (Poole et al., 2012). However, neither the function of Tar1 nor whether the amount of ERCs influences the levels of Tar1 is known.

1.4 Vacuole

Autophagy

Macroautophagy mediates the degradation and recycling of organelles through their engulfment into autophagosomes and targeting to the vacuole. The vacuole resembles the lysosome in metazoa and is required for both storage of ions and amino acids, and turnover of proteins and lipids (Armstrong, 2010). The turnover of macromolecules through autophagy is believed to be cytoprotective. Accordingly, survival of cells in several stress conditions depends on the autophagy machinery. In *C. elegans* and *D. melanogaster*, several manipulations leading to prolonged lifespan enhanced autophagy, suggesting that autophagy has an anti-aging effect (Rubinsztein et al., 2011). However, little is known about the role of autophagy during yeast aging. A genetic screen for shortened chronological lifespan revealed that many genes involved in autophagy are required for a normal lifespan (Fabrizio et al., 2010; Matecic et al., 2010). However, cells with defects in the autophagy pathways might suffer from stress that does not occur naturally during aging. Treating cells with spermidine, which activates autophagy, increases chronological lifespan. The effect of spermidine addition on replicative aging is less clear: treatment of young cells does not affect their lifespan but treating aged cells isolated by elutriation does (Eisenberg et al., 2009). In this study elutriation severely shortened lifespan even in the control cells, suggesting that spermidine might rather protect from the induced stress than prolonging the normal replicative lifespan. Microfluidics could be used here as a tool to reinvestigate these questions.

Vacuoles and pH

As cells age, the vacuole grows drastically (Lee et al., 2012; Tang et al., 2008). Indeed, vacuolar morphology affects aging; cells defective in vacuolar fusion, *osh6Δ* and *erg6Δ* cells, exhibit shortened replicative lifespan, whereas overexpression of Osh6 prolongs lifespan (Gebre et al., 2012; Tang et al., 2008). Osh6 mediates vacuolar fusion by maintaining sterol levels in the vacuolar membrane, whereas overexpression of Osh6 depletes sterols from the plasma membrane. Similarly, Erg6 is directly involved in ergosterol biosynthesis. Therefore, these perturbations not only affect vacuolar fusion but also change sterol homeostasis, which might affect

longevity through other pathways, as e.g. by modulating the strength of the diffusion barrier (described later).

Insights into the age-associated changes occurring in the vacuole and their impact on mitochondrial physiology arise from work by Hughes and Gottschling. Acidity in the vacuole drops rapidly early in age (after 4 divisions) and is followed by changes in mitochondrial structure and membrane potential. Vacuolar acidity is established by the V-ATPase and overexpression of Vma1, a subunit of the V-ATPase, delays the drop of acidity in the vacuole ((Hughes and Gottschling, 2012; Li and Kane, 2009) Model Fig. 1.5). Remarkably the same perturbation also delays the dysfunction of mitochondria and extends lifespan. Furthermore, while acidity declines in mother cells as they age, the acidity in their daughter's vacuoles is reset. Together, these observations indicate that a very early change in the vacuolar pH affects mitochondrial function in the aging mother cell and contributes to the replicative aging process. It would be interesting to test whether the pH changes in more compartments during aging, since a general drop of pH might affect many more cellular functions besides mitochondrial integrity.

Fig. 1.5

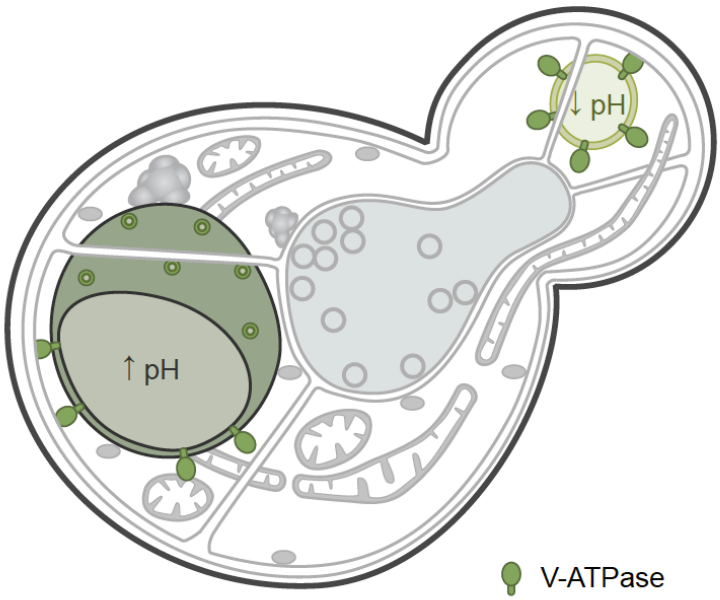

Fig. 1.5 Changes in the vacuolar pH during aging

Already early during the aging process (after 4 generations), acidity drops in the vacuole (dark green), which leads to a decrease in mitochondrial integrity. Overexpression of Vma1, a component of the V-ATPase (green) prevents the drop of acidity and prolongs lifespan.

1.5 Cytoplasm & Endoplasmatic Reticulum

Carbonylated proteins

As previously discussed, ROS levels are elevated in old yeast mother cells (18 generations) compared to young cells (4 generations) (Laun et al., 2001). This spurred the Nyström lab to investigate protein carbonylation, a form of irreversible oxidative damage to proteins (Stadtman, 2006). Carbonylated proteins segregate asymmetrically towards the mother cell and accumulate with replicative age. Interestingly, the asymmetry depends on Sir2 and the actin cytoskeleton ((Aguilaniu et al., 2003) Model Fig. 1.6). Furthermore, age-induced carbonylated proteins interact with Hsp104, a chaperone involved in disassembly of protein aggregates, and the asymmetric distribution of carbonylated proteins depends on Hsp104 function. Cells lacking Sir2 exhibit increased carbonylation of different chaperones including Hsp104, which might impair their function and explain the increased symmetry of oxidized proteins. Accordingly, overexpression of Hsp104 rescues both the symmetric segregation of carbonylated proteins and the replicative lifespan of *sir2Δ* mutant cells (Erjavec et al., 2007). How overexpression of Hsp104 rescues the lifespan of *sir2Δ* cells, which contain high ERC load, remains unclear. Furthermore, the retention of carbonylated proteins was proposed to be important for the rejuvenation of daughter cells; when aged mother cells were treated with Latrunculin-A (Lat-A), a chemical compound that disrupts the actin cytoskeleton, more carbonylated proteins were passed to the daughter cell. The daughter cells that were produced during the Lat-A treatment displayed shortened lifespan, whereas the daughter cells born after removal of Lat-A were fully rejuvenated (Erjavec et al., 2007). However, it is unclear whether the Lat-A treated daughter cells suffer more from their higher load of carbonylated proteins or from the lack of actin-dependent transport during bud growth. Together, these experiments demonstrate that carbonylated proteins are retained in the mother cell, leading to their accumulation with age. However, they do not definitely clarify whether oxidative damage is indeed a lifespan determinant.

Protein aggregates

The Hsp104 chaperone facilitates the refolding of denatured and aggregated proteins (Parsell et al., 1994). Unlike chaperones involved in the folding of newly synthesized proteins, Hsp104 is a disaggregase and interacts with aggregated proteins. Therefore, Hsp104 is frequently used as a marker of protein aggregation within the cell (Winkler et al., 2012). To investigate how Hsp104 foci are segregated at mitosis, such foci have been induced through heat shock in young cells (42°C, 30 min) and their behavior has been monitored by microscopy. Using this method, Zhou *et al.* describe their movement as rather slow and random, and mathematical modeling revealed that the geometry of dividing yeast cells might be sufficient to retain Hsp104 aggregates in the mother cell. The remarkably slow movement might suggest that these Hsp104 foci are not freely diffusing in the cytoplasm but are rather associated with an organelle. Using long-term microscopy, the dissolution of these heat induced aggregates was observed in both mother and bud (Zhou et al., 2011). Using the same method, Liu and colleagues reported that, in approximately 10% of the cells, Hsp104 foci moved in a seemingly directed manner from the bud to the mother cell. This retrograde transport depended on Sir2 and the polarisome (Liu et al., 2010). Hsp104 forms such foci even without heat stress as the cells age (Erjavec et al., 2007; Liu et al., 2010; Zhou et al., 2011). Age-induced Hsp104 aggregates are not cleared by dissolution but are retained in the mother cell and their diffusion is similar to that of heat induced ones ((Liu et al., 2010; Zhou et al., 2011) Model Fig. 1.6). However, little is known about age-induced Hsp104 aggregates, how they behave and to which extend they are comparable to the stress-induced aggregates. In addition, it is not known whether Hsp104 aggregates are toxic or have a protective function for the cell.

Analysis of protein aggregates in proteasome-deficient cells indicates that they are not all equivalent. Different reporter proteins chosen for their tendency to misfold show a two step dynamics. They first aggregate into stress foci, and then are sequestered into either one of two distinct compartments within the cell: soluble ubiquitinated proteins are targeted to the JUNQ for degradation by the proteasome and insoluble aggregates are deposited in a protective compartment called IPOD (Kaganovich et al., 2008). Interestingly, the IPOD compartment is associated with the vacuole and is entrapped in ER membranes whereas the JUNQ compartment is associated with the nucleus. Therefore, the movement of these deposits into the bud is constrained by their attachment to organelles. In cells lacking Hsp104, the stress foci are neither degraded nor deposited into IPOD or JUNQ and are no longer

asymmetrically retained in the mother cell (Spokoini et al., 2012). Accordingly, *hsp104Δ* mutant cells are short-lived, indicating that Hsp104 function is important for normal lifespan (Erjavec et al., 2007).

Fig. 1.6

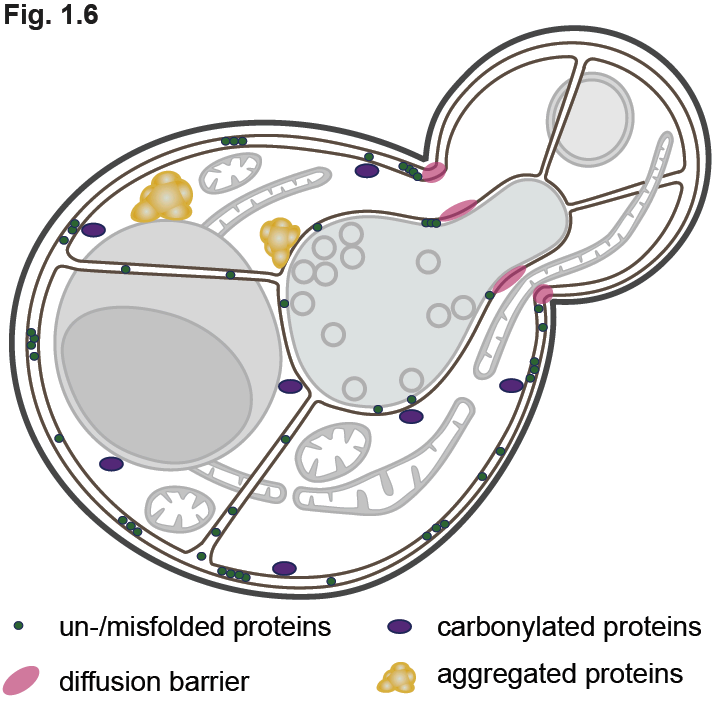

Fig. 1.6 Cytoplasmic and ER-associated changes occurring with age

Carbonylated proteins (violet) as well as aggregated proteins (yellow) are found in old cells and are segregated asymmetrically. Aggregated proteins are attached to membranes (IPOD and JUNQ) and are diffusing rather slow (Hsp104-containing foci), which, together with the diffusion barrier and the geometry of a dividing yeast cell, might explain their retention in the mother cell. The asymmetric segregation of misfolded proteins (green) in the lumen of the ER depends on the ER diffusion barrier.

Together, studies on Hsp104-recruiting aggregates suggest that there are several parallel mechanisms ensuring their asymmetric segregation: A) aggregates are efficiently retained in yeast mother cells through attachment to organelles, B) once an aggregate is segregated into the bud it can be either cleared by dissolution or C) possibly brought back into the mother cell by retrograde transport (Liu et al., 2010; Spokoini et al., 2012; Zhou et al., 2011). It has to be noted that both heat shock treatment and blocking the proteasome machinery might not reflect the characteristics of aggregates arising throughout the aging process. Therefore, Juha Saarikangas, a PostDoc in our lab, studies age-induced aggregates more carefully and asks which proteins are sequestered to these aggregates, when and how they are formed and whether different aggregates behave differently. Importantly, the

question remains whether aggregates that appear with age act as aging factors or sequester aggregates from the cytoplasm, thereby ensuring a normal lifespan.

A very recent report from our lab showed that unfolded proteins in the ER contribute to aging in cells that are defective for the unfolded protein response machinery (Clay et al., 2014). Interestingly, the unfolded proteins are retained in the mother cell due to a diffusion barrier at the bud neck in the ER membrane ((Luedeke et al., 2005); Model Fig. 1.6). This barrier was proposed to be mediated by tethering of the ER to septins via Scs2 and to consist of sphingolipids (Chao et al., 2014; Clay et al., 2014). Accordingly, interfering with sphingolipid biosynthesis weakened the barrier and allowed the propagation of unfolded proteins into the bud, which prolonged the lifespan of mother cells with defects in the unfolded protein response. However, it seems that in wild type cells the pathways responding to unfolded proteins are efficient enough to prevent the accumulation of unfolded proteins, suggesting that they do not contribute to aging under normal growth conditions. Nevertheless, the diffusion barrier in the ER might help confining different factors to the mother cell by their attachment to ER membrane-associated proteins both in the ER lumen and in the cytoplasm.

All together we can conclude that several changes occur within the cell as it ages but for the majority of changes it remains difficult to dissect whether they cause aging or appear as a consequence of aging. Protein aggregates, as an example, are clearly connected to aging; however, it is still unclear whether the formation of aggregates becomes toxic or rather protects the cell from free diffusing carbonylated and misfolded proteins. So far only ERCs fulfill all four requirements for an aging factor discussed earlier. Nevertheless, the evidences are strong that mitochondrial decay, high levels of ROS, carbonylated and misfolded proteins contribute to aging, probably dependent on their levels within a cell. It also seems that beneficial factors, such as multidrug resistance proteins, chaperones, proton pumps, the retrograde response, autophagy, proteasome machinery as well as the deacetylases preventing DNA recombination are important players to prevent accelerated aging. Still, ERCs seem to be the most limiting factors of age in laboratory conditions and even though the formation of ERCs is well characterized, very little is known about how they are retained in the mother cell.

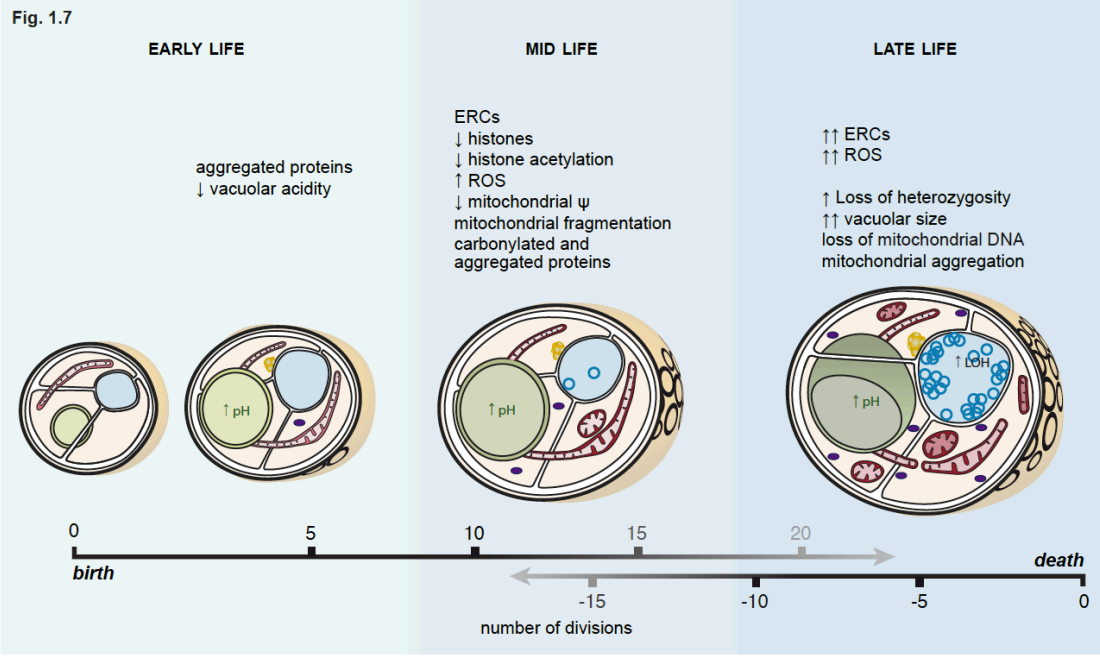

Fig. 1.7 Different stages of life

This scheme divides the aging process into three different stages: early age, during which first changes occur but do not impair cell growth; intermediate age, during which aging factors start to accumulate; and late age, which corresponds to the last divisions before death, during which damage accumulation ultimately leads to cell death. Importantly, the changes depicted here summarize the trends observed in average in a population of cells and are unlikely to happen in a stereotyped manner in all individual cells.

1.6 Retention of ERCs in yeast mother cells

Mathematical modeling predicted that an ERC retention above 0.99 is required in order to simulate experimentally obtained aging curves (Gillespie et al., 2004). Another modeling study revealed that the geometry of the nucleus and the speed of anaphase ensure a retention frequency of 0.75-0.90 (Gehlen et al., 2011). Thus, mechanisms beyond geometry and speed of anaphase are likely to contribute to this process. In particular, ERC retention was proposed to involve a diffusion barrier at the bud neck of early anaphase nuclei ((Shcheprova et al., 2008) Model Fig. 1.3). This diffusion barrier impairs free diffusion of proteins embedded in the outer nuclear membrane from the mother part into the daughter part of a dividing nucleus. Our laboratory discovered that this diffusion barrier depends on septins and Bud6, both localizing to the bud neck. Interestingly, there is a strong correlation between the strength of this diffusion barrier and the retention of ERCs (Shcheprova et al., 2008). Investigating ERC levels in *bud6Δ* mutant cells at different ages revealed that ERCs are still formed but accumulate much slower (Lindstrom et al., 2011). Accordingly, *bud6Δ* mutant cells are longer lived compared to wild type cells (Shcheprova et al., 2008). The prolonged lifespan is not further extended by the deletion of *FOB1*, suggesting that ERC accumulation is no longer limiting lifespan. The diffusion barrier in the nuclear envelope depends on intact sphingolipid biosynthesis, suggesting that sphingolipids are involved in establishing both diffusion barriers, the one in the outer nuclear envelope and the one in the cortical ER. However, the nuclear diffusion barrier seems to be more sensitive to different environmental stresses. For example, the nuclear diffusion barrier is weakened when the cells experience mild heat stress (growth at 37°C) and increased when the cells were grown in calorically restricted medium (Sandro Baldi, unpublished data). Both treatments were proposed to extend replicative lifespan (Lin et al., 2000; Swiecilo et al., 2000). Thus, the nuclear diffusion barrier is highly regulated allowing the cells to react to various changes occurring in natural environments.

How the diffusion barrier in the outer nuclear membrane restricts the diffusion of ERCs in the nucleoplasm is currently debated. Since nuclear pore complexes (NPCs) span both inner and outer nuclear membrane they are subjected to the diffusion barrier and it was proposed that ERCs are attached to nuclear pores. This hypothesis was supported by the localization of non-centromeric plasmids to the nuclear rim and the co-localization with NPC clusters in *nup133Δ* mutant cells. Additionally, cells

lacking the basket proteins Mlp1 and Mlp2 were defective in plasmid retention. Thus, it was hypothesized that pre-existing nuclear pores are retained in the mother cell ensuring the retention of ERCs attached to NPCs and that the NPCs in the bud are newly synthesized (Shcheprova et al., 2008). However, newer reports show that the bulk of pre-existing pores is not efficiently retained in the mother cell and can thus not account for ERC retention (Colombi et al., 2013; Khmelinskii et al., 2010; Terweij et al., 2013). Therefore, several questions remained: Are ERCs and other non-centromeric plasmids indeed attached to NPCs? How can attachment of circles to NPCs ensure their high retention although NPCs are not efficiently retained in the mother cell? If they are attached to NPCs, what are the proteins tethering them to NPCs? Is there a molecular mechanism recognizing non-centromeric DNAs to attach them to NPCs whereas centromeric DNAs are allowed to be segregated to the bud? And what are the cellular consequences of such attachment during aging?

1.7 Aim of this project

The aim of this project was to identify molecular players that attach non-centromeric DNA molecules to NPCs in order to I) reinvestigate whether circles are indeed attached to NPCs II) investigate the cellular consequences of detachment of DNA circles in young and old cells III) gain insights into what is retained by the diffusion barrier in order to ensure ERC retention and IV) to identify mechanisms that allow the cells to distinguish self from non-self DNA in order to allow the segregation of centromeric DNA but simultaneously prevent spreading of non-centromeric DNA molecules. Finally, we also wondered how mammalian cells react to non-centromeric DNA molecules.

2. Results

2.1 The SAGA complex mediates retention of non-centromeric DNA molecules in yeast mother cells

The SAGA and TREX-2 complex are required for the retention of non-centromeric plasmids in the mother cell

To investigate the segregation of non-centromeric DNA circles the previously described plasmid pPCM14 (Fig. 2.1A) containing a replication origin (ARS1) and 224 repeats of the TetO sequence was used (Megee and Koshland, 1999). In cells expressing a TetR-mCherry fusion protein, which binds the TetO sequence, the plasmid is observed as a focus of red fluorescence. Additionally, the plasmid contains an excisable centromere leading to the formation of a labeled non-centromeric DNA circle upon expression of the R-recombinase. The plasmid also contains two auxotrophic selection markers: *URA3* located between the two recombination sites to prevent accidental centromere excision and *LEU2* on the residual backbone, allowing selection for the plasmid after centromere excision. In budding yeast all centromeres co-localize with SPBs throughout the cell cycle (Kitagawa and Hieter, 2001). Accordingly, we observe the centromeric plasmid in close proximity to the SPBs (Fig. 2.1A). 3 h after addition of estradiol plasmids localized away from the SPBs in 68% of the cells. Most of those cells displayed one or two small plasmid foci (61% or 33%, respectively; Fig. 2.1A) and only 6% of the cells showed more than two foci. Using cells containing one, two or four plasmid foci the propagation frequency for each individual plasmid was determined as described in Materials and Methods. In brief, the lower the propagation frequency the better is the plasmid retained in the mother cell. The propagation frequency in wild type (wt) cells was extremely low (pf = 3.9 ± 1.1; Fig. 2.1B), thus this plasmid is stringently retained in the mother cell. And the propagation frequency was increased in *yku70Δ* and *bud6Δ* cells as previously reported ((Gehlen et al., 2011; Shcheprova et al., 2008); pf = 10.3 ± 1.3 and 11.8 ± 0.8, respectively, N = 3 clones, $p < 0.001$; Fig. 2.1B).

To investigate how the plasmid might be anchored to the nuclear periphery we screened different strains lacking proteins known to interact with both chromatin and the nuclear periphery using this assay. No effect on circle retention was observed in

cells lacking any of the sirtuin proteins, Sir1-4, which are involved in chromatin silencing and telomere anchorage to the inner nuclear membrane (Gotta et al., 1996), in cells lacking the nucleoplasmic domain of the Sun-domain protein Mps3, involved in NPC and SPB insertion (Jaspersen and Ghosh, 2012) and telomere tethering to the nuclear envelope (Bupp et al., 2007), in cells lacking the lamin-binding-related proteins Src1 or Heh2 (Grund et al., 2008) and in cells lacking Slx5, a protein involved in DNA double strand break repair (Mullen et al., 2001) and forming perinuclear foci (Cook et al., 2009) (Fig. 2.1B).

In contrast, cells lacking Gcn5, a component of the Spt-Ada-Gcn5 acetyltransferase (SAGA) complex, showed a clear increase in plasmid propagation (pf = 11.1 ± 2.8, N = 3 clones, $p < 0.001$). The SAGA complex is a multiprotein complex that was first discovered for its role in histone acetylation (Grant et al., 1997). Gcn5, a core component of the SAGA complex, acetylates histones in vitro and forms together with Ada2 and Ada3 a minimal catalytic complex able to acetylate histones present in nucleosomes (Brownell et al., 1996; Grant et al., 1997; Kuo et al., 1996). In vivo SAGA acetylates various lysines on both histone H3 and histone H2B tails (Zhang et al., 2010). Besides its acetylation activity, SAGA further contains a deubiquitination module (dub) consistent of Ubp8, the deubiquitinating enzyme, Sgf73, Sgf11 and Sus1 (Kohler et al., 2008; Rodriguez-Navarro et al., 2004). It was proposed that the acetylation of these histones opens the chromatin structure and thus facilitates transcriptional initiation by RNA polymerase II (Pol II). Indeed, SAGA plays an important role in the transcription of several stress-induced genes (Huisinga and Pugh, 2004). And a very recent report even suggests that SAGA acetylates promoters and deubiquitinates the transcribed region of all transcribed genes in the yeast genome (Bonnet et al., 2014). The GAL genes, for example, are highly expressed when cells are shifted to galactose containing medium and this depends on SAGA (Larschan and Winston, 2001). Simultaneously the activated genes relocate to the nuclear periphery (Dieppois and Stutz, 2010; Luthra et al., 2007; Vinciguerra and Stutz, 2004). However, whether these changes in nuclear positioning facilitate transcription and fast mRNA export or rather enable fast repression is a topic of current investigations (Green et al., 2012; Taddei et al., 2006; Texari et al., 2013). Nevertheless, SAGA brings chromosomal loci to the nuclear periphery by linking them to nuclear pores via the TREX-2 complex (Luthra et al., 2007).

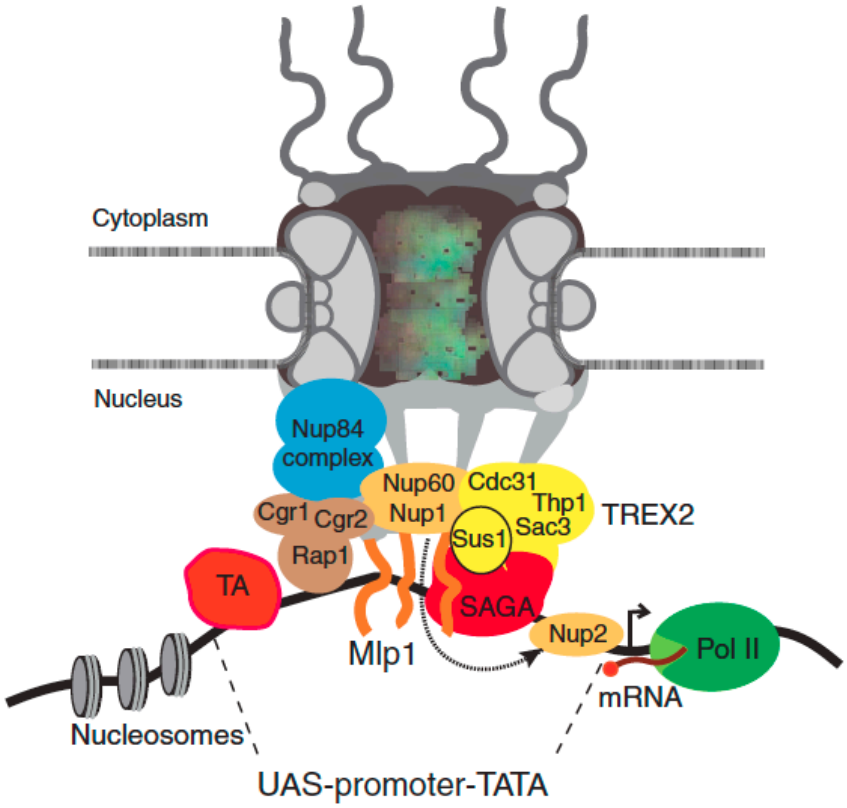

Dieppois and Stutz, 2010

2.0 SAGA anchors chromatin to NPCs via TREX-2

The SAGA complex tethers chromatin to nuclear pores by interacting with the TREX-2 complex, an NPC-binding complex, and the nuclear basket proteins Mlp1 and Mlp2. Figure is taken from Dieppois and Stutz, 2010.

All SAGA mutants tested, including *spt3Δ*, *sgf73Δ*, *sgf11Δ*, and *ubp8Δ* displayed similar defects in DNA circle retention (pf = 9.7 ± 1.7, 11.8 ± 1.6, 9.4 ± 1.2, 8.5 ± 1.0 respectively, N = 3 clones, $p < 0.001$; Fig. 2.1B). The function of Sgf73 in plasmid retention did not depend on the low complexity domain of Sgf73 (aa 454-657). However, replacement of the GCN5 gene with a point mutant allele abrogating its acetyl-transferase activity, *gcn5-E173A* (Wang et al., 1998) led to a similar increase in plasmid propagation to the daughter cell as observed in *gcn5Δ* mutant cells (pf = 11.0 ± 1.5, N = 3 clones, $p < 0.001$). Thus, SAGA and its acetyl-transferase activity, which are known for their ability to link chromatin to NPCs, promote the retention of DNA circles in the mother cell.

SAGA's function in chromatin anchorage to NPCs depends on the TREX-2 complex. Thus we wondered whether components of the TREX-2 complex were required for circle retention. Inactivation of the core TREX-2 gene, *SAC3*, caused circles to

propagate to the bud 3 times more frequently than in wild type cells, i.e., at a frequency similar to SAGA defective cells (pf=11.5 ± 3.0, N = 3 clones, $p < 0.001$; Fig. 2.1B). Deletion of *SUS1,* which inactivates both SAGA and TREX-2 complexes (Pascual-Garcia and Rodriguez-Navarro, 2009), led to similar effects (pf=11.3 ± 1.4, N = 3 clones, $p < 0.001$), indicating that inactivation of SAGA and TREX-2 were not additive. We conclude that the SAGA complex and the NPC component TREX-2 act together in a pathway mediating the targeted retention of non-chromosomal circles in the mother cell.

16-18 h after addition of the estradiol and growth in selective medium (-LEU), the majority of the cells (96%) contained no red focus, 1% contained few small foci as above, and 6% of the cells carried one large and intense signal (Fig. 2.1C). This big focus remained inside the nucleus, localized away from the SPB and was 8 fold brighter compared to the nuclear background level (Fig. 2.1D). This plasmid mass was clearly distinguishable from the individual plasmids observed 3h after excision of the centromere. As previously described, growth in selective medium of cells containing non-centromeric plasmids leads to the accumulation of 50-100 plasmids in a single cell (Hyman et al., 1982). Thus, we propose that the big and intense plasmid foci correspond to accumulated plasmids. Interestingly, these accumulated plasmids localized mainly to one focus and only rarely a part of it was transmitted to the daughter cell (2%, N = 50 cells pooled from all experiments). The propagation of parts of the accumulated plasmids was increased in cells lacking Bud6 or Gcn5 (11% or 12%, N = 50 cells pooled from all experiments). Thus, the retention of individual and accumulated non-centromeric plasmids depends on the SAGA complex and an intact diffusion barrier at the bud neck.

Fig. 2.1

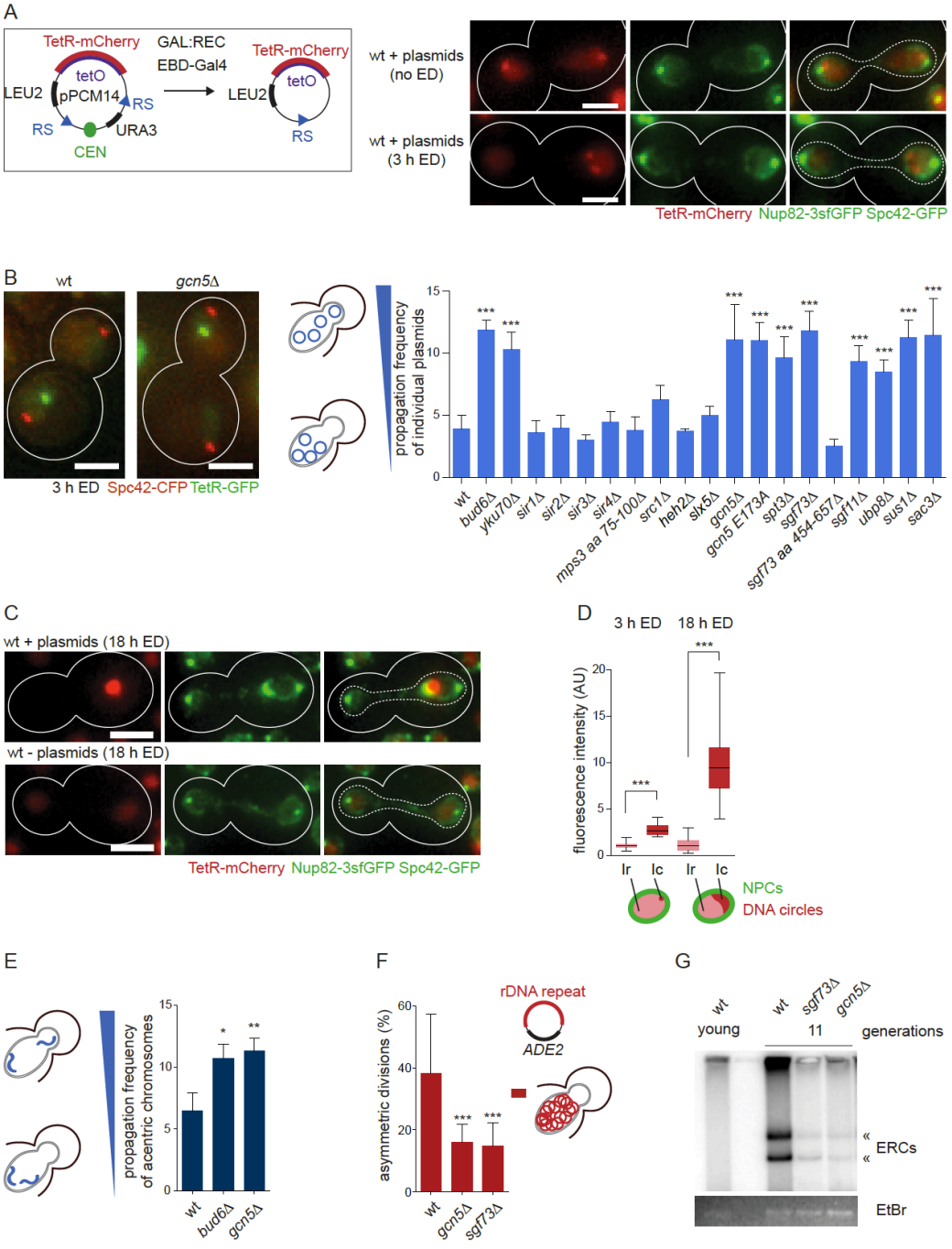

Fig. 2.1 SAGA ensures the retention of non-centromeric DNAs, including ERCs, in the mother cell

(A) Scheme of the plasmid pPCM14 and fluorescent images of pPCM14 before and 3 h after excision of the centromere by addition of estradiol (ED) in cells expressing TetR-mCherry, Nup82-3sfGFP and Spc42-GFP. (B) Representative images and quantification of the plasmid propagation frequencies (pf) in wt and different mutant cells (mean ± sd, N ≥ 3 clones). (C) Florescent images of cells with and without accumulated plasmids (pPCM14) 18 h after centromere excision. (D) Quantifications of the TetR-mCherry intensity in the circle area (Ic) and the residual nuclear area (Ir) 3 or 18 h after centromere excison (box plots represent min to max, line represents median, N ≥ 30 cells).

(E) Propagation frequencies of chromosome IV after centromere excision in wt and depicted mutant cells (mean ± sd, N ≥ 3 clones) (F) Mother-bud distribution of a marked ERC (pDS163) in wt, *gcn5Δ* and *sgf73Δ* mutant cells (mean ± sd, N = 10 independent experiments). (G) Detection of ERC levels in wt, *sgf73Δ* and *gcn5Δ* mutant cells by Southern blotting (« depicts ERCs) in 11 generations old cells. (B-F) ***p < 0.001, **p < 0.01, *p < 0.05; Images are max Z projections; Scale bar always represents 2 µm.

The SAGA complex prevents propagation of non-centromeric chromosomes and ERCs to the daughter cell.

Next, we wondered whether SAGA functioned specifically in the retention of this particular plasmid or whether we discovered a general mechanism to retain pieces of non-centromeric DNA. Since the plasmid is rather small we aimed for a bigger piece of DNA and removed the centromere of chromosome IV, the largest chromosome in *S. cerevisiae*. This strain contains two lox sites on both sites of the centromere and a *KanMX4* cassette to test for centromere excision (Warsi et al., 2008) and 256 TetO repeats inserted into the *TRP1* locus on the same chromosome. Similarly to pPCM14, 3 h of estradiol-induced expression of the Cre recombinase, allows the visualization of one to four individual fluorescent foci localizing away from the SPBs. In contrast, the foci were close to the SPBs throughout the cell cycle in untreated control cells. Thus, these foci represent non-centromeric chromosomes.

Interestingly, the non-centromeric chromosomes were highly retained in the mother cell (pf = 6.5 ± 1.4, N = 3 clones, Fig. 2.1E; previously observed by Barbara Böttcher using the *GAL* promoter to repress the centromere, unpublished data). Remarkably, however, the retention was decreased in cells lacking Bud6 or Gcn5 (pf = 10.7 ± 1.2 and 11.3 ± 1.0, N = 3 clones, *p < 0.05, **p< 0.01). Thus, a full acentric chromosome is retained in the mother cell in a SAGA- and barrier-dependent manner.

As described in the introduction, ERCs are non-centromeric molecules of special interest, since they are naturally occurring with age and were shown to contribute to the aging process. ERCs are highly retained in the mother cell and we wondered whether their retention involved the SAGA complex.

We first monitored the inheritance of an ERC marked with the *ADE2* gene (pDS163; (Sinclair and Guarente, 1997)) in wild type and SAGA mutant cells, by dissecting daughters off their mothers and following the inheritance of the *ADE2* marker between them. Following the segregation of the *ADE2* gene did not determine the segregation of single ERCs but solely whether all ERCs remained in the mother cell

or not. In 38% (± 6%) of the wild type cells, all ERCs accumulated in the mother cell segregated asymmetrically towards the mother cell, as demonstrated by the fact that their daughters failed to inherit a single copy of the *ADE2* marker and formed a red colony (see Material and Methods, (Sinclair and Guarente, 1997)). This percentage was reduced more than 2 fold in cells lacking Gcn5 or Sgf73 (16 ± 2% and 15 ± 2%, $N \geq 3$ clones, $p < 0.001$; Fig. 2.1F), indicating that full retention of ERCs in the mother cell requires SAGA function.

To test this conclusion further we investigated whether the accumulation of ERCs in aged yeast mother cells depended on SAGA function. We purified wild type, *sgf73Δ* and *gcn5Δ* mother cells after 11 generations using the mother enrichment program (Lindstrom and Gottschling, 2009), normalized the extracted DNA using qPCR against the *ACT1* gene and monitored ERC levels using Southern blotting. While no ERCs were detected in young wild type cells, substantial ERC accumulation was observed in wild type mothers after 11 generations. In contrast, SAGA mutant cells of the same age contained fewer ERCs (Fig. 2.1G). Together, these data establish that SAGA generically promotes the retention and accumulation of non-centromeric DNA molecules, including ERCs, in yeast mother cells.

SAGA acts independently of the nuclear diffusion barrier and anaphase duration

The SAGA complex is required for the efficient transcription of certain genes; therefore preventing its function might modulate gene expression and therefore affect previously known mechanisms involved in plasmid retention. To test this possibility we asked whether SAGA disruption interfered with the duration of anaphase and the morphology of the dividing nucleus, particularly the width of the bridge linking the two daughter nuclei (Gehlen et al., 2011), or with the compartmentalization of the nuclear envelope (Shcheprova et al., 2008). Measuring anaphase duration using time lapse movies of cells expressing Nsg1-GFP revealed that indeed deleting *YKU70* prolonged anaphase, whereas deletion of *BUD6, GCN5* and *SGF73* did not ($N \geq 180$ cells, $p < 0.001$; Fig. 2.2A). Furthermore, nuclear bridges were not wider in *gcn5Δ* cells ($N \geq 70$ cells; Fig. 2.2B). To determine whether SAGA inactivation affected the compartmentalization of the nuclear envelope during anaphase, the strength of the diffusion barrier was measured using fluorescence loss in photobleaching (FLIP), as previously described (Shcheprova et al., 2008). The barrier strength was measured in *gcn5Δ* mutant as well as in wild type and *bud6Δ* mutant cells, using Nup49-GFP as

a reporter. Although the *bud6Δ* mutation reduced compartmentalization of the envelope, as reported (Shcheprova et al., 2008), no effect was observed in wild type and *gcn5Δ* mutant cells (N ≥ 20 cells; Fig. 2.2C). Thus, changes in nuclear geometry, anaphase duration and the diffusion barrier do not account for the role of SAGA in circle retention.

Fig. 2.2

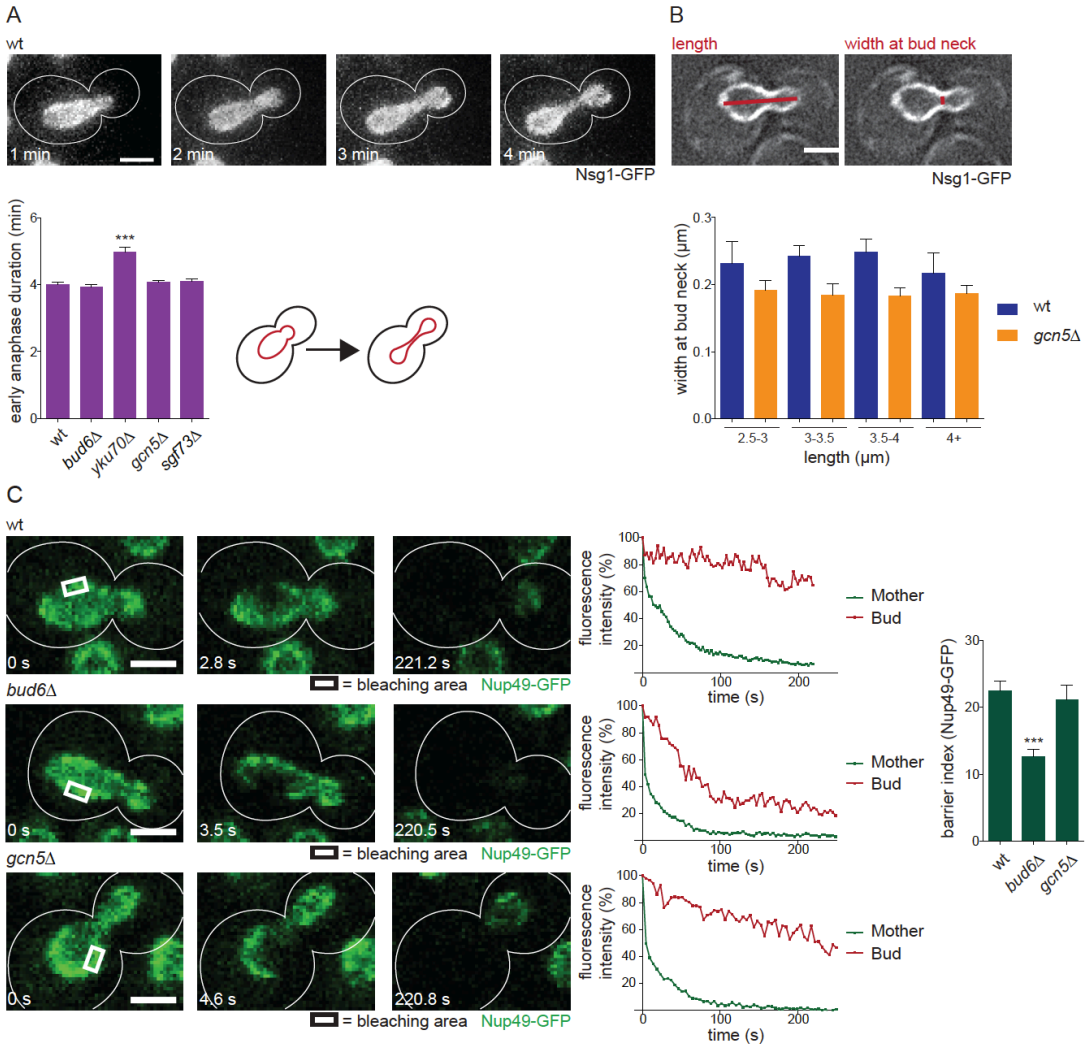

Fig. 2.2 Previously described mechanisms for plasmid retention are not affected in SAGA deficient cells

(A) Duration of early anaphase in wt cells and cells lacking Bud6, Yku70, Gcn5 or Sgf73 (mean ± sd, N ≥ 180 cells). (B) Measurements of the width of early anaphase nuclei at the bud neck categorized by different length of the nucleus in wt and *gcn5Δ* mutant cells (mean ± sem, N ≥ 70 cells). (C) Photobleaching analysis of wt, *bud6Δ* and *gcn5Δ* cells expressing Nup49-GFP. Graph shows the Barrier Index (ratio of the time to decay to 70% of initial fluorescence in the mother compartment to the bud compartment of early anaphase nuclei, mean ± sem, N ≥ 20 cells). (A-C) ***p < 0.001. Images are max Z-projections (A) or represent one focal plane (B&C).

2.2 The SAGA complex binds non-centromeric DNA circles and promotes their accessibility

The SAGA complex preferentially interacts with non-centromeric DNA

Since SAGA deficient cells showed no major defects in pathways previously reported to ensure plasmid retention in the mother cell, we wondered whether SAGA was directly involved in plasmid retention. To this end we first asked whether SAGA interacts with non-centromeric DNA circles. We visualized the SAGA components Gcn5 and Sgf73 labeled with GFP in cells accumulating non-centromeric DNA circles labeled with TetR-mCherry. Both SAGA components were strongly enriched in the plasmid area, suggesting that SAGA interacts more readily with non-chromosomal DNA than with the rest of the genome (Fig. 2.3A).

Additionally, chromatin immunoprecipitation (ChIP) experiments performed by Catherine Stober showed an enrichment of the SAGA proteins Gcn5 and Spt20 on a non-centromeric reporter plasmid (pYB1670/CEN-), as judged by probing for the autonomous replication sequence (ARS) and two non-coding sequences of bacterial origin. Strikingly, this enrichment was reduced 2 to 2.8 fold (average 2.4 ± 1.7 fold, $p < 0.05$, N = 5 ChIP experiments) when the same plasmid contained a centromere (CEN+; Fig. 2.3B). Thus, SAGA is recruited to higher levels on non-centromeric than on centromeric DNA circles. Together, these data indicate that SAGA shows a preference of non-chromosomal over chromosomal DNA, and provides a means to distinguish these two types of molecules.

The SAGA complex increases accessibility of non-centromeric DNA

At highly induced genes the SAGA complex is recruited to sequences upstream of the promoter to induce Pol II-dependent transcription by acetylating histones, which was proposed to open the chromatin structure and to thereby facilitate gene transcription (Baker and Grant, 2007). We reasoned that if SAGA interacts preferentially with non-centromeric DNA circles they might be in a more open state compared to circles containing a centromere and thus more accessible for DNA binding molecules such as TetR. To test this, the total green fluorescence of TetR-GFP on centromeric and non-centromeric pPCM14 (see Fig. 2.1A) was measured. Remarkably, fluorescence of TetR-GFP bound to centromeric plasmids was

decreased in anaphase compared to G1 cells (1.2 ± 0.1 AU, sem, N = 96 cells in anaphase compared to 2.5 ± 0.2 AU, sem, N = 70 cells in G1, $p < 0.001$; Fig. 2.3C,D). Since DNA is more condensed in anaphase this data suggests that we are able to detect some kind of compaction using this method. However, whether the reduced tetR accessibility indeed reports increased DNA compactions requires further investigations.

Interestingly, however, fluorescence was increased on non-centromeric plasmids independently of whether the cells were in G1 or anaphase (4.4 ± 0.4 AU and 5.5 ± 0.4 AU, sem, $p < 0.001$, $N > 40$ cells, Fig. 2.3D). Thus, non-centromeric plasmids are more accessible for TetR suggesting that they are in a constitutively more open state. Whereas the fluorescence on centromeric plasmids was unaffected, deletion of *GCN5* abolished the increased TetR binding on non-centromeric plasmids (2.8 ± 0.2 AU in anaphase and 2.7 ± 0.2 AU in G1, sem, $N > 35$ cells, Fig. 2.3D). Therefore, SAGA specifically facilitates TetR binding to non-centromeric DNA molecules.

To further test whether acetylation influences plasmid compaction, we artificially attached Gcn5 to the plasmid by fusing Gcn5 to TetR. Although Gcn5-TetR might compete with TetR-GFP for binding on the plasmid the GFP signal was highly increased on both centromeric and non-centromeric plasmids in cells expressing Gcn5-TetR (11.7 ± 1.1 AU on centromeric and 16.5 ±1.3 AU on non-centromeric plasmids in G1 cells, sem, $N > 50$ cells; Fig. 2.3E). In contrast, artificial attachment of Sir2, a deacetylase, to the plasmid reduced TetR binding on both centromeric and non-centromeric plasmids (2.7 ± 0.3 AU on centromeric and 3.9 ± 0.3 AU on non-centromeric plasmids, sem, $N > 50$ cells, Fig. 2.3E). Thus, artificial recruitment of Gcn5 increases and Sir2 decreases accessibility of the plasmid suggesting that SAGA-dependent acetylation opens chromatin whereas deacetylation leads to a more compact chromatin state. Together with the data that the non-centromeric plasmid binds more TetR compared to its centromeric form and that this depends on SAGA we propose that SAGA binds preferentially to the non-centromeric plasmid and opens its chromatin structure by acetylation, which might help its retention in the mother cell.

To test whether the chromatin state could indeed influence plasmid segregation we probed for the propagation frequency of the plasmid in cells expressing Gcn5-tetR and Sir2-tetR. Indeed, attachment of Gcn5 to the plasmid increased its retention (pf = 0.9 ± 0.1) whereas tethering Sir2 to the plasmid increased its propagation into the bud (pf = 12.3 ± 0.6, sd, $p < 0.001$, $N = 3$ clones; Fig. 2.3F). This suggests that

SAGA-dependent acetylation increases plasmid retention whereas deacetylation inhibits it. Thus, plasmid retention might be mediated by opening of the chromatin structure and therefore facilitating binding to a certain receptor in the nuclear envelope. The presence of a centromere might increase DNA compaction and inhibit the binding to such a receptor leading to increased propagation to the bud. Alternatively, attachment of Gcn5 might relocate the plasmid to the NPC bound TREX-2 complex whereas Sir2 would transfer the plasmid to the telomeres, rDNA and HML/HMR, and increase its partitioning by hitchhiking the chromosomes. To distinguish these two possibilities investigating plasmid segregation in cells expressing non-acetylatable histones would be very insightful.

Finally, the retention of the non-centromeric plasmid was also increased when the cells were grown in –LEU medium instead of YPD, which induces transcription on the plasmid containing the *LEU2* gene (pf = 2.3 ± 0.2, $p < 0.05$, N = 3 clones; Fig. 2.3F), strengthening the idea that recruitment of SAGA increases plasmid retention.

Fig. 2.3

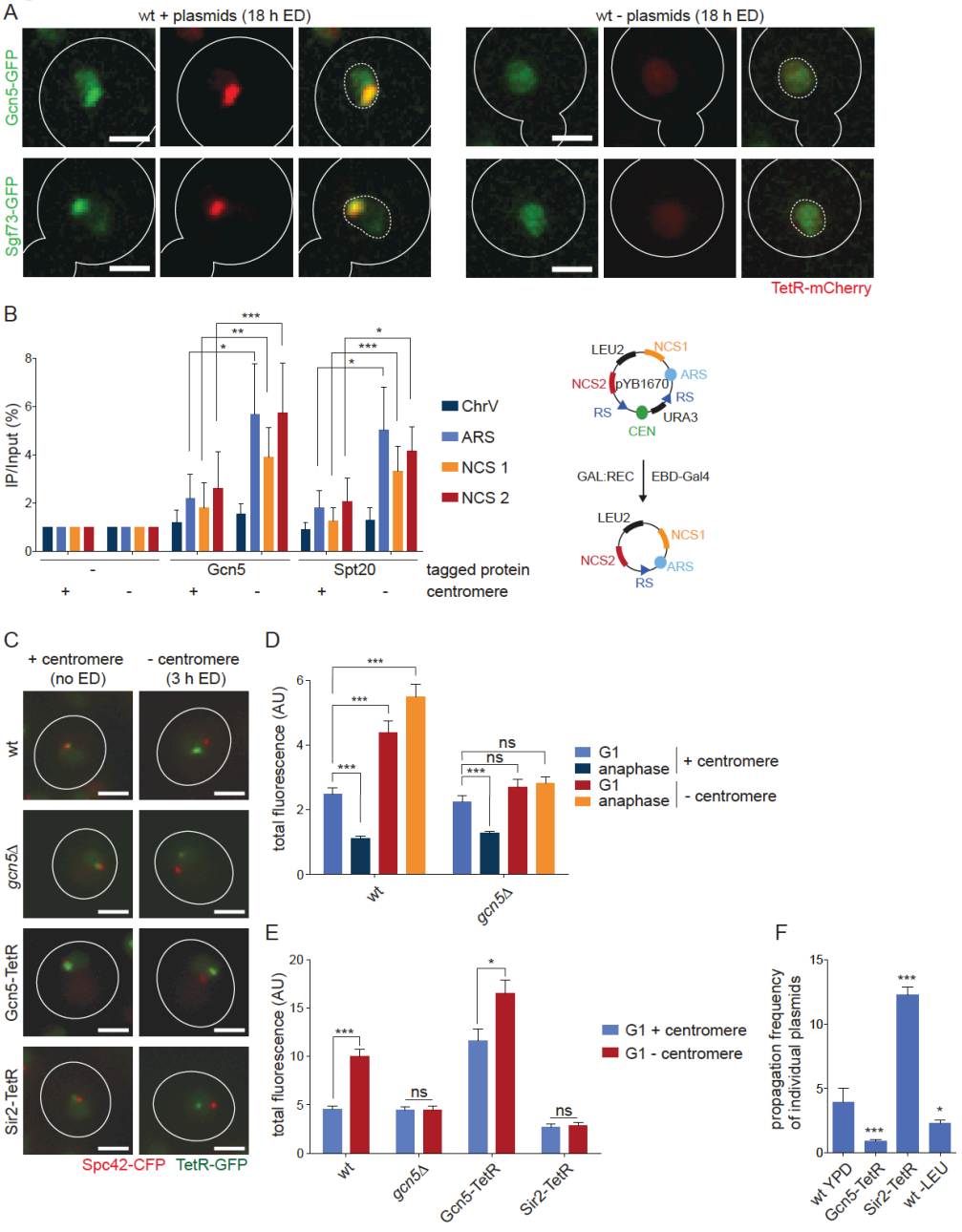

Fig. 2.3 SAGA interacts with non-centromeric DNA circles and promotes their accessibility

(A) Fluorescent images (deconvolved max Z-projections) of Gcn5-GFP and Sgf73-GFP (green) in cells with and without accumulated plasmids (red). (B) ChIP-qPCR analysis to test binding of the SAGA components Gcn5 and Spt20 to three sequences on pYB1670 (ARS, non-coding sequences (NCS) 1 and 2; see scheme of plasmid) and a control sequence on chromosome V (mean ± sd, N = 5 independent experiments). (C) Representative images of G1 cells containing a centromeric (no ED) or non-centromeric (3 h ED) plasmid pPCM14. (D) Quantifications of total TetR-GFP intensity of pPCM14 with or without the centromere in G1 or anaphase cells (mean ± sem, N ≥ 50 cells). (E) Quantifications as in (D) in wt cells, *gcn5Δ* mutant cells and wt cells expressing Gcn5 or Sir2 fused to TetR (mean ± sem, N ≥ 50 cells). (F) pf in cells expressing Gcn5 or Sir2 fused to TetR or wt cells grown in media lacking leucine (mean ± sd, N = 3 clones). (B-F) ***p < 0.001, **p < 0.01, *p < 0.05.

2.3 The SAGA complex attaches non-centromeric DNA circles to NPCs

The SAGA complex reduces mobility of DNA circles

Investigating non-centromeric plasmids in wt and *gcn5Δ* mutant cells we realized that the plasmid moved differently in SAGA deficient cells. To investigate the movement of the plasmids more carefully movies of cells containing non-centromeric plasmids were recorded taking stacks of 20 slices every 3 s for 3 min. Using Imaris three dimensional tracks of individual plasmids were generated, with which the speed of every plasmid at every time point was calculated. This revealed that the average speed of non-centromeric plasmids was significantly higher in cells lacking Gcn5 (0.09 ± 0.027 µm/s, N ≥ 50 plasmids, $p < 0.001$) than in wt cells (0.05 ± 0.019 µm/s; Fig. 2.4A). These data suggest that non-centromeric plasmids are attached to something and that this depends on SAGA function.

The SAGA complex anchors DNA circles to nuclear pores

This data together with the fact that the SAGA complex is known to interact with the TREX-2 complex and thereby with nuclear pores prompted us to test whether the SAGA complex attached DNA circles to NPCs. Thus, we asked whether individual non-centromeric plasmids co-localize with nuclear pores and whether this would require SAGA function. Consistent with this idea, the vast majority of non-centromeric circles localized to the nuclear rim in wild type cells: only 15% (± 2.8%) of them were at a resolvable distance from the nuclear envelope (Fig. 2.4B). In contrast, this fraction was substantially increased in cells lacking SAGA (*gcn5Δ* mutant cells) or both SAGA and TREX-2 function (*sus1Δ* mutant cells; 31.9% ± 1.3%, and 24.1% ± 2.6%, respectively, N = 3 clones, $p < 0.001$). To determine whether the plasmids localizing to the periphery co-localized with nuclear pores, Nup82-3sfGFP intensity traces (N > 50 cells) were measured along the nuclear envelope in equatorial focal sections of nuclei containing a single labeled, acentric DNA circle at the rim. High LED-based illumination and fast image acquisition minimized blur due to NPC movement. Aligning all traces with the position of the DNA circle showed that the average Nup82-3sfGFP intensity increased in the vicinity of the circle compared to elsewhere (+33.2% ± 0.09%, Fig. 2.4C). No such increase in nuclear pore signal was observed near DNA circles in *gcn5Δ* and *sus1Δ* mutant cells (+4.6% ± 0.05% and -

2.0% ± 0.07%, p < 0.01). Thus, we conclude that SAGA indeed mediates the recruitment of non-chromosomal DNA circles to nuclear pores (see model Fig. 2.4D).

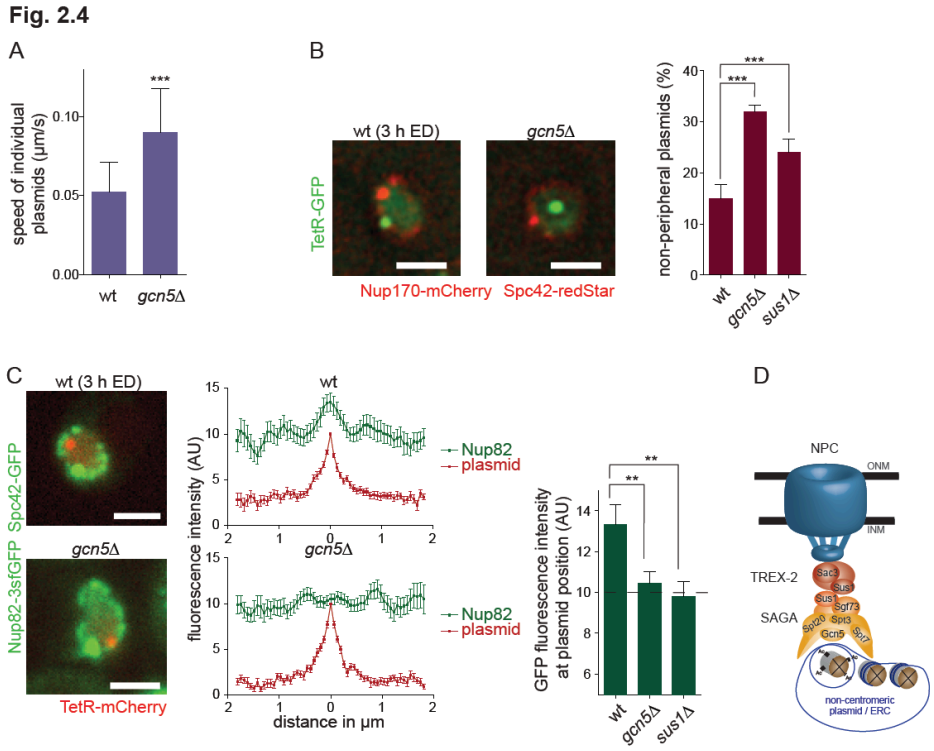

Fig. 2.4 SAGA attaches DNA circles to NPCs

(A) Speed of individual plasmids in wt and *gcn5Δ* cells expressing TetR-GFP measured from time lapse movies with 3s intervals (mean ± sd, N ≥ 50 plasmids). (B) Percentage of plasmids at a resolvable distance to the nuclear periphery in wt, *gcn5Δ* and *sus1Δ* mutant cells (mean ± sd, N = 3 clones). (C) Normalized fluorescence intensity of Nup82-3sfGFP in green (NPCs) and TetR-mCherry in red (plasmid) aligned by the peak of TetR intensity. Quantifications of average Nup82-3sfGFP intensity 130 nm around the plasmid (mean ± sem, N = 50 cells). (D) Model of how non-centromeric plasmids / ERCs might be attached to NPCs via the SAGA and TREX-2 complexes. (A-C) ***p < 0.001, **p < 0.01. Images represent one focal plane.

Artificial tethering of circles to stable NPC components bypasses the need for SAGA

Next, we wondered whether detachment from pores was the main reason for the increased circle propagation into the bud observed in SAGA-deficient cells. In order to test this, we artificially tethered circles to the core nucleoporins Nup49 and Nup170, as previously reported (Khmelinskii et al., 2011), and monitored their segregation during mitosis in wild type and SAGA deficient cells. Neither fusion protein had any effect on circle retention when replacing the corresponding endogenous nucleoporin in otherwise wild type cells (pf = 5.5 ± 0.7 in *NUP170-TetR*

and 4.6 ± 1.6 in *NUP49-TetR* cells; Fig. 2.5A), as reported. In contrast, when expressed in *gcn5Δ*, *sgf73Δ* or *sus1Δ* mutant cells, these fusion proteins fully or nearly fully restored the retention of the reporter circle in the mother cell. In support of the TetR-fusion proteins mediating circle attachment to NPCs, the labeled circles localized close to the envelope in these cells (Fig. 2.5B). Importantly, tethering of the circles to nuclear pores did not bypass the requirement for the diffusion barrier in plasmid retention in the mother cell, since *bud6Δ* mutant cells expressing Nup170 or Nup49 fused to TetR, displayed plasmid propagation frequencies similar to *bud6Δ* cells (pf = 11.9 ± 1.8 and 10.8 ± 1.2, respectively; Fig. 2.5A). Thus, non-chromosomal DNA circles artificially tethered to NPCs no longer need SAGA for being efficiently retained in the mother cell by the diffusion barrier.

A previous report using TetR-fusions concluded that artificial attachment of plasmids to NPCs increases their propagation (Khmelinskii et al., 2011). However, this study showed that fusing TetR to 11 different core nucleoporins did not affect the partition of a TetO-containing circle, but TetR fusion to the peripheral nucleoporins Mlp1 and Nup2 did. The first set of observations is expected either if the TetR fusions are not accessible to the circles, or if the circles are already tethered to NPCs by SAGA. Our data indicate that at least two of these core nucleoporins, Nup170 and Nup49 are accessible to the circles since fusing them to TetR restores the circle localization and retention defects of the SAGA mutant cells. Concerning the second set of observations, it is noteworthy that Nup2 localizes only transiently to NPCs (Dilworth et al., 2001) and is therefore not an ideal NPC anchor. Supporting this view, Nup2, Mlp1 and Nup60 show higher mobility by FRAP than the core nucleoporins Nup1, Nup49 and Nup170 (Fig. 2.5C). This, in part, may explain their effect when targeted to a circle. Actually, we found a nice correlation between the stability of different pore components and their ability to retain the plasmid when artificially attached to it (Fig. 2.5D). Thus, SAGA-dependent attachment to stable NPC components is required for DNA circles to be tightly retained in wt mother cells. And we conclude that SAGA mediates the retention of non-chromosomal DNA circles through anchoring them to NPCs.

To address whether the effect of SAGA on circle anchorage to NPCs was direct, we asked whether physical interaction between SAGA, TREX-2 and NPCs was required for circle retention. We generated fusion proteins to covalently link the SAGA complex to the TREX-2 complex (Gcn5-Sac3) or directly to NPCs (Spt7-Nup49) and tested whether this was sufficient to restore the retention of DNA circle in cells

lacking Sgf73 or Sus1, which mediate SAGA/TREX-2 interaction (Kohler et al., 2008). Expression of these fusion proteins did not significantly alter plasmid retention in otherwise wild type cells (pf = 5.2 ± 0.4 and 4.1 ± 1.0, respectively; Fig. 2.5E). However, it extensively bypassed the need for Sgf73 (pf = 6.1 ± 1.3 with Gcn5-Sac3 and 6.8 ± 2.0 with Spt7-Nup49, compared to 11.8 ± 1.6 in *sgf73Δ* cells) and Sus1 (pf = 6.5 ± 1.3 with Gcn5-Sac3 and 5.6 ± 0.2 with Spt7-Nup49 compared to 11.3 ± 1.4 in *sus1Δ* cells, N = 3 clones, $p < 0.001$). We conclude that the main function of Sgf73 and Sus1 in plasmid retention is to physically link SAGA to nuclear pores. Hence, SAGA needs to be at NPCs to function in circle retention.

Fig. 2.5

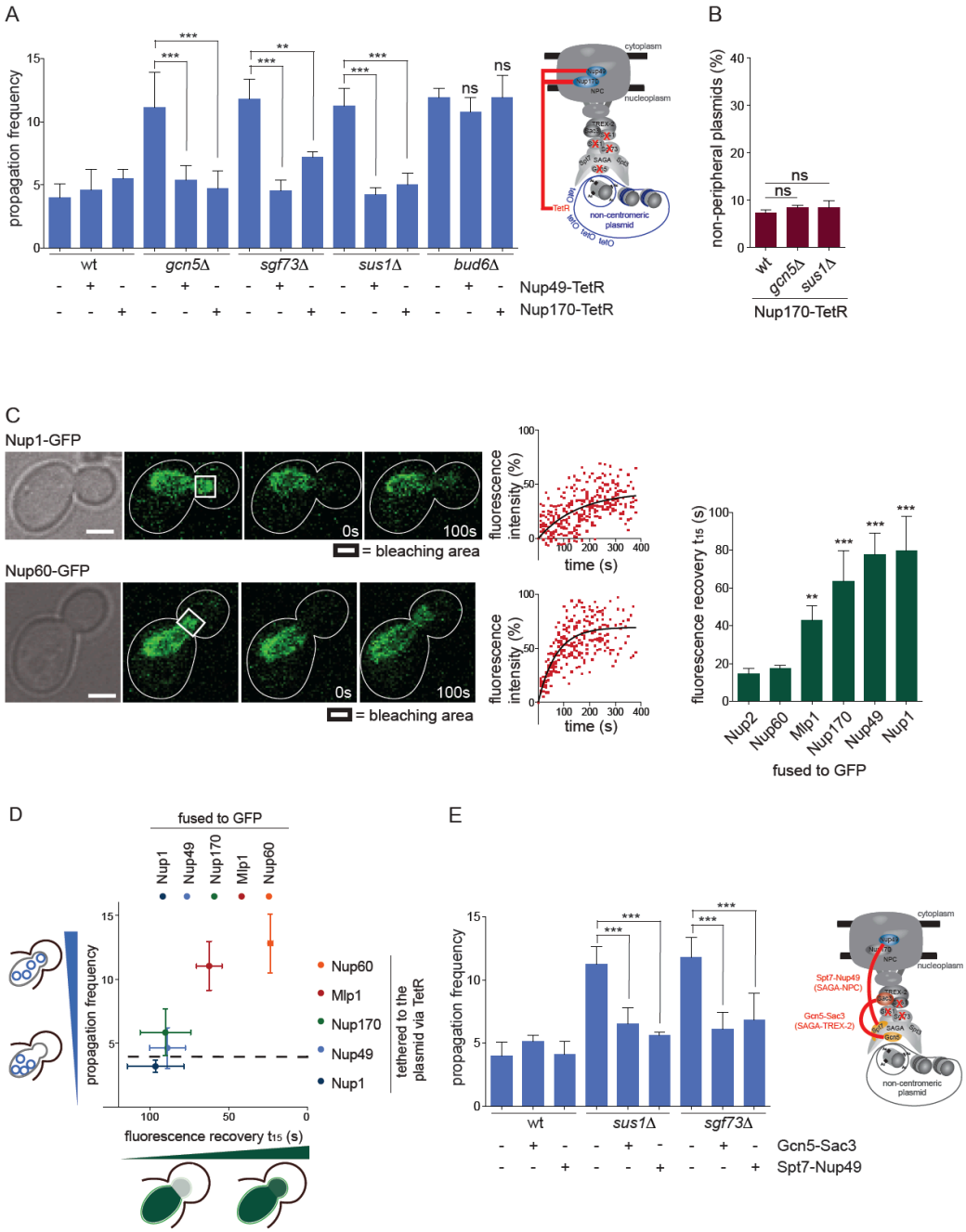

Fig. 2.5 SAGA-dependent attachment of circles to stable NPC components ensures their asymmetric segregation

(A) pf in wt and different mutant cells expressing Nup170 or Nup49 fused to TetR (mean ± sd, N ≥ 3 clones). Scheme of the fusion proteins. (B) Percentage of plasmids at a resolvable distance to the nuclear periphery in wt, *gcn5Δ* and *sus1Δ* mutant cells expressing Nup170 fused to TetR (mean ± sd, N = 3 clones) (C) Fluorescence recovery after bleaching the bud part of early anaphase nuclei measured in cells expressing several NPC components tagged with GFP. Quantification of the time to recover 15% of fluorescence intensity (t_{15}, mean ± sem, all compared with Nup2 for statistics) (D) Correlation between the fluorescence recovery in the bleached bud compartment (t_{15}) of the depicted proteins fused to GFP and the pf in cells expressing the same proteins fused to TetR. Dashed line represents pf in wt cells. (E) pf in wt and mutant cells expressing the fusion proteins Gcn5-Sac3 or Spt7-Nup49 (mean ± sd, N ≥ 3 clones). Scheme of the fusion proteins. (A-E) ***p < 0.001, **p < 0.01.

2.4 Attachment of DNA circles affects localization, mobility and mitotic segregation of nuclear pores

Accumulated DNA circles induce the formation of an adjacent cap of NPCs

To determine the localization of accumulated plasmids within the nucleus, we investigated wild type cells co-expressing TetR-mCherry with different nuclear markers fused to GFP. Nup82-3sfGFP was used to visualize the morphology of the nuclear envelope, Spc42-GFP indicated the position of the spindle pole body (SPB) and Fob1-GFP labeled the nucleolus. In most cases, the accumulated DNA circles localized adjacent to but excluded from the nucleolus (Fob1-GFP; Fig. 2.6A). Accordingly, they localized opposite to the SPB, indicating that they are excluded from the area occupied by the bulk of chromosomes. Strikingly, labeling of the NPCs indicated that accumulation of DNA circles drastically affected NPC distribution. First, the circle-loaded cells contained on average 2.7 fold more nuclear pores compared to cells without plasmids (Fig. 2.6A). This was independent of the NPC reporter used (Nup82-3sfGFP, 2.7 folds, N = 50 cells, $p < 0.001$; Nup82-GFP, 2.6 fold, N = 25 cells, $p < 0.001$; Nup49-GFP, 3.0 fold, N = 25 cells, $p < 0.001$; Fig. 2.6A). In order to accumulate plasmids these cells had to divide several times. Visualization of the bud scars with calcofluor white depicted that they had divided in average 5 times (5.2 ± 1.9 bud scars on cells with accumulated plasmids compared to 0.7 ± 0.9 bud scars in cells without plasmids**;** Fig. 2.6B). Nevertheless, the increase in number of NPCs in these cells was specific for cells containing DNA circles since 5 generations old wild type cells lacking plasmids did not show such changes (see below, Fig. 2.9).

However, more strikingly than the increase in NPCs was that the NPC distribution over the nuclear envelope was no-longer uniform. A substantial fraction of NPCs formed a cap covering one side of the nucleus (Fig. 2.6A). Remarkably, in all cells this cap was adjacent to the plasmid area, and all circle-loaded cells contained such a cap. As a consequence, the fluorescence intensity of Nup82-3sfGFP was on average two fold higher in the vicinity of the circles (Ic = 202 ± 79.8 A.U.) compared with the rest of the nucleus (Ir = 100 ± 34.5 A.U., N = 50 cells, $p < 0.001$; Fig. 2.6C). In time-lapse movies (5 min intervals for 60 minutes) the NPC cap and the accumulated plasmid patch moved together (Fig. 2.6D), suggesting that DNA circles

and NPC cap were linked to each other. Thus, the accumulated circles affected the morphology of the nucleus by forming an NPC cap adjacent to them.

Investigating the NPC localization in SAGA deficient cells containing accumulated plasmids revealed that both the formation of the NPC cap as well as the clustering of the plasmids was affected. Whereas in wt cells most of the plasmids localized to one big focus the plasmids were more scattered throughout the whole nucleus in *gcn5Δ* and *sgf73Δ* mutant cells (Fig. 2.6E). This suggests that the interaction between plasmids and pores is required to form an NPC cap, which in turn might support the clustering of the plasmids into one focus. In some SAGA deficient cells a small NPC cap seemed to appear when bigger plasmid foci were formed, however, these interactions were very transient. This might indicate that plasmids have a weak but intrinsic affinity to NPCs and that SAGA functions rather in maintaining than in establishing the NPC-plasmid interactions. However, further experiments will be required to clarify this.

Fig. 2.6

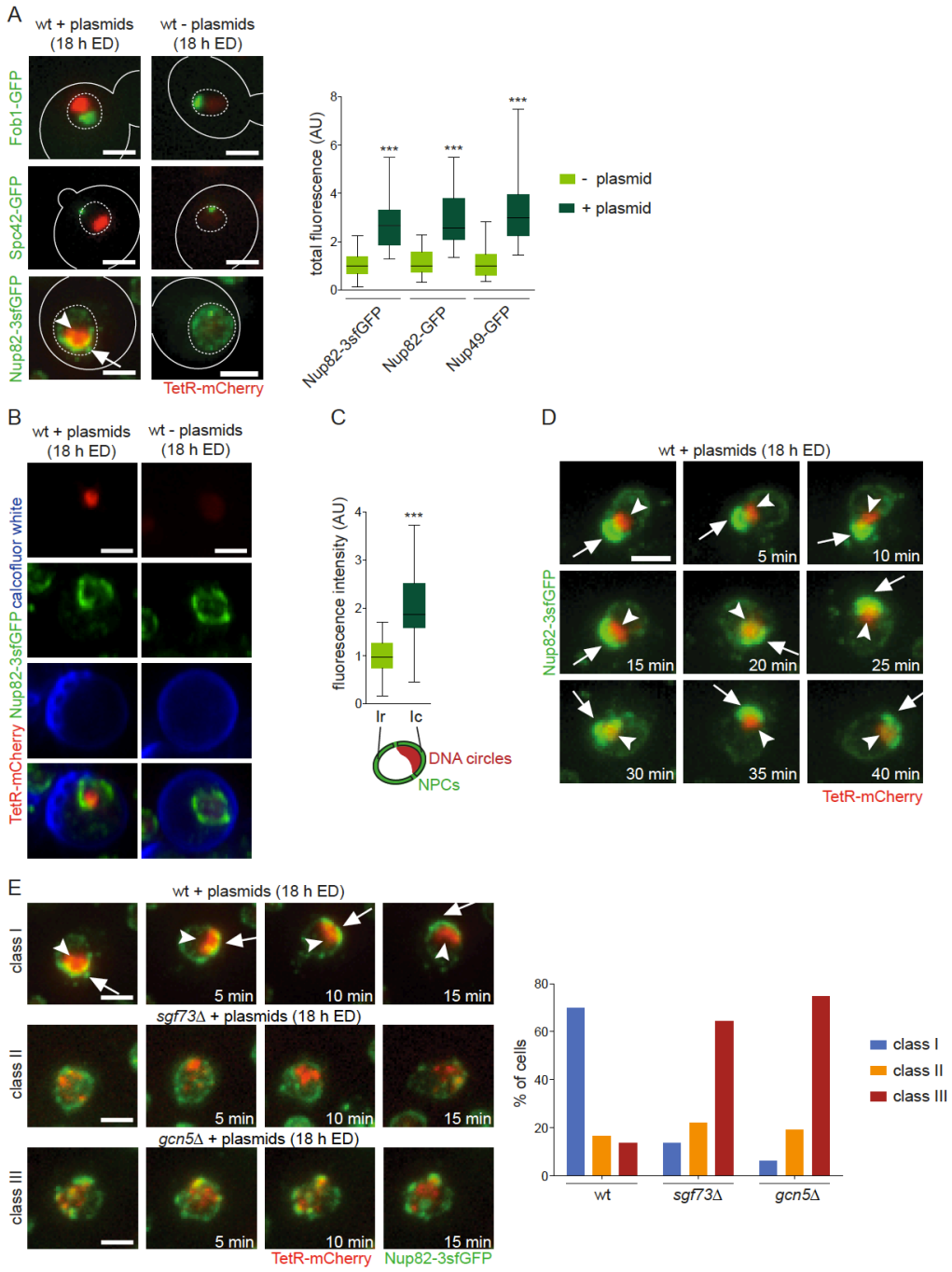

Fig. 2.6 SAGA-dependent formation of an NPC cap adjacent to accumulated DNA circles

(A) Fluorescent images of the nuclear proteins Fob1, Spc42 and Nup82 (green) in cells with or without accumulated plasmids (red, 18 h after addition of ED). Quantifications of total fluorescence of different nuclear pore markers in cells with or without accumulated plasmids normalized by the median of cells without plasmids (N > 30 cells). (B) Fluorescent images of cells containing accumulated plasmids, expressing Nup82-GFP and stained for bud scars using calcofluor white. (C) Quantifications of fluorescence intensity of Nup82 within the nucleus in the vicinity of the DNA circle (Ic) and the rest of the nucleus (Ir) normalized by the median Ir (N = 50 cells). (D) Time lapse images of a nucleus with accumulated plasmids (red) and the NPC cap (green). Images were taken every 5 min. (D) Quantification of plasmid clustering in wt and SAGA deficient cells. Cells were divided in 3 categories: plasmids localized always, partially or never to one focus throughout a 1 h time lapse movie (mean, N ≥ 160 cells). (A-E) ***p < 0.001; Images are max Z-projections; Arrow depicts the NPC cap, arrow head the accumulated circles.

NPCs attached to DNA circles are less mobile

Next we wondered whether the interaction of DNA circles and nuclear pores changed the mobility of NPCs. To test this we performed FLIP experiments in wt and *gcn5Δ* mutant cells both with and without accumulated plasmids. In wt cells fluorescence dropped slower in cells with accumulated plasmids (t_{50} = 58 ± 13.2 s) compared to cells lacking plasmids (t_{50} = 35 ± 5.9 s, N = 20 cells, $p < 0.001$; Fig. 2.7A). In contrast, in SAGA deficient cells, fluorescence decayed homogenously over the entire nuclear envelope, whether they contained circles or not (t_{50} = 46 s ± 9.1 s or 41 s ± 6.7 s; N = 20 cells, $p > 0.05$; Fig. 2.7B). This suggests that SAGA-dependent attachment of circles to pores reduces their mobility. However, we did not control for different sizes of these nuclei, which might influence the fluorescence decay if measured in the whole nucleus. Therefore, we proceeded by measuring fluorescence intensity both in the vicinity of the circles (Ic) and at opposite side of the nucleus (Io) within the same nucleus in wild type cells loaded with circles. Importantly, both measurement regions were equidistant from the bleached spot. The signal decayed slower and to a lesser extent in regions associated with the circles (t_{70} = 82 s ± 39 s) than in those on the opposite side (t_{70} = 25 s ± 8 s, N = 20 cells, $p < 0.001$; Fig. 2.7 C,D). Therefore, we concluded that accumulated DNA circles decrease the diffusion of the associated NPCs.

Fig. 2.7

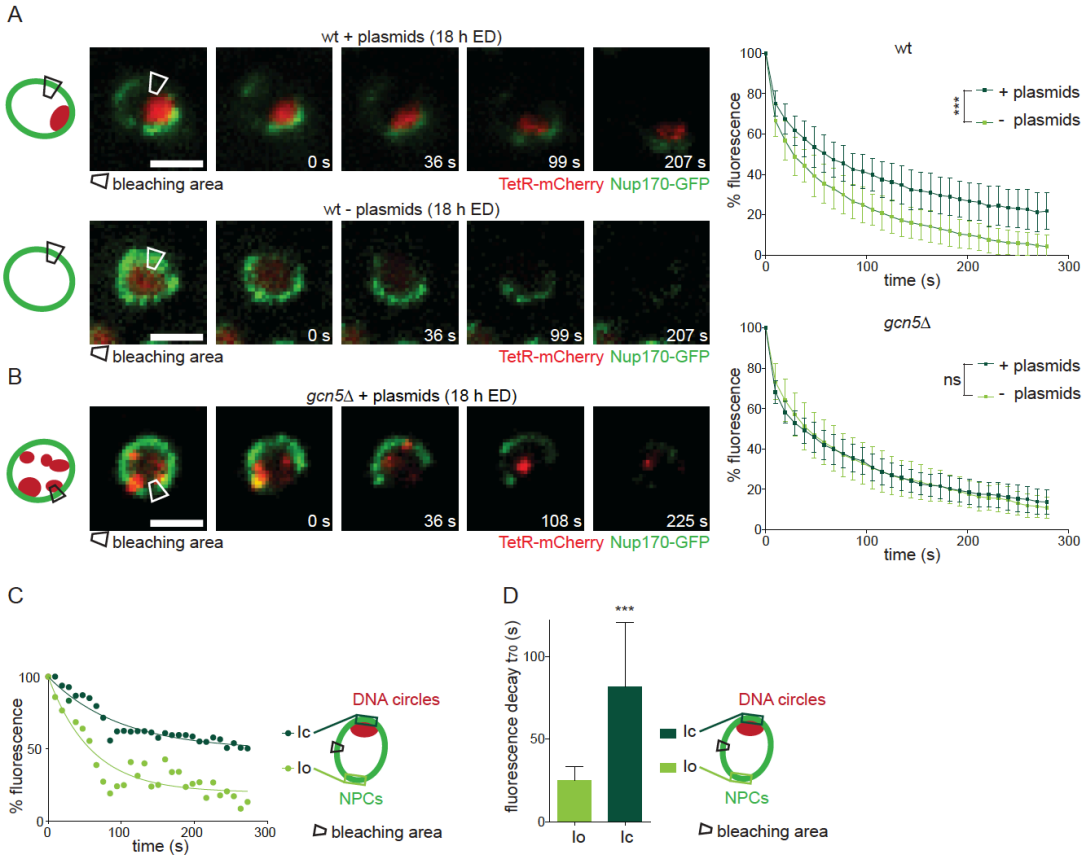

Fig. 2.7 Attachment of DNA circles reduces NPC mobility

(A) Time lapse images of a photobleaching experiment in wt cells expressing Nup170-GFP (green) and containing accumulated plasmids (red). Rectangle depicts the bleaching area. Plotted is the average total fluorescence of the whole nucleus over time in wt cells with (dark green) and without plasmids (light green), set to 100% prior to bleaching (mean ± sd, N ≥ 20 cells). (B) Bleaching experiment as in (A) in and *gcn5Δ* mutant cells (mean ± sd, N ≥ 20 cells). (C) Plotted Nup170-GFP intensity in the circle area (Ic) and an equidistant area opposite of the circles (Io) over time, set to 100% prior to bleaching. (D) Quantification of the time 30% of fluorescence decays (t_{70}; mean ± sd, N = 20 cells). (A-D) ***p < 0.001; Images represent one focal plane.

Accumulated DNA circles retain NPCs in the mother cell at mitosis in a SAGA-dependent manner

Since DNA circles reduced the dynamics of the associated NPCs we investigated how these NPCs segregate during mitosis. Strikingly, circle-loaded mother cells retained a larger fraction of their NPCs (median = 78%, N = 50), compared to cells containing no circles (63%, N = 50 cells, p < 0.001; Fig. 2.8A). In these cells both the TetR-mCherry signal and the GFP cap localized to the entry of the nuclear bridge

linking mother and bud lobes of the dividing nucleus, and only in rare cases a fraction of it passed to the bud (2%, N > 50 cells). Qualitatively, the same effect was observed whether using Nup82-3sfGFP, Nup82-GFP or Nup49-GFP as reporters. Irrespectively of plasmid accumulation, tagging Nup49 slightly enhanced NPC retention (Fig. 2.8A), as previously reported (Chadrin et al., 2010; Makio et al., 2013). The increased asymmetry of NPC segregation in cells containing accumulated plasmids resulted from both increased NPC density (64% with plasmid compared to 55% without) and increased volume difference (65% with plasmid compared to 55% without, $p < 0.001$, N = 25; Fig. 2.8B). Consistent with these phenotypes resulting from DNA circle accumulation, cells where the centromere was not excised from the plasmid and untransformed cells of similar age did not show such NPC distribution and segregation (Fig. 2.1 and 2.9). Together, these data indicate that the accumulation of non-chromosomal DNA circles affects the size of the nucleus, the organization of the nuclear envelope and promotes the mitotic retention of NPCs in yeast mother cells.

In cells lacking Bud6 the NPC cap still formed around the plasmid, however, in 11% of them part of the plasmid mass was transmitted to the daughter cell (compared to 2% in wild type cells, N = 50 cells). The propagated plasmid foci were rather small but when a bigger part was transmitted an NPC cap was visible around it (see representative images Fig. 2.8D). The percentage of NPCs retained in the mother cell in wt and barrier deficient cells revealed that NPCs tend to be better retained in the presence of the diffusion barrier, independent of the presence of plasmids. Still, the difference between wt and *bud6Δ* cells in NPC segregation towards the mother cell was more pronounced in cells with accumulated plasmids (Fig. 2.8C). Thus, retention of the circles and the NPC cap partially depends on the nuclear diffusion barrier at the bud neck.

Interestingly, the increased retention of NPCs in circle loaded cells clearly depended on SAGA: In both *gcn5Δ* and *sgf73Δ* mutant cells the presence of DNA circles had no effect on pore segregation (66% vs. 64% or 64% vs. 61%, respectively, N = 50 cells; Fig. 2.8D). This indicates that SAGA-dependent attachment of circles to pores is required for their concomitant retention in the mother cell.

Fig. 2.8

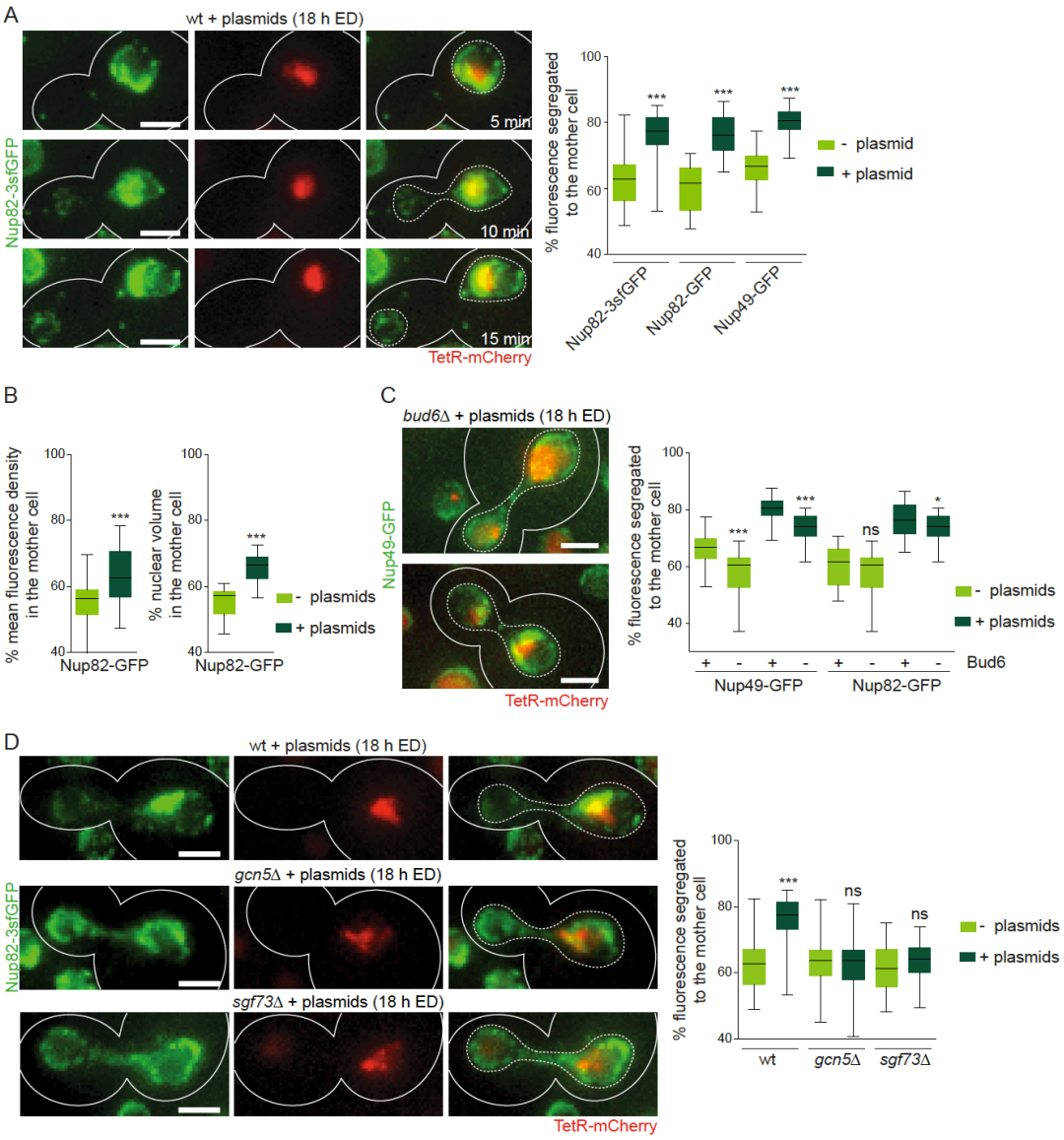

Fig. 2.8 SAGA mediates the retention of the NPC cap in the mother cell

(A) Time lapse images of a dividing nucleus in a cell expressing Nup82-3sfGFP (green) and containing accumulated plasmids (red). Percentage of the total green fluorescence segregated to the mother cell in telophase cells with and without plasmids using different nuclear pore markers (N > 25 cells). (B) Quantification of the percentage of the mean Nup82 fluorescence and the nuclear volume segregated to the mother cell. (C) Representative pictures and quantifications of NPC segregation in wt and *bud6Δ* cells using different nuclear pore markers. (D) Fluorescent images and quantifications of the percentage of NPCs segregated to the mother cell in wt, *gcn5Δ* and *sgf73Δ* cells with or without plasmids (N = 50 cells). (A-D) Box plots: min to max, median = line; Images are max Z-projections; ***p < 0.001, *p < 0.05.

2.5 Accumulation of NPCs in old cells depends on SAGA and ERCs

NPCs accumulate as the cells age

Together, our data suggest that SAGA targets non-chromosomal DNA circles and mediates their retention in the mother cell by linking them to NPCs. However, since these results were all obtained with reporter plasmids, we next asked whether SAGA function was also relevant for endogenous circles. We reasoned that, if endogenous ERCs rely on interaction with NPCs for their retention in the mother cell, then the NPCs attached to these ERCs should also be retained and accumulate with age. To test this possibility, we monitored nuclear pores labeled with Nup49-, Nup170- or Nup82-GFP fusions in cells grown in a microfluidic device that allows the observation of individual cells over multiple cell cycles (all microfluidic chips were run by Marek K. Krzyzanowski; (Lee et al., 2012)). In this chip, the mother cells are selectively retained, due to their larger size, while their daughter cells are removed by the medium flow. Transmission pictures were taken for 64 h at 20 min intervals, providing information about the age of all cells present. In addition, 2h fluorescence movies at 15 min intervals were recorded after 48 h and 64 h. At both time points, the original cells and some cells born on the chip and coincidentally trapped are present, allowing simultaneous monitoring of pores in cells of different ages (ranging from 0 to 38 generations; Fig. 2.9A). Strikingly, most aged cells showed a non-uniform distribution of NPCs on the nuclear surface, consistent with the formation of an NPC cap (Fig. 2.9B). A number of cells formed a cap even more intense than observed in circle-loaded cells. Cells containing such a cap were rather old and very close to the end of their life, since they divided maximally three more times before dying.

To investigate NPC distribution quantitatively, the total fluorescence of the Nup49-, Nup170- and Nup82-GFP reporters was measured in image stacks through the entire volume of mother and daughter nuclei of telophase cells, and plotted as a function of the age of the mother cell. For all three NPC markers, fluorescence intensity increased significantly in the mother nuclei as they aged (Fig. 2.9C). This effect was strongest for Nup49-GFP, as above (Fig. 2.8A). The increasing amount of NPCs in the mother cell did not happen at the cost of the daughter cells. On the contrary, occasionally an increased amount of nuclear pores was also observed in daughter cells of old mother cells (>15 generations; Fig. 2.9C). Thus, like in young cells loaded

Fig. 2.9

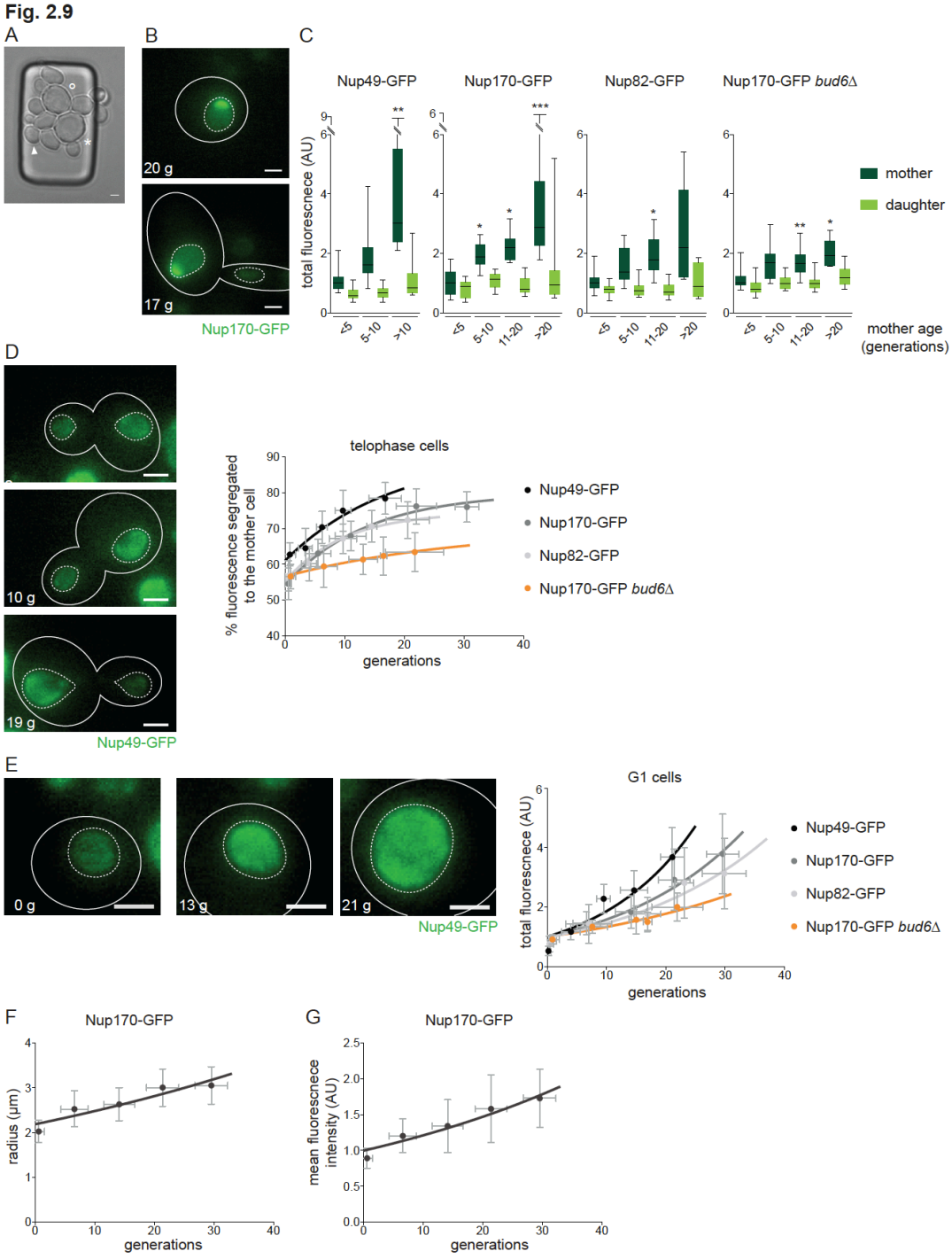

Fig. 2.9 NPCs segregate increasingly asymmetric with age leading to their accumulation in old cells in a barrier dependent manner

(A) Transmission image of cells trapped in the microfluidic device after 64 h. Cells of different age are trapped (➤,° and * depicts 0, 27 and 31 generations old cells, respectively). (B) Cells expressing Nup170-GFP showing a pronounced NPC cap. (C) Total fluorescence of the depicted NPC marker in the mother (dark green) and daughter cell (light green) grouped by age categories of the mother cells (N ≥ 50 cells, ***p < 0.001, **p < 0.01, *p < 0.05). (D) Percentage of NPC fluorescence segregated to the mother cell plotted against their age in wt cells expressing different NPC markers and *bud6Δ* cells. Line show fitted curves; dots represent the average of 10 data points grouped by age (mean ± sd, N ≥ 50 cells). (E-G) Quantifications of total fluorescence (E), nuclear radii (F) and mean fluorescence intensity (G) in G1 cells of increasing age (mean ± sd, N ≥ 50 cells) quantified as in (D). (A-E) numbers in white depict the age of the corresponding cell (g = generations). Images are sum Z-projections.

with artificial circles the number of NPCs increases in aging mother cells whereas the number of pores transmitted to the daughter cells remains fairly constant.
Also recapitulating our observations with artificial circles, the fraction of nuclear pores that segregate towards the mother cell during mitosis increased as the cells age, indicating that these cells partitioned NPCs in an increasingly asymmetric manner (Fig. 2.9D). Young mother cells expressing Nup170-GFP or Nup82-GFP retained 56% ± 1.9% and 57% ± 2.5% of the signal in the mother cell. The retention of pores in the mother cell increased after 25 generation to 73% ± 5.0% (Nup82-GFP) and 78% ± 3.8% after 35 generations (Nup170-GFP; Fig. 2.9D). Cells expressing Nup49-GFP showed the same trend, although asymmetry was higher in both young (63% ± 3.3%), and older cells (81% ± 16.1% after 20 generations; Fig. 2.9D). Analysis of nuclei in G1 cells of increasing age confirmed that old mothers contained more NPCs than young cells (on average 4.7 ± 1.2 fold more in cells expressing Nup49-GFP after 25 generations, 4.0 ± 1.1 fold in Nup170-GFP expressing cells after 30 generations and 4.1 ± 1.4 fold in Nup82-GFP expressing cells after 35 generations; Fig. 2.9E). These nuclei were both larger (radius = 1.5 fold larger; Fig. 2.9F) and more densely populated with pores (1.9 fold increase in density; Fig. 2.9G) compared to nuclei in young cells. Remarkably, the increase in NPC asymmetry, NPC retention, and NPC number with age was much slower in the *bud6Δ* mutant cells (Fig 2.9C-E). Thus, consistent with the possibility of ERC accumulation affecting NPC segregation, aging mother cells retain an increased number of NPCs as they age, in a diffusion barrier-dependent manner.

ERC accumulation and SAGA promote the age-dependent accumulation of NPCs

In order to test whether NPC accumulation in old cells indeed depended on ERCs, we next characterized the NPC content of aging *sir2Δ* mutant cells, which form more ERCs, and *fob1Δ* mutant cells, which form less of them (Defossez et al., 1999; Kaeberlein et al., 1999). Remarkably, the proportion of NPCs retained in the mother cell at mitosis and the total amount of pores in G1 cells increased much slower with age in *fob1Δ* mutant cells compared to wild type, irrespective of the reporter used (Nup49-GFP or Nup170-GFP), and faster in the *sir2Δ* mutant mother cells (Fig. 2.10A-C). Thus, the presence of ERCs largely drives NPC retention in aging cells.
Consistent with pore accumulation relying on ERC attachment to NPCs, the *sgf73Δ* mutant cells accumulated NPCs only slowly as they aged (Fig. 2.10A-C).

Furthermore, artificially linking SAGA to NPCs using the Gcn5-Sac3 and Spt7-Nup49 fusion proteins restored NPC accumulation in aging *sgf73Δ* mutant cells (Fig. 2.10D). Based on these and our findings above, we conclude that SAGA links ERCs to NPCs, leading to the joined retention and accumulation of both ERCs and NPCs in aging yeast mother cells.

Fig. 2.10

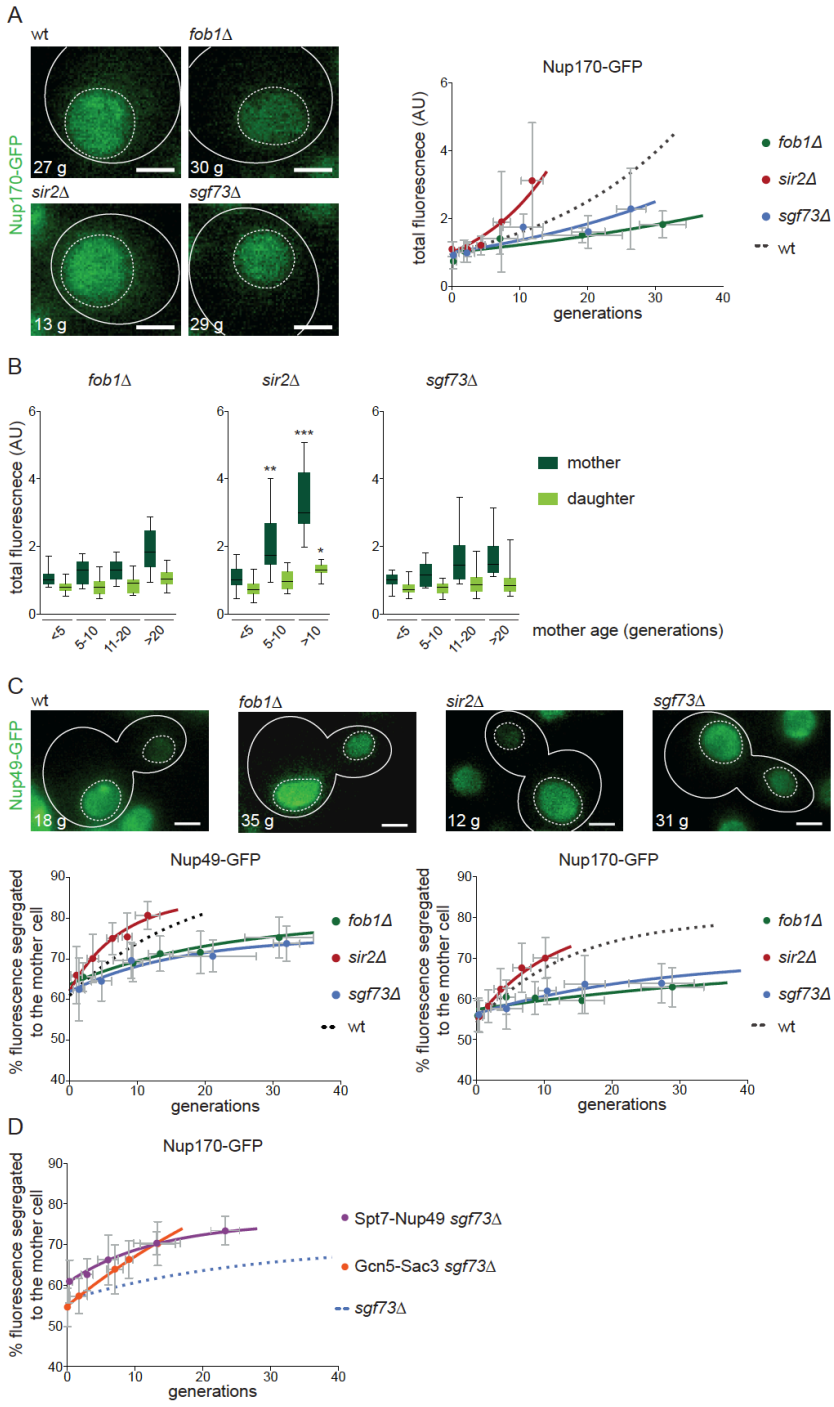

Fig. 2.10 The accumulation of NPCs in old mother cells depends on ERCs and SAGA

(A) Total Nup170-GFP intensity in G1 cells plotted against their age in wt and depicted mutant cells. (B) Total fluorescence of Nup170-GFP in mother (dark green) and daughter cells (light green) grouped by age categories of the mother cells (N ≥ 50 cells, ***p < 0.001, **p < 0.01, *p < 0.05). (C) Percentage of fluorescence segregated to the mother cell in wt and depicted mutant cells expressing Nup170-GFP or Nup49-GFP. (D) Percentage of total Nup170-GFP fluorescence segregated to the mother cell in cells lacking Sgf73 and expressing either Spt7-Nup49 or Gcn5-Sac3. (A,C,D) Lines show fitted curves; dashed lines for comparison; dots represent the average of 10 data points grouped by age (mean ± sd, N ≥ 50 cells). Images are sum Z-projections.

2.6 The SAGA complex promotes aging in yeast

The retention of DNA circles contributes to replicative aging in yeast and SAGA deficient cells accumulated less ERCs and NPCs. Therefore, we next wondered whether these cells lived longer. The lifespan of cells lacking Gcn5, Sgf73, Sus1, Spt20 and Sac3 was determined by pedigree analysis, using microdissection. Wild type cells showed a median lifespan of 27 generations, whereas the different SAGA and TREX-2 mutants showed various aging phenotypes. Cells lacking Sac3, the core component of the TREX-2 complex, were extremely short lived (9 generations; Fig. 2.11A). Due to the global role of the TREX-2 complex in mRNA export this was rather expected. Cells lacking Spt20, a structural component of SAGA were also short lived (17 generations; Fig. 2.11A) Cells lacking Gcn5 lived similar to wt cells (27 generations) which either suggests that Gcn5 has no impact on aging or that beneficial effects are masked by other toxic consequences of deleting *GCN5*. Cells depleted of Sus1 and Sgf73 were both long lived, however, to different extends (29 and 44 generations, N = 150 cells, $p < 0.001$; Fig. 2.11A; (Schleit et al., 2013)). Notably, *sus1Δ* and *sgf73Δ* mutant cells showed very similar, flat aging curves compared to the typical sigmoidal wt curves. The observation that the aging curve of *sus1Δ* cells is shifted to the left might result from Sus1 i.a. being part of the TREX-2 complex whereas Sgf73 is not. Additionally, cells lacking Sgf73 are extremely long lived, even compared to *fob1Δ* cells, which were so far the prime example for prolonged life span (32 generations; Fig. 2.11A).

Next, we wondered whether the observed lifespan of *spt20Δ* and *gcn5Δ* mutant cells was the result of a balance between the advantages and disadvantages of losing SAGA functionality. We rationalized that if this was the case, the longevity of *spt20Δ* and *gcn5Δ* mutant cells would be limited by other factors than ERC accumulation, and thus preventing ERC formation should not increase the longevity of these cells. Accordingly, removal of Fob1 failed to extend the lifespan of cells lacking Spt20 (16 generations, N = 50 cells; Fig. 2.11B). Similarly, deleting *FOB1* did not extend the lifespan of *gcn5Δ* mutant cells (median lifespan of *gcn5Δ fob1Δ* double mutant cells = 27 generations, N = 150 cells; Fig. 2.11C). Thus, cells lacking Spt20 or Gcn5 age through mechanisms independent of ERC accumulation.

To test whether lacking Gcn5 is advantageous if ERC accumulation kills the cells early in their lifetime, aging experiments were performed in wt and *gcn5Δ* cells starting with a non-centromeric plasmid. Indeed, wt cells were very short lived (10

generations) whereas lacking Gcn5 extended the lifespan (14 generations, N = 50 cells, $p < 0.05$; Fig. 2.11D). However, this experiment was performed using the plasmid visualization strains and would need to be repeated with the uninduced wt control strain in parallel or, alternatively, in the background used here for aging experiments transformed with pDS316, the ERC plasmid (Sinclair and Guarente, 1997).

Next, we tested whether cells lacking Sgf73 still died from ERC accumulation. Performing pedigree analysis on *sgf73Δ fob1Δ* double mutant cells revealed, that decreasing ERC formation by deleting *FOB1* does not further prolong the lifespan of cells lacking Sgf73. Actually, the double mutated strain was shorter lived compared to *sgf73Δ* alone (27 generations, N = 50 cells, $p < 0.01$; Fig. 2.11E). This experiment was performed only once and would need to be repeated. Nevertheless, it suggests that deleting *FOB1* interferes with some cellular functions, probably due to the lack of the replication fork barriers built by Fob1, which in turn reduces the longevity of cells lacking Fob1.

Sgf73 contains a low complexity domain composed of mainly glutamines (Alberti et al., 2009). Deleting this domain had no influence on plasmid segregaion (*sgf73 aa 454-657Δ;* Fig. 2.1B). This allowed us to test whether this domain of Sgf73 has an ERC segregation-independent function in aging. Cells lacking the low complexity domain of Sgf73 showed a similar aging curve as wt cells, however, the curve dropped more steeply leading to a slightly shortened lifespan (25 generations, N = 50 cells, $p < 0.01$; Fig. 2.11F). A similar effect was observed in *fob1Δ sgf73 aa 454-657Δ* double mutant cells. Therefore, the low complexity domain of Sgf73 is not required early in life but prolongs the lifespan of old cells. This might suggest that in wt cells Sgf73 aggregates in old cells, impairing its function in ERC retention and thereby slow down ERC accumulation in old cells. Such a model would predict that Sgf73 aggregates in a low complexity domain-dependent manner, which would be nice to test.

Adding an additional layer of complexity, these results were different when performed in a different background than to one from EUROSCARF. Performing pedigree analysis using wt 384, a lab specific background, revealed a very similar aging curve (28 generations; Fig. 2.11G). Deleting *SGF73* still clearly prolonged life span (35 generations), however, to a lesser extend. Deleting only the low complexity domain of Sgf73 increased the lifespan compared to wt cells (32 generations, N = 100 cells,

Fig. 2.11

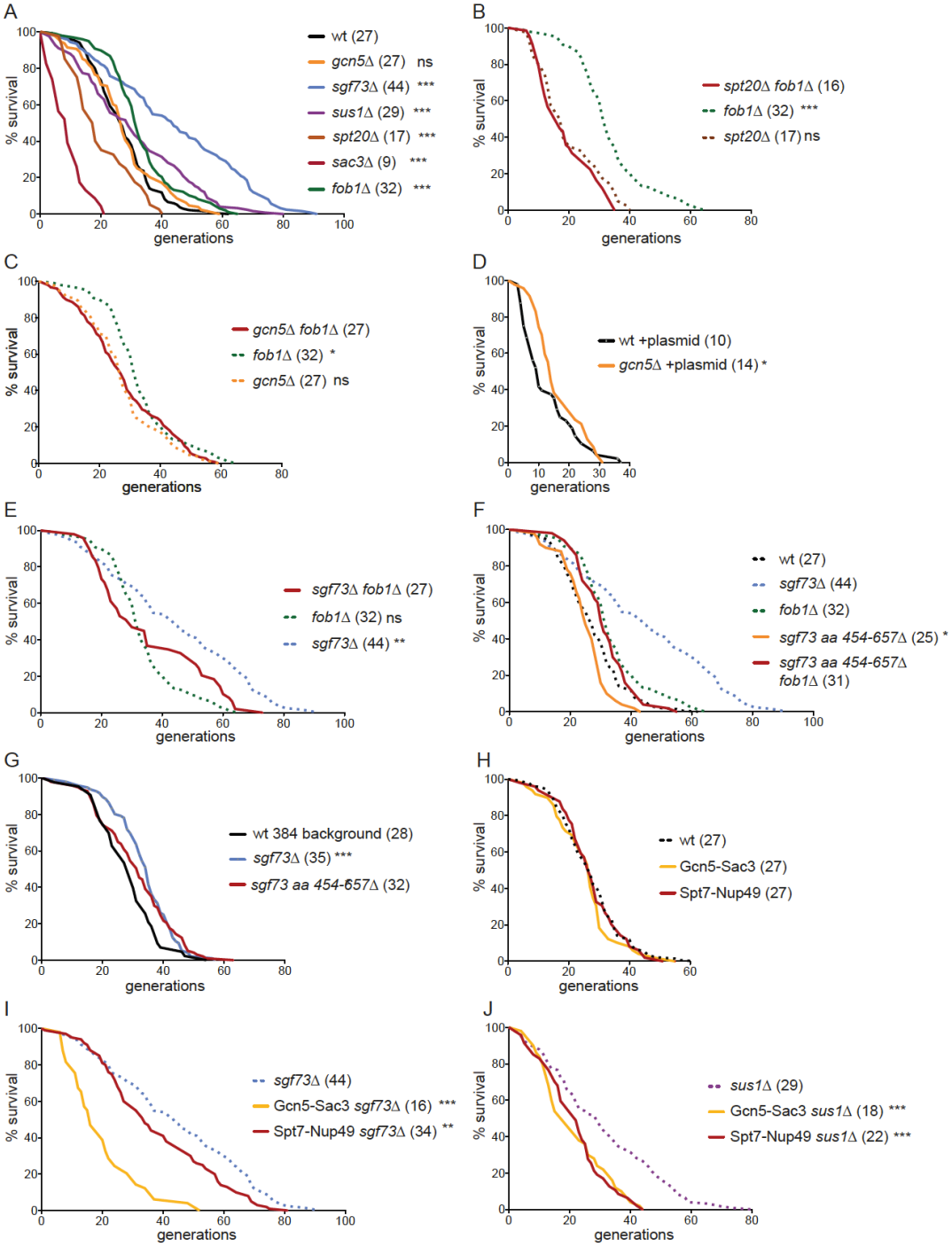

Fig. 2.11 The SAGA complex promotes aging

(A) Replicative lifespan (RLS) of wt, *gcn5Δ, sgf73Δ, sus1Δ, spt20Δ, sac3Δ* and *fob1Δ* mutant cells. (B,C,E) RLS of *spt20Δ fob1Δ, gcn5Δ fob1Δ* and *sgf73Δ fob1Δ* double mutant cells. (D) RLS of wt and *gcn5Δ* cells containing non-centromeric plasmids. (F) RLS of cells expressing Sgf73 lacking the prion like domain. (G) RLS as in (F) but in a lab specific background. (G) RLS of wt cells expressing Gcn5-Sac3 and Spt7-Nup49. (E) RLS of cells lacking Sgf73 and expressing Gcn5-Sac3 or Spt7-Nup49. (A-D) Median lifespan is depicted in brackets; dashed lines represent RLS of depicted wt and mutant cells of (A) for comparison; N = 50-150 cells; ***$p < 0.001$, **$p < 0.01$, *$p < 0.05$.

$p < 0.05$; Fig. 2.11G). This would be seminal in the identification of a prion domain contributing to yeast aging. However, first the differences between the two backgrounds need to be unveiled in order to understand the contribution of this domain to the aging process.

Finally, to test whether Sgf73 promotes aging via the retention of ERCs and NPCs in the aging cell, we asked whether targeting SAGA back to NPCs restored aging in the *sgf73Δ* mutant cells in the EUROSCARF background. Expression of the fusion proteins Gcn5-Sac3 and Spt7-Nup49 did not alter the longevity of the wild type cells (27 generations, N = 50 cells; Fig. 2.11H). However, it substantially shortened the lifespan of both *sgf73Δ* mutant cells (16 and 34 generations) and *sus1Δ* mutant cells (18 and 22 generations, respectively, $N \geq 50$ cells, $p < 0.01$; Fig. 2.11I and J). Therefore, we conclude that decreased levels of SAGA at pores largely accounts for the extended lifespan observed in *sgf73Δ* cells. Based on these data, we further conclude that SAGA promotes aging at least in part through attaching non-chromosomal DNA circles to NPCs and promoting their joint retention and accumulation with age. Furthermore, the presence of non-chromosomal DNA circles alone does not contribute to aging if these are not associated with NPCs.

2.7 DNA circles cluster and are excluded from the nucleus in HeLa cells

Finding the mechanisms in yeast contributing to the retention of non-centromeric DNA molecules in the mother cell and thereby preventing their propagation within the population we were curious to know how mammalian cells react to DNA circles. In mammalian cells the existence of a wide range of extrachromosomal DNA molecules was reported. This includes I) small microDNAs, circular DNA pieces excised from various regions within the genome (Shibata et al., 2012), II) extrachromosomal DNA circles derived from repetitive sequences, such as rDNA, telomeres and satellite DNA (Cohen et al., 2010; Tomaska et al., 2004), III) double minutes (DMs), circular DNA molecules mainly found in metastasized tumor cells and containing several copies of oncogenes such as c-myc (Benner et al., 1991) and IV) chromosomal fragments, often resulting from broken anaphase bridges of dicentric chromosomes (Hoffelder et al., 2004; Itoh and Shimizu, 1998). Among those, DMs are the best characterized, probably due to their high abundance in cancer cells.

DMs are mainly found at the nuclear periphery in G1 cells (Itoh and Shimizu, 1998). However, one fraction relocates to the nuclear center in S-phase and hitchhikes on chromosomes during mitosis through an unknown mechanism. Another fraction is excluded from the nucleus into a micronucleus (Shimizu, 2011). Interestingly, after damaging DNA by low concentrations of hydroxy urea, chromosomal DNA was rapidly repaired but DMs not (Shimizu et al., 2007). Following the damaged DMs revealed that they clustered within the nucleus and were excluded from the nucleus. DMs in micronuclei are proposed to be transcriptionally active (Utani et al., 2007), however, it is not known for how long they persist within the cell. Since cancer cells depend on the DMs encoding oncogenes, DMs might be a very special form of extrachromosomal DNAs.

Chromosomal fragments as well as lagging chromosomes also form micronuclei. Whereas micronuclei containing a whole chromosome contain NPCs and allow transcription, micronuclei containing chromosomal fragments show normal lamina but no or only few NPCs, no import of a reporter protein and no Pol II staining (Hoffelder et al., 2004; Terradas et al., 2010). This suggests that the presence of the centromere strongly influences the characteristics of the micronucleus. After micronuclei formation there are four possible fates for the incorporated DNA: I) the DNA is reincorporated into the primary nucleus, possibly during the following mitosis, II) the micronucleus is expelled from the cell, III) the micronucleus is degraded or IV)

the micronucleus is maintained within the cell and diluted from the population by asymmetric segregation to only one cell. Evidence exists for the expulsion of micronuclei containing DMs, since DMs entrapped in lamina and an additional layer of plasma membrane were found in extracellular fluid (Shimizu et al., 2000). Additionally, 60% of the micronuclei containing lagging chromosomes are disrupted by a collapse of the nuclear envelope followed by invasion by the ER (Hatch et al., 2013). Nevertheless, the two other options cannot be discarded and it is likely that the fate of the micronucleus depends on the enclosed DNA.

Even though it is well known that transfected plasmid DNA is rapidly lost from the population, very little is known about their fate within the cell. One study reported that microinjected plasmids associate with SAF-A, a marker protein for the nuclear scaffold (Mearini et al., 2004), another study showed that injected plasmids diffuse rapidly within the nucleus, aggregate into one or few foci and are subsequently expelled from the nucleus (Shimizu et al., 2005). It remains unknown how the plasmids aggregate, when and how they are excluded from the nucleus, to which compartment they localize in the cytoplasm and what their final destination is.

Thus, we aimed to investigate the fate of non-centromeric DNA circles in HeLa cells. A plasmid expressing LacI lacking its tetramerization sequence, containing the SV40 NLS sequence and fused to GFP or mCherry was constructed ((Kumaran and Spector, 2008); Model Fig. 2.12A). HeLa cells transfected with the LacI-GFP encoding plasmid showed a uniform green nuclear signal (Fig. 2.12A). When cells were co-transfected with the LacI plasmid and a plasmid containing 128-256 LacO repeats (Rohner et al., 2008) the uniform green background in the nucleus was still visible but additional brighter foci were observed. 12 h after transfection most cells containing green foci showed many of them dispersed throughout the whole nucleus, whereas 24 h after transfection most cells showed only one or few big and bright focus excluded from and adjacent to the nucleus (Fig. 2.12A). Since in cells transfected solely with the LacI encoding plasmid never such bright foci were observed, we propose that we monitor the LacO plasmids. Furthermore, the transfected plasmids showed a similar localization as the previously described microinjected plasmids, suggesting a general behavior of plasmid DNA independent of how they were introduced into the nucleus (lipid-based transfection vs. microinjection).

To investigate how the plasmids were excluded from the nucleus, cells expressing LacI-mCherry were monitored over night starting 12 h after transfection. Most cells

Fig. 2.12

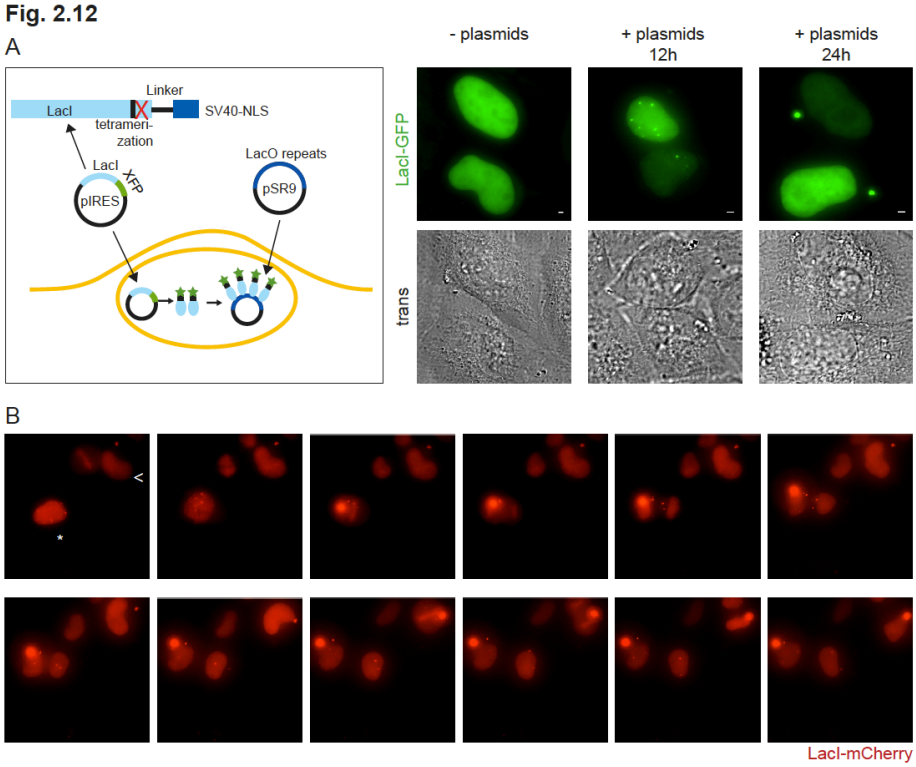

Fig. 2.12 Non-centromeric DNA is excluded from the nucleus in HeLa cells

(A) Scheme and representative images of co-transfected HeLa cells with a plasmid encoding for LacI-GFP and a plasmid containing LacO repeats. Images show cells transfected with only LacI plasmids or with both plasmids 12 h and 24 h after transfection. (B) Florescent images of a representative time lapse movie of cells transfected with LacI and LacO plasmids 12 h after transfection. * depicts a cell that contained fluorescent foci within the nucleus before mitosis and excluded from the nucleus after mitosis; < depicts a cell containing a extranuclear focus before and after mitosis.

containing small plasmid foci in the nucleus showed one or a few big foci in metaphase, which were later excluded from the nucleus (* marked cell in Fig. 2.12B). In cells already containing one big focus excluded from the nucleus this focus persisted throughout division and was present only in one cell after nuclear division (< depicted cells in Fig. 2.12B). Interestingly, also the foci that were excluded from the nucleus when we started monitoring the cells showed an increase in intensity in metaphase, suggesting that more LacI could bind to the plasmid after nuclear envelope breakdown. Together, these data suggest that plasmids are first in the nucleus, cluster into one or few big foci in metaphase and are excluded from the nucleus after the first nuclear division. However, we can not exclude that a small dot was outside the nucleus, became more intense in metaphase and the remaining plasmids in the nucleus were degraded. To investigate whether all plasmids were inside the nucleus time lapse movies would need to be recorded using cells

expressing a nuclear envelope marker. Nevertheless, we propose that episomes cluster in the nucleus, are excluded from the nucleus after mitosis and once excluded, they stay in a clustered form for several divisions.

To investigate the compartment the plasmids localized to after exclusion of the nucleus, we visualized different nuclear markers in cells containing extranuclear plasmids. First, antibodies against Lamina-associated polypeptide 2 isoform beta (Lap2-β), a protein integrated in the inner nuclear membrane and interacting with lamins, was used (Fig. 2.13A). A defined ring was observed around the plasmids, suggesting that the plasmids are enwrapped in a micronucleus containing Lap2-β.

To test if these micronuclei contained NPCs a stable cell line expressing Nup58-GFP (provided by the Kutay lab) was used. Additionally NPCs were stained with an antibody against FG repeats, phenylalanine and glycine rich parts of the core NPC proteins forming a disordered structure in the central channel of the pores. Both ways to visualize NPCs showed a clear enrichment in the nuclear envelope surrounding the primary nucleus but no enrichment was observed around the micronucleus containing plasmids (Fig. 2.13B). To exclude side effects caused by fixation, live imaging of cells expressing Nup58-GFP and containing plasmids was performed, however, no clear enrichment of Nup58 was observed (Fig. 2.13C). Although we cannot fully exclude the presence of NPCs, these data strongly suggest that there are no or only few NPCs present in micronuclei containing plasmids, as it was previously proposed for acentric chromosomal fragments (Hoffelder et al., 2004).

To functionally test for the presence of NPCs the import of Ibb, the importin beta binding domain, fused to mCherry was monitored using a stable cell line provided by the Gerlich lab. Although Ibb was efficiently imported into the primary nucleus after nuclear envelope reassembly, no Ibb was detected in the micronuclei containing plasmids (Fig. 2.13D). In some cells an additional micronucleus devoid of plasmids was observed, presumably containing a whole chromosomes, since most micronuclei formed in untreated HeLa cells arise from lagging chromosomes (Rao et al., 2008). Interestingly, while Ibb was imported into this micronucleus (depicted with *), it was not into the micronucleus containing plasmids (depicted with <; Fig. 2.13D second row). These data strongly suggest that the micronucleus surrounding plasmid circles is lacking functional NPCs.

Fig. 2.13

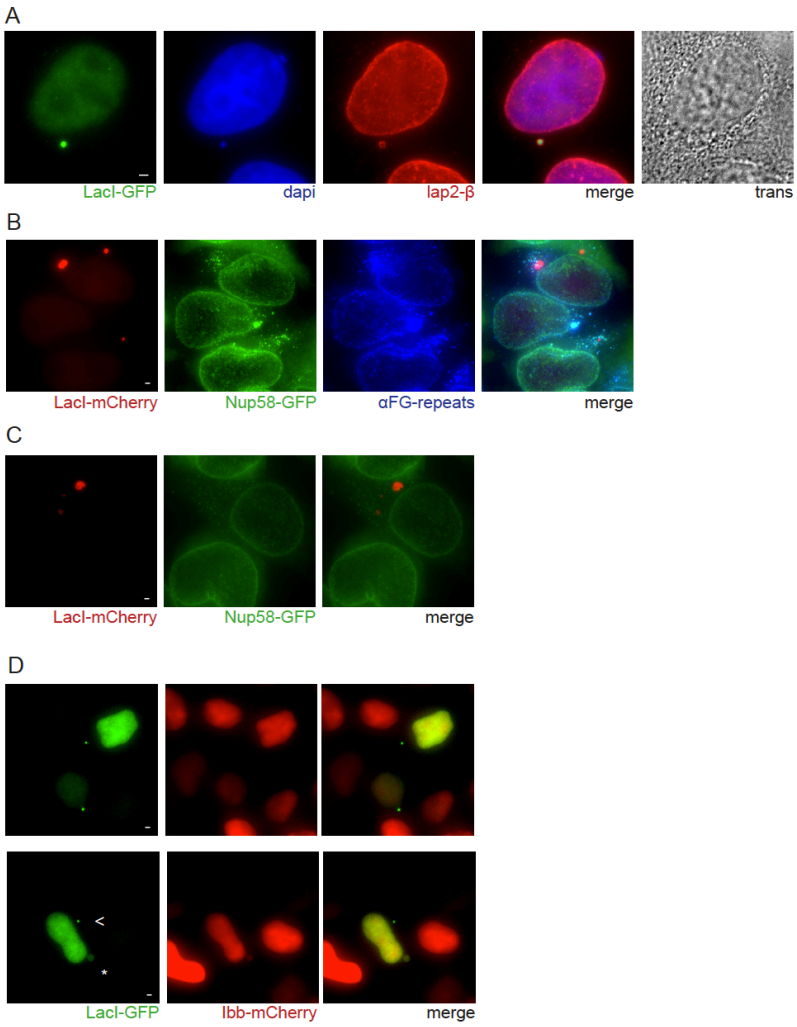

Fig. 2.13 Acentric DNA circles localize to a micronucleus probably containing lamina but no NPCs

(A) Representative image of HeLa cells containing a LacI/LacO focus stained with DAPI and antibodies recognizing Lap2-β. (B) Images of cells stably expressing Nup58-GFP containing LacI/LacO foci and stained with antibodies raised against FG-repeats. (C) Representative images of cells containing LacI/LacO foci expressing Nup58-GFP using life cell imaging. (D) Images of cells expressing Ibb-mCherry and containing LacI/LacO foci. * depicts a micronucleus containing Ibb but no LacO plasmids, < depicts the micronucleus containing the LacO plasmids but no Ibb.

3. Discussion

3.1 The SAGA complex ensures retention of non-centromeric DNA molecules in yeast mother cells

We discovered that the yeast SAGA complex is required for the retention of non-centromeric DNAs, including whole acentric chromosomes, ERCs and different non-centromeric plasmids. We observed that in SAGA deficient cells plasmids detach from NPCs, move freely in the nucleoplasm and thereby enter more frequently into the bud compartment. Accordingly, cells lacking the SAGA complex accumulate less ERCs, which prolongs their lifespan. These data strongly suggest that SAGA anchors non-centromeric DNAs to nuclear pores to ensure their retention in the mother cell and thus assigns a new function to SAGA.

SAGA was previously described to be involved in transcriptional activation of several stress-activated and highly induced genes (Timmers and Tora, 2005). Thus, the observed increase in plasmid propagation in SAGA deficient cells might be indirect, resulting from decreased gene expression of genes required for plasmid retention, such as e.g. those involved in establishing the nuclear diffusion barrier. To test this, SAGA deficient cells were tested for barrier strength, nuclear geometry and anaphase duration, mechanisms that were previously reported to be required for DNA circle retention. None of these parameters was affected. An even stronger argument for SAGA being directly involved in the attachment of circles to pores arose from experiments using different fusion proteins: artificial attachment of the circles to NPCs bypassed the need for SAGA. Thus, detachment from pores is the main cause for the increased segregation of circles into the bud in SAGA deficient cells. Additionally, the fusion of SAGA to TREX-2 and SAGA to NPCs showed that SAGA has to interact with NPCs to fulfill this function. Therefore, we conclude that the SAGA complex directly mediates attachment of circles to pores. Whether SAGA fulfills this function by modifying proteins associated with the DNA and/or the nuclear pores to allow them to interact or whether SAGA acts as a physical linker remains unknown. Observing the SAGA complex co-localizing with the accumulated plasmids suggests that SAGA not only mediates the circle-NPC interaction but also remains associated with them.

A very recent report proposed that the deubiquitinase module of SAGA, particularly Sgf73, is involved in ERC formation (McCormick et al., 2014). Since the *sgf73Δ*

mutant strain is the longest lived strain reported so far, it seems likely that deletion of *SGF73* affects several pathways that lead to prolonged lifespan. It will be interesting to compare the levels of ERC formation between cells lacking Sgf73 and Fob1 in order to estimate the contribution of reduced ERC formation on longevity of the *sgf73Δ* mutant cells.

There is an ongoing debate in the literature whether non-centromeric DNA circles attach to a receptor in the nuclear envelope allowing their retention by the diffusion barrier (Shcheprova et al., 2008) or whether the geometry of the nucleus combined with the short duration of anaphase is sufficient to mediate their retention (passive model; (Gehlen et al., 2011)). Here, we propose that both morpho-kinetic parameters, as proposed in the passive model, as well as tethering to NPCs are required for sufficient circle retention in vivo. Indeed, circle retention is affected in mutations that prolong anaphase (*yku70Δ*) and mutations that weaken the nuclear diffusion barrier (*bud6Δ*) and detach plasmids from NPCs (*gcn5Δ)* without prolonging anaphase. Therefore, we propose that morpho-kinetic constraints provide the baseline for circle retention and ensure that free-moving plasmids are still reasonably well retained, as observed for the circles in SAGA defective cells. Above this baseline, SAGA-mediated attachment of plasmids to NPCs and the nuclear diffusion barrier tighten circle retention to achieve full retention.

In contrast to our findings, a previous study argued that anchorage of circles to NPCs leads to symmetric segregation of circles (Khmelinskii et al., 2011). This study showed that fusing TetR to 11 different core nucleoporins did not affect the partitioning of a TetO-containing circle, but TetR fusion to the peripheral nucleoporins Mlp1 and Nup2 did. The first set of observations is expected either if the TetR fusions are not accessible to the circles, or if the circles are already tethered to NPCs by SAGA. Our data indicate that at least two of these core nucleoporins, Nup170 and Nup49 are accessible to the circles since fusing them to TetR restores the circle localization and retention defects of the SAGA mutant cells. Concerning the second set of observations, it is noteworthy that Nup2 localizes only transiently to NPCs (Dilworth et al., 2001) and is therefore not an ideal NPC anchor. Supporting this view, Nup2, Mlp1 and Nup60 all show higher mobility in FRAP experiments than the core nucleoporins Nup1, Nup49 and Nup170. Accordingly, we observed a correlation between the mobility of a protein at NPCs and its capacity to mediate retention of a circle when attached to it. However, why tethering Nup2, Mlp1 and Nup60 to the circle interferes with its normal attachment remains elusive. Possible explanations

might be that the attachment of Nup2, Mlp1 or Nup60 hinders them to bind to NPCs, that the interaction sites on the plasmid are blocked for SAGA or core NPC components, that attachment to components of the nuclear basket positions the plasmid to an inaccessible location on the NPC or that Nup2, Mlp1 and Nup60 mediate detachment of the plasmid from NPCs possibly by recruiting a SAGA inhibitor. Nevertheless, the data show that attachment of plasmids to stable nuclear pore components promotes their retention if the nuclear diffusion barrier at the bud neck is present. This is important to understand how attachment of DNA circles to pores leads to their retention in the mother cell.

We can think of different scenarios how the interaction of DNA circles to NPCs leads to their restriction to the mother cell: I) Circles detach from NPCs specifically in the bud. II) Circles are peeled off NPCs when they pass the barrier at the bud neck. III) Cells contain two distinct subsets of NPCs and circles are attached to the one that is better retained by the diffusion barrier. IV) Preexisting NPCs are retained in the mother cell and thus circles are retained independently of which NPC they are bound to. V) NPCs attached to a circle are specifically retained by the diffusion barrier. The observation that circles artificially attached to Nup49 and Nup170, two core components of the NPC, are retained as efficiently as wt plasmids, discards the first possibility, since detachment is obviated. Nevertheless, detachment of circles from NPCs in the bud might act as a rescue mechanism in case a circle containing NPC is accidentally passed to the bud. This could explain the very subtle increase in propagation frequency of the attached plasmid compared to wt plasmids. A possible detachment mechanism might involve a bud-specific deacetylase (as eg. Hos3) to counteract SAGA-dependent acetylation and its deletion would rather effect circle propagation in *bud6Δ* mutant cells, when plasmids are passed to the bud, than in wt cells. The artificial attachment experiments also discard the second possibility, because attachment would interfere with a mechanism peeling circles off the pores and the third possibility, since artificial attachment targets the plasmid unselectively to any NPC containing Nup49 or Nup170, unless cells contain a pool of NPCs lacking Nup49 and Nup170, which is rather unlikely. Finally, also the fourth possibility was dismissed because it would require the retention of most preexisting pores, which was shown not to be the case (Colombi et al., 2013; Khmelinskii et al., 2010; Menendez-Benito et al., 2013). Thus we investigated the last possibility: the specific retention of circle loaded NPCs.

3.2 A refined model for ERC retention

To test the effect of circles on NPC diffusion and segregation, cells containing high amounts of non-centromeric plasmids were examined. Remarkably, the plasmids localized mainly to one focus and NPCs were clearly enriched around this area. We named this enrichment of nucleoporins the NPC cap and showed that it is always associated with non-centromeric plasmids, follows the movement of the circles and remains together with the circles in the mother cell during mitosis. Thus, attachment of circles to NPCs not only increases the retention of circles but also of NPCs in the mother cell.

FLIP experiments on the NPC cap showed that NPCs associated with circles diffuse slower compared to circle-free NPCs and both circles and NPCs were less retained in barrier mutant cells. This suggests that the diffusion barrier retains NPCs interacting with DNA circles more efficiently than circle-free NPCs (see Model, Fig. 3.1). There are different possible explanations to explain this observation: First, enhanced retention might simply be due to the fact that these NPCs are less mobile. Indeed, a reduction in mobility is expected to reduce the frequency at which NPCs approach the barrier, and therefore their chances of passing it. Reduced mobility may be due to the added mass of the attached plasmid. However, if the added mass was pivotally ensuring retention we would expect better retention for bigger non-centromeric DNA molecules (chromosome IV) compared to non-centromeric plasmids. Since this was not observed we predict that retention is not solely based on the increased mass. Decreased mobility might be due to the propensity of circle-bound NPCs to cluster, by a yet unknown mechanism. Indeed, different mutations inducing NPC clustering lead to increased NPC retention in the mother cell (Shcheprova et al., 2008). Additionally, post-translational modification of the NPC might reduce its mobility. Here, the acetyl transferase or deubiquitination activity of SAGA could promote NPC clustering or reduce their mobility through another yet unknown mechanisms. Alternatively, based on very recent results from our laboratory, palmitoylation could be involved (Tom Kruitwagen, unpublished data). The covalent binding of a palmitoyl group, a fatty acid, is of special interest because it promotes anchorage of proteins into membranes and might thereby reduce the mobility of pores within the nuclear membrane.

Second, the barrier might be selective. For example, remodeling of the NPCs and their clustering might interfere with their ability to pass the barrier. In any case, the

immobilization and segregation effects observed upon circle attachment to NPCs are strikingly reminiscent of the phenotypes caused by removing the nucleoporin Nsp1 (Colombi et al., 2013; Makio et al., 2013). It is therefore tempting to speculate that SAGA affects Nsp1 recruitment, stability or function in the pore, and thereby affects NPC behavior. We would predict that SAGA associated pores lack Nsp1 or that SAGA mediates Nsp1 modifications, both preventing these pores to pass the diffusion barrier. Accordingly, we would predict that SAGA detaches from the pores that are passed to the bud during mitosis but remains with the circles and therefore ensures their retention. We could test this by visualizing Nsp1 or investigating Nsp1 modifications in cells containing accumulated plasmids. Additionally we would predict Nsp1 to dissociate from ERC-loaded NPCs in old cells. Very preliminary data showed that in aged cells (average 8 generations) less Nsp1 is retained compared to Nup170, suggesting that some NPCs that are retained in the mother cell during aging are lacking Nsp1 (Melissa Amrein, semester student). It will be interesting to see whether this is even more enhanced in older cells (more than 25 generations).

Thus, together, our observations provide insights into how NPCs mediate retention of circles even though they are not plainly retained in mother cell themselves, if the cells are circle-free (Colombi et al., 2013; Khmelinskii et al., 2010; Menendez-Benito et al., 2013). Furthermore, they indicate that the diffusion barrier in the envelope of anaphase nuclei, which has limited effects on bulk NPC distribution in young cells, becomes crucial during aging.

Fig. 3.1

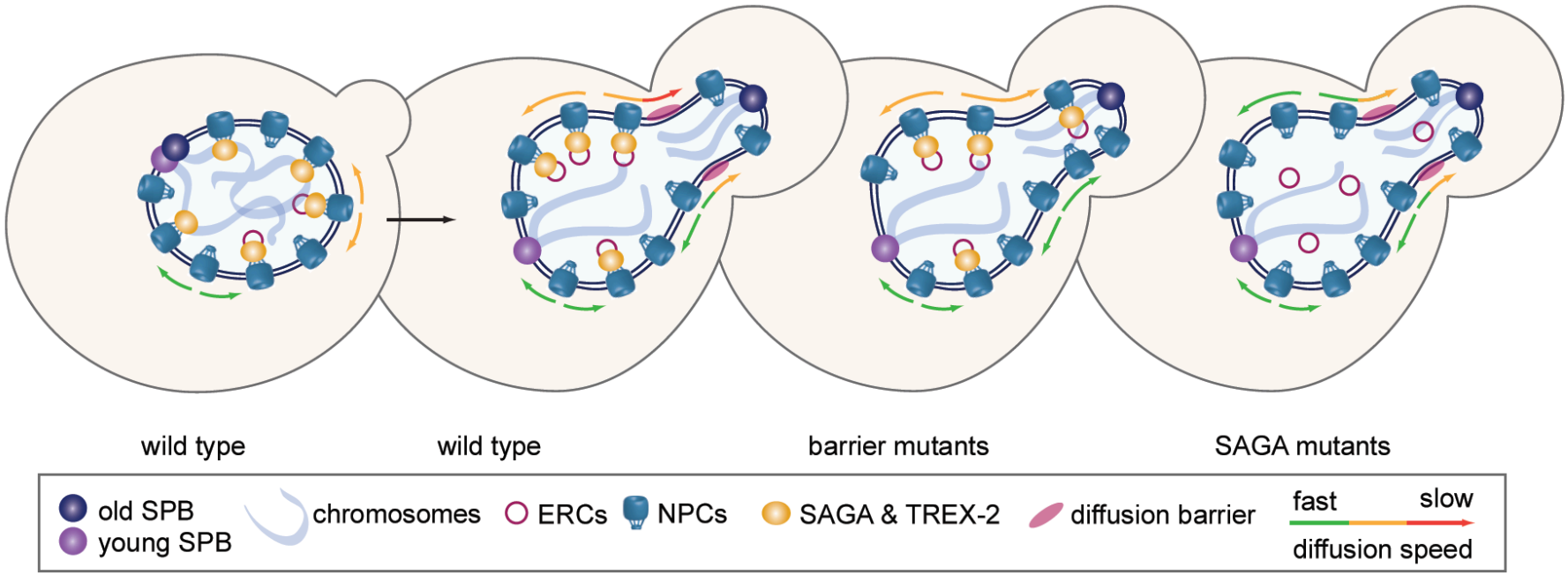

Fig. 3.1 A refined model for the retention of ERCs in yeast mother cells

The SAGA complex (yellow) attaches ERCs (red) to NPCs (blue), thereby reduces their mobility (arrows) leading to a better retention by the diffusion barrier at the bud neck (pink). In cells with a reduced barrier function both ERCs together with NPCs segregate more frequently into the bud. In contrast, the diffusion barrier is intact in SAGA deficient cells but ERCs detach from NPCs allowing their free movement in the nucleoplasm and an increased propagation into the bud.

3.3 Does SAGA change the chromatin structure of non-centromeric DNA molecules?

We found that SAGA is required for the attachment of non-centromeric DNA circles to nuclear pores and the observation that the catalytic domain of Gcn5 is involved in the retention of DNA circles suggests that SAGA-mediated acetylation somehow mediates attachment of DNA circles to NPCs. SAGA was previously described to acetylate histones and this was proposed to open the chromatin structure to allow binding of Pol II in order to start transcription (Baker and Grant, 2007; McCullough and Grant, 2010). Therefore, we wondered whether SAGA modifies the chromatin structure on non-centromeric DNA circles and whether this was involved in circle retention.

We discovered that TetR intensity on the centromeric plasmid changed during the cell cycle, it was decreased in anaphase, suggesting that we can visualize the higher compaction of DNA during mitosis that was previously described (Vas et al., 2007). The compaction was independent of SAGA but provides a nice tool to investigate whether a deacetylase is involved in the cell cycle dependent compaction of centromeric DNA. A very recent report showed that Ipl1 (Aurora B kinase)-dependent phosphorylation of histone H3 serine 10 recruits the Sir2-related deacetylase Hst2 leading to deacetylation of histone H4 lysine 16. And it was proposed that this cascade ensures compaction during mitosis (Wilkins et al., 2014). Hst2 is therefore a perfect candidate to test for the increased TetO compaction during mitosis.

Interestingly, we found that the plasmid is more accessible for TetR in its non-centromeric form. This suggests that the chromatin is in a more open state when lacking a centromere. The increase in TetR intensity observed on non-centromeric plasmids almost completely depended on Gcn5. Thus, we conclude that non-centromeric DNAs bind Gcn5, which decreases their compaction, presumably by histone acetylation. To test whether the decreased compaction of DNA promotes attachment or whether it is a secondary consequence of SAGA binding, cells expressing histones mutated in their known SAGA targets could be examined. Nevertheless, a model proposing that acetylation of the plasmid mediates its attachment to NPCs agrees with a number of observations. Artificial attachment of Gcn5 to the plasmid increased its retention in the mother cell. In contrast, the recruitment of a deacetylase interferes with the retention in the mother cell. This was observed when attaching Sir2 to the plasmid (this thesis) and it was previously

reported that insertion of sequences such as silent mating-type loci and subtelomeric regions, which recruit Sir2, into episomes, as well as targeting Sir4 to episomes causes these circles to segregate more symmetrically (Ansari and Gartenberg, 1997; Enomoto et al., 1994; Kimmerly and Rine, 1987). Thus, we propose that acetylation of non-centromeric chromatin mediates attachment to NPCs whereas their deacetylation leads to detachment and therefore to increased symmetric segregation. Taken together, we observe decreased compaction of non-centromeric DNA molecules and, concomitantly, their retention in the mother cell, both depending on SAGA. On the other hand, centromeric DNA molecules become more compact in anaphase, the exact moment when they segregate symmetrically. Thus, we could imagine that compaction is involved in the distinct segregation- asymmetric or symmetric- of DNAs during mitosis depending on the presence of a centromere. This leads to a model proposing that histone acetylation promotes attachment of acentric DNAs to NPCs whereas deacetylation occurs during mitosis to ensure detachment of centromeric DNA. Involving Hst2 in the detachment of chromosomes from NPCs would be a very elegant mechanism to combine detachment with chromatin compaction required for sufficient separation of the mitotic chromosomes. Whether centromeric DNAs indeed detach from NPCs during mitosis is currently unknown. However, it was already observed that telomeres detach from the nuclear envelope during mitosis, supporting the idea that mechanisms attaching centromeric DNA to the nuclear periphery are reverted during mitosis (Hediger et al., 2002). Alternatively, the SAGA-dependent attachment to NPCs would remain during mitosis, pulling the attached NPCs into the daughter cell. Such a mechanism was previously proposed to ensure symmetric segregation of NPCs in *Schizosaccharomyces japonicus* (Yam et al., 2013). And finally, the interaction between SAGA and non-centromeric DNAs might be stronger compared to the previously described interactions on chromosomal DNA (Ohtsuki et al., 2010). Thus, the centromeric DNA would never attach as strongly to NPCs and therefore the forces generated by the mitotic spindle would be sufficient to pull the chromosomes away from NPCs. Further studies will be required to elucidate the roles of deacetylases on centromeric DNA molecules.

3.4 How do cells distinguish non-centromeric DNAs from chromosomes?

Starting from the hypothesis that indeed, acetylation mediates retention of non-centromeric DNA in the mother cell whereas deacetylation allows the segregation of chromosomal DNA to the daughter cell we formulate the following prediction: either centromeric DNA is recognized by deacetylases whereas non-centromeric DNA by acetyl transferases or, alternatively, acetyl transferases interact with all DNA molecules but centromeric DNA specifically recruits deacetylases interfering with them. In other words, either the cells identify both centromeric and non-centromeric DNAs separately or they retain all DNA pieces in the mother cell except the centromeric DNAs, the chromosomes, which are specifically passed to the daughter cell. The first possibility would allow the cells to develop two very distinct and independent pathways dealing with either centromeric or acentric DNA. However, it would require a mechanism recognizing all kinds of non-centromeric pieces of DNA a yeast cell could possibly be exposed to, which might be very difficult or even impossible to be achieved. If the cells cannot recognize every foreign piece of DNA, the second possibility would still allow the retention of all non-centromeric DNAs: the cells would retain all DNA molecules, independent of their sequences, but allow the propagation of the chromosomes- the only pieces of DNA the cells might want to share with their progeny. Therefore, the second possibility is very appealing because it would allow the cells to react to any non-centromeric piece of DNA, of own or foreign origin, independent of its sequence. This pathway would fulfill the functions of a genomic immunity system capable of preventing the spread of both foreign and endogenous non-chromosomal DNA molecules in a population.

Identifying SAGA as a key player in the retention of acentric DNAs gave a first glimpse about how cells sort non-centromeric DNA molecules from chromosomes. Since SAGA was already described to interact with all transcribed regions on the genome (Bonnet et al., 2014), our findings that it interacts with non-centromeric DNAs and ensures their retention in the mother cell strongly supports the second possibility- that SAGA interacts with all DNA molecules but detaches from chromosomes during mitosis in order to allow their symmetric segregation. However, using fluorescence microscopy we observed that SAGA is enriched on non-centromeric DNA circles even in G1 and ChIP experiments (performed by Catherine Stober) showed an increased interaction of SAGA with non-centromeric plasmids compared to a chromosomal locus. Therefore, the question remains, whether SAGA

recognizes non-centromeric DNA molecules specifically or whether it binds all DNA molecules equally but is repelled from chromosomes. To further test this hypothesis it would be important to see whether SAGA indeed dissociates from the described interaction sites on the chromosome during mitosis. Additionally, it would be exciting to test whether versatile foreign DNAs are retained in the mother cell and whether this would depend on SAGA. So far, we know about the retention of various DNA circles, ERCs and non-centromeric chromosomes. But are bacterial, viral or synthetically designed DNA molecules lacking yeast specific sequences recognized by SAGA and retained in the mother cell?

The possibility remains that SAGA specifically recognizes non-centromeric DNA molecules. Different proteins of the SAGA complex contain bromo- and chromodomains. Gcn5 and Spt7, for example, contain a highly conserved bromodomain, which allows them to recognize acetylated lysines. Furthermore, Chd1 contains a chromodomain mediating the interaction with methylated histones and Sgf29 preferentially binds to methylated histones. More specifically it was reported that Chd1 and Sgf29 interact with trimethylated histone H3 lysine 4 (H3K4me3), a hallmark of promoters of actively transcribed genes, which was proposed to promote SAGA activity (Bian et al., 2011; Pray-Grant et al., 2005). If non-centromeric DNAs showed increased methylation of H3K4, this could increase SAGA recruitment and binding. Set1, a methyltransferase required for H3K4 trimethylation, is indeed required for retention of non-centromeric DNA circles (Tom Kruitwagen, personal communication). It would be interesting to test whether SAGA recruitment depends on Set1 and H3K4 methylation. SAGA is recruited by methylated H3K4 but was also reported to acetylate the same lysine residue. Thus, acetylation and methylation might compete for this residue suggesting that a demethylase is required to allow SAGA-dependent acetylation. A demethylase of interest might be Gis1, since its deletion promotes longevity (Managbanag et al., 2008). Still, the question remains why non-centromeric DNA would differ from centromeric DNA. Why would non-centromeric chromatin show increased methylation leading to enhanced SAGA binding?

This brings us to the second possibility, that SAGA might be repelled from chromosomal DNA. Different possibilities could result in SAGA deactivation on centromeric DNA: I) Proteins recruited to chromatin in a centromere dependent manner might compete with SAGA for binding sites. II) A specific SAGA inhibitor could be recruited by the centromere. III) Histone acetylation mediated by SAGA

could be constantly (or every cell cycle) reverted by a centromere-dependent deacetylase. As previously described, Ipl-dependent histone phosphorylation could recruit Hst2 specifically to centromeric DNA during mitosis and thus interfere with SAGA binding on chromosomes. Interestingly, the acetylation of H4K16 can promote SAGA binding (Zhang et al., 2010). Thus, acetylation would recruit SAGA whereas deacetylation would reject SAGA from centromeric DNA. It was previously reported that acetylation of H4K16 is mediated by the acetyltransferase Sas2 and reverted by the deacetylase Sir2 (Suka et al., 2002). Interestingly, cells lacking Sas2 show prolonged lifespan (Dang et al., 2009). Thus, it would be interesting to investigate whether Sas2 is involved in SAGA recruitment and thus in circle retention. Additionally, to test whether Hst2 rejects SAGA form centromeric DNAs, ChIP experiments combined with DNA sequencing are planned to investigate differential binding of Gcn5 and Hst2 on chromosome IV with or without a centromere. Investigating the epigenetic marks on both the non-centromeric chromosome IV and its centromeric equivalent combined with the retention of non-centromeric DNA in different histone mutants would provide important insights into which histone modifications promote retention of acentric DNAs. Together, we conclude that SAGA is a key player in the process of identifying acentric DNAs, however, requiring additional proteins either stabilizing SAGA interaction with non-centromeric DNAs or repelling SAGA from centromeric DNAs in order to distinguish the two.

Furthermore, we wonder whether the interaction of SAGA with non-centromeric DNAs is influenced by the DNA sequence. Speaking in favor of SAGA interacting with acentric DNAs independently of their sequence is the observation that SAGA interacted with non-coding regions of bacterial origin when present on a non-centromeric plasmid (ChIP experiments). However, since these regions are in close proximity to the *LEU2* gene and the ARS sequence on our reporter plasmid this could result from SAGA spreading on DNA as it was previously proposed for SAGA (Baker and Grant, 2007). On chromosomes SAGA was mainly found at promoter regions of stress-induced genes, t-RNA encoding genes, ARS sequences and Ty elements (Ohtsuki et al., 2010). The tetO and rDNA containing plasmids used in this study harbor both an ARS sequence and a marker gene. Thus, SAGA might be recruited to plasmids by the ARS sequence or the transcribed element. This idea is supported by the finding that retention is increased in selective medium, which induces transcription of the marker gene present on the plasmid. Additionally, this would explain the discrepancy in the literature: whereas we observe our reporter plasmid at

the nuclear periphery and highly retained (this study and (Shcheprova et al., 2008)) others reported random distribution within the nucleus and less efficient retention for a reporter plasmid that is loxed out from the chromosome (Gehlen et al., 2011). Interestingly this DNA circle neither contains an ARS sequence nor a transcribed unit. Additionally, DNA circles with strong replication origins are more highly retained in mother cells than those with weak origins (Futcher and Cox, 1984). Thus, replicating circles may also be better retained than non-replicating circles. Together, a transcribed unit and a replication sequence might increase SAGA recruitment and mediate retention.

From the aging perspective we are especially interested in the retention of ERCs. Thus it is important to test whether ERCs also recruit SAGA. The observation that ERCs and NPCs accumulate slower in SAGA deficient cells and that we never observed an NPC cap in old *sgf73Δ* mutant cells suggests that indeed SAGA interacts with ERCs and attaches them to NPCs. Transcription of the rDNA repeats requires RNA Polymerase (Pol) I and III, whereas SAGA was only reported to mediate Pol II-dependent transcription. Interestingly, it was reported that the polymerase transcribing rDNA switches to Pol II once the rDNA repeat is present on a DNA circle (Conrad-Webb and Butow, 1995). This remarkable observation suggests that SAGA does not bind chromosomal rDNA but is recruited to rDNA repeats once excised from the chromosome. Additionally, every rDNA unit contains an ARS, which might further increase SAGA binding. To investigate whether SAGA interacts with ERCs ChIP experiments probing for SAGA interacting with rDNA sequences in young and old cells would be very interesting. Alternatively, we could investigate SAGA localization in old cells. We would predict that SAGA accumulates in close proximity to the NPC cap observed in very old wt cells. Additionally, we would predict an ERC-dependent increase in SAGA asymmetry visualizing SAGA in old wt or *sir2Δ* mutant cells compared to young cells.

All together, we could imagine that SAGA binds non-centromeric DNA in general, but interacts stronger with replicating and transcribed acentric DNA molecules. However, we cannot exclude the possibility that the cells specifically detects foreign and endogenous non-centromeric DNA molecules solely if a specific sequence, a transcribed gene or an ARS, is present. To test this, plasmids lacking both an ARS and a transcribed unit would need to be tested for their mitotic segregation and their association with SAGA and NPCs. Additionally, it would be interesting to investigate whether NPCs cluster in proximity of non-transcribed accumulated plasmids and

whether they cause aging to a similar extend as circles containing a transcribed gene. If transcription and replication are indeed increasing SAGA recruitment and circle retention we propose a SAGA-based mechanism that primarily targets non-chromosomal DNA molecules based on their expression and replication potential, i.e., on their potential toxicity.

A mechanism in which SAGA interacts with DNA in general and is removed from centromeric DNA molecules specifically would allow cells to react to any piece of DNA that does not contain a centromere. Such a system would be extremely powerful not only to prevent spreading of DNA byproducts (as ERCs) but also all foreign DNAs entering the nucleus. Yeast cells are constantly exposed to DNA molecules of very different origins, thus a mechanism recognizing DNA molecules which the cells have never encountered before is presumably very important for yeast cells in their natural environment. The fact that we found the same complex involved in transcription of many chromosomal genes being required for the retention of different artificial introduced plasmids and endogenous ERCs supports the idea of SAGA binding DNA in general and the existence of an antagonizing mechanism liberating chromosomes to allow their segregation to the bud. However, the possibility still remains that SAGA recognizes specifically non-centromeric DNAs, binds them much stronger and that the weak interaction of SAGA with chromosomes is not strong enough to interfere with the pulling forces generated by the mitotic spindle. Identifying a centromere-dependent and SAGA antagonizing pathway would strengthen our hypothesis that SAGA binds DNA in general but is repelled from chromosomes.

3.5 A novel role for ERCs in aging

How ERCs contribute to aging is unknown. It was previously proposed that accumulated ERCs would increase rDNA instability or titrate essential binding proteins (see Introduction; (Ganley et al., 2009; Sinclair and Guarente, 1997)). Interestingly, we discovered that ERCs interact with NPCs and that this interaction leads to major nuclear rearrangements during aging. We observed an increase in NPC asymmetry as the cells age, which depended on ERCs and SAGA. Furthermore, the reduced accumulation of NPCs in SAGA deficient cells was partially reverted upon expression of the SAGA-TREX-2 or SAGA-NPC fusion proteins. Together, we conclude that SAGA-mediated attachment of ERCs retains NPCs in old

mother cells leading to their accumulation as the cells age (Model Fig. 3.2). Based on these observations we propose that NPCs are one of these previously proposed essential ERC binding proteins and speculate whether NPC accumulation finally kills the cells. Replicative aging in yeast might be at least in part the secondary consequence of a mechanism involved in restricting the propagation of non-chromosomal DNAs and thereby altering nuclear organization and NPC number.

To test the hypothesis that ERCs promote aging by accumulating NPCs we would first ask whether nuclear cytoplasmic transport is affected in old cells. If this was the case, the import of inner nuclear membrane proteins through NPCs might be perturbed leading to their mislocalization to the ER (Meinema et al., 2011). Or the nucleo- cytoplasmic shuttling of proteins required for cell cycle progression (such as e.g. Mcm4) could be examined. Indeed, it was observed that old cells slow down their cell cycle and often arrest during cytokinesis (Egilmez and Jazwinski, 1989). Nevertheless, even if we could observe aberrations in nuclear homeostasis in old cells, this would not yet demonstrate the cause of aging. To announce NPC accumulation as an aging factor we would like to induce or prevent NPC accumulation and test their effect on aging. We tested the first possibility by tagging Nup49 with GFP, which is known to increase NPC asymmetry and thus leads to a faster accumulation of NPCs as the cells age (this thesis and (Makio et al., 2013)). Performing pedigree analysis of cells expressing Nup49-GFP we found that this indeed shortened lifespan (19 generations, data not shown). However, mutations shortening the replicative lifespan have to be treated with caution since they might rather represent sickness of the cells than accelerated aging. Finally, mutations preventing NPC accumulation, such as deleting Fob1 or Sgf73, prolonged lifespan. However, these mutations also decreased ERC accumulation, thus preventing us from dissecting whether ERC or NPC accumulation causes aging. It will be a major challenge to uncouple ERC from NPC accumulation due to their concomitant retention in the mother cell.

A role for nuclear organization in aging was already known from human diseases. As described in the introduction, nuclear organization of patients suffering from HGPS is severely affected leading to premature aging phenotypes. However, it is still mysterious how the altered shape of the nucleus translates into all these specific aging phenotypes. Thus, studying the defects related to altered nuclear structure in aging yeast cells might give important insights into which mechanisms are affected by aberrant nuclear organization in these patients.

The Bloom and Werner syndromes originate from dysfunctions in two helicases leading to very similar premature aging phenotypes (see Introduction). Since these helicases inhibit the formation of Holliday junctions and thus circle formation it might be that cells from these patients accumulate more extrachromosomal DNA circles. However, why these patients show very similar symptoms as patients suffering from HGPS is unknown. Showing that DNA circles cause nuclear disorganization in yeast suggests that circle accumulation in Werner or Bloom patients similarly affects nuclear structure as mutations in HGPS patients. Indeed, an altered nuclear structure including the formation of micronuclei was reported for cells from Bloom patients (Yankiwski et al., 2000). Similarly, WRN knockout cells show nuclear alterations including defects in Lamin B1, NPC and RAN distribution (Li et al., 2013). Together these different observations indicate a link between genomic instability, DNA circle formation and changes in nuclear organization during aging, and suggest that NPCs might be at the center of these relationships. Our data indicate that yeast will be a powerful system to dissect how NPC number and modifications affect nuclear homeostasis and cellular viability.

Fig. 3.2

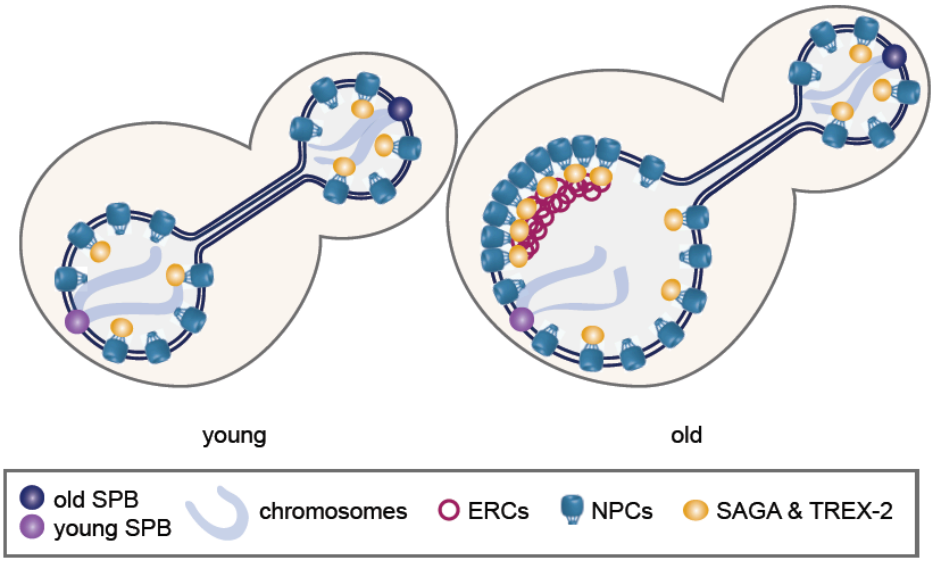

Fig. 3.2 The effects of ERCs on NPCs during aging

The attachment of ERCs to NPCs leads to their retention in the mother cell. Thus, NPCs start to accumulate as the cells age leading to enlarged nuclei containing massive amounts of NPCs. This might become toxic for the cells and contribute to the aging process.

3.6 DNA circles accumulate and are excluded form the nucleus in mammalian cells

To investigate whether mammalian cells react similarly to non-centromeric DNA circles, we investigated the localization and segregation of plasmids containing LacO repeats in HeLa cells expressing LacI fused to either GFP or mCherry. Early after transfection many LacI foci scattered in the whole nucleus were observed whereas at later timepoints mainly one focus excluded from the nucleus was visible. This, together with time lapse movies of dividing cells suggested that plasmids cluster before or during nuclear envelope breakdown and are not included into the nucleus when the nuclear envelope is reformed (Model Fig. 3.3). Such observations were previously reported by observing microinjected DNA into the nucleus (Shimizu et al., 2005). After micronucleus formation the structure was very persistent throughout several divisions and was not observed to be re-integrated into the nucleus. However, to determine the fate of the micronucleus more carefully long term imaging would be required to follow the plasmids for many divisions.

The plasmids entrapped in the micronucleus were enclosed by Lap2-β, suggesting there might be at least some lamina components, but no staining for NPCs was observed. Additionally, no IBB was imported into the micronucleus, suggesting that indeed, the micronuclei containing plasmids are lacking NPCs. This was previously proposed for DNA fragments lacking a centromere, whereas whole chromosomes are rather entrapped in micronuclei with NPCs (Terradas et al., 2010). This suggests that NPC recruitment is triggered by the centromere which would allow the cells the distinction between centromeric and acentric DNA.

Since the circles are surrounded by Lap2-β in the micronucleus, lamins and lamin-associated proteins might even play a role in the formation of the micronucleus. Thus, it would be extremely interesting to test plasmid localization in progeria expressing cells. It could be that cells from HGPS patients are defective in the exclusion of DNA circles from the nucleus leading to their accumulation and probably contributing to the nuclear disorganization observed in these cells.

The majority of the cells accumulated all plasmids into one micronucleus, which allows the cells to always segregate the plasmids asymmetrically. Investigations of Xuan Wang, a PhD student from the Kroschewski lab who continued on this project, showed that the micronucleus containing plasmids preferentially segregates to the cell containing the younger centrosome in both HeLa (human) and MDCK (dog) cells

(unpublished data). This would be similar to yeast cells, although the asymmetry is less stringent (about 70% co-segregation with the younger centrosome in HeLa and MDCK cells compared to 94% in *S. cerevisiae*). It would be interesting to investigate plasmid segregation in stem cells to see whether the percentage of cells co-segregating the plasmids with the young centrosome is increased compared to HeLa and MDCK cells. Nevertheless, HeLa and MDCK cells transfected with LacO plasmids are an ideal model system to investigate the basic mechanisms ensuring asymmetric segregation of acentric plasmids in mammalian cells.

3.7 Are the mechanisms ensuring asymmetric segregation of DNA circles conserved from yeast to humans?

All together these data showed that DNA circles segregate asymmetrically in both mammalian and budding yeast cells. Thus, the question arises whether the mechanisms ensuring asymmetry are conserved from yeast to humans. Interestingly, the circles clustered in both cell types, which facilitates their segregation to only one daughter cell. We discovered that in yeast cells the SAGA complex is involved in both clustering of the circles and their attachment to NPCs. Since we could not detect NPCs present in the micronucleus enclosing DNA circles in mammalian cells, we would predict that these circles are not attached to NPCs. Nevertheless, clustering of the circles prior to their exclusion from the nucleus might indeed depend on the human SAGA complex (hSAGA). It would be tempting to test whether the transfected circles would remain scattered within the nucleus or form many micronuclei in hSAGA depleted cells.

Clustering of many DNA circles to only one focus fully ensures their asymmetric segregation. However, Xuan's observation that their segregation is non-randomly in respect to the age of the centrosomes indicates an additional layer of regulation. Interestingly, work from Lori Clay, a former PostDoc in the lab, proposed the existence of a diffusion barrier in the ER of dividing HeLa cells (unpublished data). Supporting this, Darcie Moore showed that the ER membrane is compartmentalized in dividing neuronal stem cells (personal communication). It would thus be possible that a diffusion barrier in the ER regulates the segregation of the circle-containing micronucleus to the cell containing the younger centrosome. Indeed, Xuan observed that the micronucleus is embedded in the ER, which would allow their subjection to the diffusion barrier (unpublished data).

Relocating the plasmids from the primary nucleus to the micronucleus might have several advantages: First, the circle DNA might no longer be transcribed, inhibiting a potential toxic effect of foreign DNA. Second, the circles might not replicate in the micronucleus. To investigate these hypotheses co-localization of DNA- and RNA-polymerases together with the clustered circles in the micronucleus could be examined. Third, once separated from the chromosomes, the enclosed DNA might be degraded or rejected by the cell. Accordingly, separating the DNA circles from the chromosomes might be a great advantage if the circle DNA is foreign and potentially toxic but also if it is of endogenous origin and could contribute to aging, as in budding yeast cells. Since endogenously formed DNA circles exist in all tested organisms so far, including human cells (Cohen et al., 2010), it would be exciting to know where they localize within the cell and how they are segregated during mitosis. We would first ask whether they also localize to a micronucleus and whether they co-segregate with the younger centrosome. However, this might be very difficult since the studies observing endogenous DNA circles were performed on collected DNA of several hundred thousands of cells and even in yeast cells ERCs are only detectable after selecting for old cells (see Introduction). Thus, the visualization of extrachromosomal DNA circles might be rather possible in cells collected from old animals, WRN-/- cells or cells with induced circle formation.

Even though the circles are excluded from the nucleus they are still present in the cell, which might be a burden for the receiving cell. It would be interesting to know whether the circle containing micronucleus is segregated together with other deposits such as the aggrosome, IPOD and JUNQ as well as unfolded proteins in the ER and fragmented mitochondria during cell division, as it was observed in yeast cells. It could be imagined that during cell division the diffusion barrier retains all these factors simultaneously in one part of the cell and that the spindle orients accordingly.

While endogenously formed circles and foreign non-centromeric DNA molecules are retained in the mother nucleus of dividing budding yeast cells, they replicate every cell cycle and thus accumulate exponentially in the mother cell. The stringent retention in the mother cell allows the formation of a rejuvenated daughter cell but concomitantly leads to aging of the mother cell. In contrast, mammalian cells expel the circles from the nucleus during nuclear envelope disassembly, which might inhibit replication and accumulation and might inhibit their contribution to aging. Thus, excluding acentric DNA molecules from the nucleus might be a major advantage of cells undergoing open mitosis arising the hypothesis that open mitosis evolved to

Fig. 3.3

A

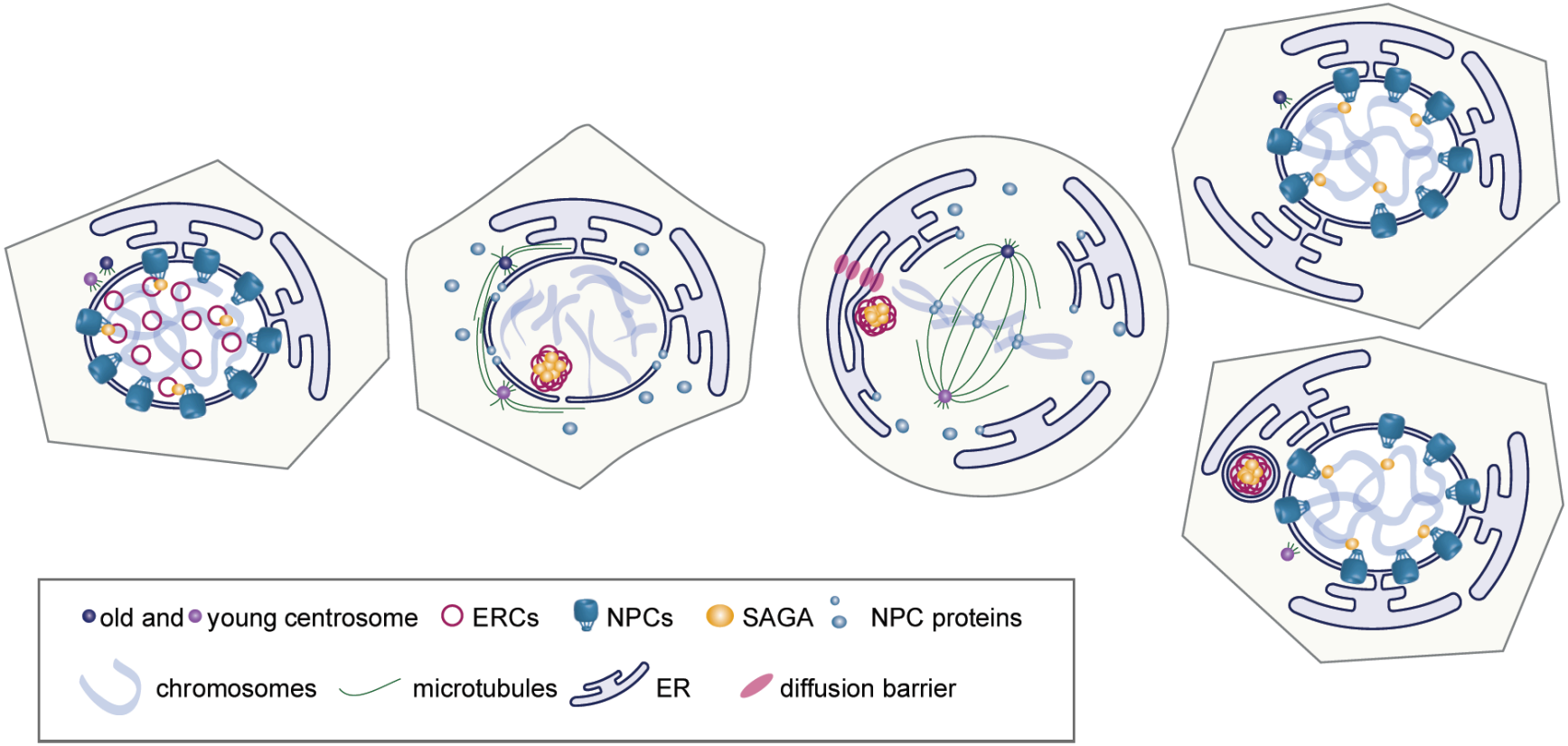

Fig. 3.3 In mammalian cells non-centromeric DNA circles cluster together, are excluded from the nucleus and segregate asymmetrically during mitosis

In HeLa cells DNA circles cluster into one focus and are excluded from the nucleus, most probably during nuclear envelope breakdown. Once excluded from the nucleus, they remain in a micronucleus surrounded by lamina but lacking NPCs. Since they mainly cluster into one focus they segregate asymmetrically to one of the two daughter cells. They preferentially stay in the daughter cell harboring the younger centrosome, a process that might involve their tethering to the ER and the presence of a later diffusion barrier in the ER membrane. Drawing is partially adapted from (Guttinger et al., 2009).

allow the exclusion of non-chromosomal DNA. To get a glimpse into this, plasmid localization could be examined in yeast species undergoing partially open mitosis, such as e.g. *Schizosaccharomyces japonicus*.

3.8 Closing remarks

In this study, we investigated the mechanisms that allow yeast cells to efficiently retain ERCs and other non-centromeric DNA circles in the mother cell, allowing the formation of circle-free daughter cells. We discovered that the SAGA complex mediates the attachment of DNA circles to NPCs, impairs their diffusion and prevents their passage through the previously described diffusion barrier at the bud neck. However, many questions still remain. For example, how do cells distinguish non-centromeric DNAs from chromosomes? The identification of SAGA, a complex previously known to interact with chromosomal DNA, as being involved in the retention of non-centromeric DNAs proposes that SAGA interacts with DNA in a general manner and thereby mediates the retention of all DNA molecules present in the nucleus. Thus, only approved DNA fragments would be incorporated into a chromosome, allowing their segregation into the bud.

But why would yeast cells develop a mechanism ensuring the strict retention of ERCs in the mother cell? This seems unprofitable, especially since the retention and concomitant accumulation of ERCs leads to the accumulation of NPCs and drastic changes in nuclear architecture. One possible answer is that small amounts of ERCs received early in the life of yeast cells drastically shorten their lifespan and would be a disadvantage for the newborn daughter cells. However, these cells would also have the advantage of propagating ERCs to their offspring and thus, a slower accumulation of ERCs. Currently, we don't know whether the daughter cells of aged mother cells show a reduced lifespan potential compared to daughter cells from young cells if they are lacking the SAGA complex.

However, if SAGA is required for the retention of all possible non-centromeric DNA molecules a cell might encounter, we could imagine that this mechanism plays a very important role for yeast cells grown in a natural environment where cells are constantly exposed to foreign DNA. In this scenario, it might be crucial to retain foreign DNA molecules in order to impede the spread of possibly harmful and toxic DNA fragments within the population. From this point of view, we have discovered a very basic mechanism ensuring cellular immunity. In the human immune system, all

possible combinations of antibodies are created. However, antibodies against ones own proteins are degraded (Market and Papavasiliou, 2003; Palmer, 2003). Therefore, the immune system attacks all proteins except the ones recognized as "self". Analogous to this, the yeast cells would retain all DNAs in the mother cell except the ones containing a centromere, which would mark them as "self". The discovery of SAGA being involved in this unicellular immune system creates many new and exciting perspectives. Accordingly, the retention of ERCs might rather be a side effect of a mechanism originally developed to prevent the spreading of foreign DNA.

Alternatively, we could imagine that the retention of certain non-centromeric DNAs could be advantageous for the mother cells. In the case of a foreign piece of DNA encoding for a beneficial protein (e.g. a resistance gene), the mother cell would gain a growth advantage over the population, given the retention of such a DNA molecule, and in extreme cases survive when other cells die. As this cell ages, the beneficial DNA would accumulate and either start leaking into the daughter cell after reaching a critical number or even integrate into the genome. Thus, mother cells might become extremely valuable for the maintenance of a population under certain stress conditions. Mother cells in a population would collect and retain different foreign pieces of DNA over many generations and would contribute to the rescue of the population if all other cells died in conditions that suddenly change.

Interestingly, the rDNA locus encodes for several antisense transcripts, most of which are uncharacterized. However, one of them encodes a protein called Tar1, which localizes to mitochondria but its function is still unknown. The amount of Tar1 might increase with increasing ERCs, providing a beneficial role for ERCs in regulating the amounts of Tar1. It would be very interesting to investigate whether ERCs indeed provide an advantage for cells in certain stress conditions.

Finally, we found that mammalian cells not only segregate non-centromeric DNA circles to the cell containing the younger centrosome (analogous to the mother cell in yeast), but even exclude them from the primary nucleus. Thus, open mitosis allows cells to separate non-centromeric DNAs from chromosomes into different cellular compartments. However, if the DNA in the micronucleus is not degraded but remains with the cell line receiving the young centrosome, these cells might still be able to reintegrate the DNA into the primary nucleus in case the DNA pieces render an advantage for the cells. To investigate such possibilities, we would need to know whether the micronucleus remains in the cell for many divisions.

In budding yeast, ERCs were the first aging factors discovered. Since then, several other factors were found to play a role in the aging process and they are all highly retained in the mother cell. Similarly, we could imagine that in mammalian cells, the micronucleus, which contains non-centromeric DNA circles, is only one factor segregated to the daughter cell containing the younger centrosome. It is already known that the aggrosome stays with one centrosome and that damaged proteins and proteins targeted for proteasomal degradation segregate asymmetrically in stem cells (Bufalino et al., 2013; Fuentealba et al., 2008; Wigley et al., 1999). Thus, mammalian cells might retain all these factors together in one half of the cell during mitosis whereas the spindle would orient accordingly and the diffusion barrier might play a very important role in this process.

Finally, it would be extremely interesting to follow cells receiving the DNA circles throughout their lifetime. By constant removal of cells lacking the circle containing micronucleus, it could be possible to follow the cell containing the circles and count how many division cycles this cell can undergo before it dies, exactly as pedigree analysis was performed on yeast cells. This technique might allow first glimpses into whether DNA circles contribute to aging in mammalian cells.

4. Materials and Methods

4.1 Strains and plasmids:

Yeast strains used in this study are in chapter 6 “Strain list”. All strains are isogenic to S288C. GFP and knock out strains derived from collections (http://web.uni-frankfurt.de/fb15/mikro/euroscarf/index.html and http://clones.lifetechnologies.com/cloneinfo.php?clone=yeastgfp) or were manually created as described (Janke et al., 2004). Cells were grown using standard conditions: YPD and 30°C unless otherwise indicated. pYB1601 containing 3sfGFP was created by Mathias Bayer. pDS316 containing one rDNA repeat was a gift from D. A. Sinclair (Sinclair and Guarente, 1997) and pYB1382 containing *gcn5-E173A* was a gift from S. L. Berger (Wang et al., 1998). *gcn5-E173A* was integrated into the genome to replace *GCN5*. To allow the visualization of SPBs and the expression of the recombinase upon addition of estradiol *spc42::SPC42-CFP:kanMX4* and the estradiol binding domain fused to Gal4 *trp1::GAL4-EBD:TRP1* were introduced into the plasmid visualization strain used in (Shcheprova et al., 2008). To create TetR fusion proteins a plasmid pYB1666 containing *linker-TETR-mCHERRY-hpHNT1* was created by homologous recombination into pRS314. To generate the Gcn5-Sac3 and Spt7-Nup49 fusion proteins pYB1665 containing *GCN5-linker-SAC3-SAC3(3’UTR)-hphNT1-GCN5(3’UTR)* and pYB1739 containing *SPT7-linker-NUP49-NUP49(3’UTR)hphNT1-SPT7(3’UTR)* were created by homologous recombination into pRS314. PCR fragments containing the fusions were treated with DpnI and gel-purified before integration into yeast. Integrations of the fusion proteins were verified by microscopy (TetR-fusions) or PCR (Gcn5-Sac3 and Spt7-Nup49). For all fusions the linker sequence is as described in (Gruber et al., 2006).

4.2 Fluorescent microscopy:

For microscopy cells were resuspended in non-fluorescent medium (SD –TRP) and either mounted on a glass cover slip (for still images or movies of max. 5 min duration) or immobilized on a 2% agar pad containing non-fluorescent medium.
To visualize the accumulated plasmids cells were grown on SD –URA to maintain the centromere on the plasmid, then shifted to SD -LEU containing β-Estradiol (1 μM final concentration; Sigma) to induce excision of the centromere (*rec-CEN4-URA3-*

rec) and to select for the presence of the plasmid. After 16-18 h a Deltavision microscope (Applied Precision) equipped with a CCD HQ2 camera (Roper), 250W Xenon laps, Softworx software (Applied Precision) and a temperature chamber set to 30°C was used to visualize the plasmids and the depicted proteins tagged with GFP. Time lapse movies of 5 min intervals for 1h taking 20 Z-stacks of 0.4 µm spacing were recorded with a 100x/1.4 NA objective and 2x2 binning. To determine the total NPC fluorescence integrated density was measured of the nucleus and background in sum projections using Image J (National Institutes of Health). After subtraction of the background the fluorescence was normalized by the median fluorescence of cells without plasmids. To determine fluorescence intensity the mean gray value of the NPC area adjacent to the accumulated circles (Ic) and the residual NPC area (Ir) was measured and normalized by the median intensity of Ir. For the percentage fluorescence segregated to the mother cell the integrated density of the nucleus in the mother and the bud was measured after nuclear division and after subtraction of the background the fluorescence in the mother was divided by the total fluorescence. Box plots represent the distribution of the measurements in single cells whereas whiskers reach from min to max, the box covers 50% of the data and the line depicts the median.

To investigate plasmid propagation the cells were kept on SD –URA medium and diluted in YEPD medium containing estradiol only 3 h before imaging. Cells were washed once using 1 x PBS buffer and then resuspended in non-fluorescent medium. Images were obtained using an Olympus BX50 microscope, equipped with a piezo motor, a monochromator light source, a CCD camera (Andor) and the TillVision software (TillPhotonics). Images were acquired with a 100x/1.4 NA objective, 2x2 binning and stacks of 20 focal slices. Maximal intensity projections were used to determine plasmid propagation (described below “plasmid retention assay”).

To determine plasmid localization, nuclear geometry and anaphase duration the Deltavision microscope was used (described above). Prior to analysis the images were deconvolved. For plasmid localization images were taken with an Olympus 100x/1.4 NA objective and 1x1 binning. 15 focal sections with 0.3 μm spacing were acquired. Nuclear geometry was analyzed using an Olympus 100x/1.4 NA objective, 1x1 binning and a 1.6x auxiliary magnification. Stacks of 15 sections and 0.2 μm spacing were obtained. Nuclear length and width was measured as illustrated in Fig.

2.2B using ImageJ and average nuclear width was calculated for different categories of nuclear length.

Anaphase duration was determined using an Olympus 60x/1.42 NA objective and 1x1 binning. 30 min movies were taken with 1 min between each stack of 8 sections and 0.6 μm spacing. Early anaphase was measured form the first time point the nucleus crossed the bud neck until the nucleus contracts as shown in the cartoon and representative pictures in Fig. 2.2A.

To investigate the enrichment of NPCs close to non-centromeric plasmids a Core Deltavision containing a CCD HQ camera (Roper) and solid state LEDs was used. An Olympus 100x/1.4 NA objective, 1x1 binning was used to create stacks of 15 focal sections and 0.2 μm spacing. Using ImageJ fluorescence intensity was measured along the nuclear rim. Nup82-3sfGFP intensity was normalized by its average intensity and TetR-mCherry intensity was normalized by its highest intensity in each cell. Afterwards all obtained traces were aligned by the peak of TetR-mCherry intensity.

To determine the speed of the non-centromeric plasmids cells were imaged 3h after centromere excision using the same Deltavision with LEDs. First a Z-stack of 16 sections and 0.3 µm spacing was recorded in CFP and YFP to visualize both the plasmid and the SPBs in order to select for the non-centromeric plasmids. Then the plasmid was followed in a time lapse movie taking the same stacks every 3 s for 3 min. The plasmids were tracked using Imaris (Bitplane) to determine their 3 dimensional coordinates. The coordinates were then used to determine the distance covered by the plasmid for each time point, which was deviated by 3 to determine the distance per second. All speed values were averaged for every plasmid, then averaged over all non-centromeric plasmids recorded and plotted in the graph.

4.3 FLIP and FRAP experiments:

Both FLIP and FRAP experiments were essentially done as described in (Boettcher et al., 2012). Briefly, to measure dynamics of NPCs in cells with and without accumulated plasmids cells were grown in SD -URA, restreaked on SD -LEU 16-18 h prior to imaging and then immobilized on a 2% agar pad containing non-fluorescent medium. A Zeiss LSM 780 laser confocal microscope (Zeiss Microimaging) with a 63x/1.4 NA objective and a multiarray 32PMT GaAsP detector controlled by the ZEN 2011 software (Carl Zeiss) was used for imaging. Bleaching was performed using a

488 nm argon laser at 2.6% laser intensity and 45% output. Repeated photobleaching was performed in the depicted area with 9s intervals for 30 time points. Afterwards the fluorescence intensity of Nup170-GFP was measured in the vicinity of the circles (Ic) and an area of the same size equidistant from the bleaching region (Io) using ImageJ. Both intensities were set to 100% prior to the first bleaching. Fluorescence decay was plotted for each cell using Prism (GraphPad Software) and t_{70} was defined as the time after which 70% of the initial intensity was still recorded. Finally, the average t_{70} of several cells was calculated for both Ic and Io and shown in the graph.

To determine the strength of the nuclear diffusion barrier a Zeiss LSM 510 microscope was used. Early anaphase cells were selected and photobleaching was applied on the depicted areas. To analyze the FLIP experiments the total integrated fluorescent density in both the mother and daughter part of the nucleus was measured. After subtracting the average fluorescent loss determined by 5 neighboring cells the fluorescent signal of the mother and daughter part were set to 100% at the beginning of the experiment. All experiments were pooled and analyzed using Prism to fit a one-phase decay curve. The barrier index was defined as the ratio of the times needed to lose 40% of the initial fluorescent signal in the bud over the mother compartment.

For the FRAP experiments the whole bud compartment of early anaphase nuclei were bleached and fluorescent recovery was measured in a constant area located in the bud. After subtracting the average fluorescent loss by imaging based on three neighboring cells the fluorescence after photobleaching was set to 0%. The fluorescence recovery was fitted to a one-phase association curve for each cell using Prism. T_{15} was defined as the time to recover 15% fluorescence. The average of t_{15} of all measured cells was calculated and is shown in the graph.

4.4 Plasmid retention assay:

Late anaphase or telophase cells containing one, two or four plasmids that did not co-localize with the spindle pole body were analyzed. Propagation frequency (pf) was calculated as $100-(xa+2y\sqrt{b}+4z\sqrt[4]{c})/(x+2y+4z)$, where a, b and c being the percentages of cells retaining all plasmids in the mother cell and x, y and z the number of cells counted for one, two or four plasmids, respectively.

Retention of pDS316 (Sinclair and Guarente, 1997) was analyzed using freshly transformed wt and mutant cells. Cells were grown on SD –ADE plates and then transferred to plates containing low amounts of adenine 3h before micromanipulations. Using microdissection techniques mother cells were separated from their daughter cells. After 3-5 days both the mother and the daughter cells formed a colony whereas the appearance of white sectors depicted whether the original cell contained pDS316.

4.5 Southern blot analysis of aged cells:

Old cells were purified following the protocol of the mother enrichment program (Lindstrom and Gottschling, 2009). Briefly, $2.5x10^8$ cells were labeled with Sulfo-NHS-LC-Biotin (Pierce) and recovered for 2h at 30°C prior to addition of β-Estradiol (1 μM final concentration). After either 26 h and 27.5 h or 34 h and 35.5 h (for wt and mutant cells) cells were washed, diluted in PBS and incubated with 25 μl streptavidin-coated magnetic beads (MicroMACS, Miltenyi Biotec) for 30 min at 4°C before purification using LS MACS columns (Miltenyi Biotec). Cells were eluted using 1xPBS containing 2 mM EDTA, pelleted and split into two fractions: 1) cells were incubated in 20 μg/ml calcofluor white and bud scars were counted using fluorescence microscopy; 2) cells were lysed and DNA was purified using standard methods. DNA content was measured performing qPCR amplifying *ACT1* as follows: genomic DNA from wt non-aged cells was used to generate a dilution curve. Simultaneously, three qPCRs for two different dilutions were run for each genomic DNA sample derived from the aged wt, *gcn5Δ* and *sgf73Δ* mutant cells. The average of the six qPCR values obtained for each strain was used to calculate the volume loaded on a 0.6% agarose gel containing ethidium bromide. The gel was run in TBE containing ethidium bromide for 24 h at 50 V at 4°C. The gel was blotted to transfer membrane (magnacharge nylon, GE Water&Process Tech.) using standard protocols. Membranes were hybridized with a ^{32}P labeled probe specific to the rDNA as described (Lindstrom et al., 2011) and visualized using a Typhoon phosphoimager (GE healthcare).

4.6 ChIP assay:

ChIP analysis was essentially done as described (Chymkowitch et al., 2012): Cells were fixed with 1% (wt/vol) formaldehyde for 30 min and quenched for 5 min using glycine (final conc. of 125 mM). Cells were washed with Tris-buffered saline, resuspended in lysis buffer and lysed in a cooled freezer mill (Spex) for 6 cycles (2 min with 2 min breaks each at 12 cps). Afterwards the samples were sonicated twice for 15 min by altering cycles of 30 s pulses followed by 30 s cool down periods using a Bioruptor (Diagenode). After centrifugation, supernatants were immunoprecipitated overnight at 4°C on anti-GFP beads (Chromotek). Washing steps and elution were performed as described (Chymkowitch et al., 2012). After RNase and proteinase K treatment, DNA fragments were purified using QIAquick PCR purification kit (Qiagen) and were analyzed by qPCR using a rotorgene qPCR system (Qiagen). Primer sequences were as follows:

ChrV: GAACAAGGTTACAAATCC and CCGATTTGTGAGATTCTTCCT

ARS: AGTAAAGATTTCGTGTTCATGCAG and ATAGTGAAGGAGCATGTTCGG

non-coding sequence (NCS1): GATACCTGAGTATTCCCACAG and CACACCGCATATGGTGCACTC

non-coding sequence (NCS2): CCGCTTACCGGATACCTGTC and ATCCTGTTACCAGTGGCTGC

Fold enrichment was calculated as IP/Input of protein X normalized by the same ratio measured in wt cells where no protein was tagged with GFP to correct for unspecific binding.

4.7 Microfluidic experiments:

Pore segregation during aging was followed using the microfluidics dissection platform (Huberts et al., 2013; Lee et al., 2012) with constant flow of synthetic complete medium at 1µl / min and a Eclipse Ti fluorescent microscope (Nikon Instruments) controlled by Micro-Manager 1.4 software (µManager). Images were acquired with a Plan Apo lambda 60x/1.4 NA objective and a Orca R2 CCD camera (Hamamatsu). Cell growth and budding events were monitored by capturing images using transmitted light every 20 min. Fluorescent images were taken after 24 h and 36 h for short-lived strains (e.g. *sir2Δ* cells) and after 48 h and 64 h for normal or long-lived strains using a mercury lamp as a light source (Intensilight, Nikon

Instruments). Stacks of 14 slices covering a range of 7 µm were captured every 15 min for 2 h, to follow the nuclear division. Nuclei of cells of different ages were analyzed using sum projections of the fluorescence images from both time points (48 h and 64 h). Total fluorescence (integrated density) was measured in the mother and daughter cell after nuclear division using ImageJ. After background subtraction the values were grouped by the indicated age categories of the mother cells, normalized by the median of the daughter cells in the youngest age category and plotted using Prism. Alternatively, the fluorescence in the mother cells was divided by the total fluorescence (mother plus daughter cell) for each cell and plotted against the age of the mother cell to visualize the increase in asymmetry with age. This data was used to fit a one-phase association curve, which is shown in the graph. Additionally, 10 values were grouped age-dependently and plotted showing the average age and percentage of fluorescence segregated to the mother cell as well as the standard deviations. For G1 cells the total amount of NPCs (integrated density) was measured, plotted against their age and an exponential curve was fitted using Prism. The values were then normalized by intersection of the curve with the Y-axis and set to 1. The dots on the graph were created from 10 values as described for the dividing cells. Similarly, the mean fluorescence intensity (integrated density divided by area) was plotted in (Fig. 2.9). The radius of the G1 nuclei was measured drawing a line through the nucleus at its broadest area using ImageJ, dividing it by 2 and plotting it against the age of the cell.

4.8 Lifespan analysis:

Pedigree analysis was done as described (Shcheprova et al., 2008): Freshly streaked cells were restreaked on YPD plates and 2h later virgin daughter cells were placed to analyze their lifespan. Over night the cells were kept at 4°C (max. 10-12h). Micromanipulation was performed using a Zeiss Axioscope 40 microdissection microscope (Zeiss). Lifespan curves were analyzed using Prism.

4.9 Mammalian cells:

HeLa cells were grown in Dulbecco's modified Eagle's medium (DMEM) containing 10% FCS at 37°C and with 5% CO_2. Transfections were performed using Fugene

transfection reagent (Promega) and Optimem medium (Invitrogen). 1 µg DNA was used for transfection. Cells were imaged in FCS and Leibowitz medium (Sigma).

4.10 Statistics:

One-way ANOVA followed by Dunnett's multiple comparison was used to test for significance except the lifespan curves, which were compared using Log-rank (Mantel-Cox) tests and the ChIP experiment, for which a paired t-test (within the same experiment) was used.

5. References

Aguilaniu, H., Gustafsson, L., Rigoulet, M., and Nystrom, T. (2003). Asymmetric inheritance of oxidatively damaged proteins during cytokinesis. Science *299*, 1751-1753.

Alberti, S., Halfmann, R., King, O., Kapila, A., and Lindquist, S. (2009). A systematic survey identifies prions and illuminates sequence features of prionogenic proteins. Cell *137*, 146-158.

Ansari, A., and Gartenberg, M.R. (1997). The yeast silent information regulator Sir4p anchors and partitions plasmids. Mol Cell Biol *17*, 7061-7068.

Armstrong, J. (2010). Yeast vacuoles: more than a model lysosome. Trends Cell Biol *20*, 580-585.

Baker, S.P., and Grant, P.A. (2007). The SAGA continues: expanding the cellular role of a transcriptional co-activator complex. Oncogene *26*, 5329-5340.

Barros, M.H., Bandy, B., Tahara, E.B., and Kowaltowski, A.J. (2004). Higher respiratory activity decreases mitochondrial reactive oxygen release and increases life span in Saccharomyces cerevisiae. J Biol Chem *279*, 49883-49888.

Barton, A.A. (1950). Some aspects of cell division in saccharomyces cerevisiae. J Gen Microbiol *4*, 84-86.

Benner, S.E., Wahl, G.M., and Von Hoff, D.D. (1991). Double minute chromosomes and homogeneously staining regions in tumors taken directly from patients versus in human tumor cell lines. Anticancer Drugs *2*, 11-25.

Bian, C., Xu, C., Ruan, J., Lee, K.K., Burke, T.L., Tempel, W., Barsyte, D., Li, J., Wu, M., Zhou, B.O*., et al.* (2011). Sgf29 binds histone H3K4me2/3 and is required for SAGA complex recruitment and histone H3 acetylation. EMBO J *30*, 2829-2842.

Bodnar, A.G., Ouellette, M., Frolkis, M., Holt, S.E., Chiu, C.P., Morin, G.B., Harley, C.B., Shay, J.W., Lichtsteiner, S., and Wright, W.E. (1998). Extension of life-span by introduction of telomerase into normal human cells. Science *279*, 349-352.

Boettcher, B., Marquez-Lago, T.T., Bayer, M., Weiss, E.L., and Barral, Y. (2012). Nuclear envelope morphology constrains diffusion and promotes asymmetric protein segregation in closed mitosis. J Cell Biol *197*, 921-937.

Bonnet, J., Wang, C.Y., Baptista, T., Vincent, S.D., Hsiao, W.C., Stierle, M., Kao, C.F., Tora, L., and Devys, D. (2014). The SAGA coactivator complex acts on the whole transcribed genome and is required for RNA polymerase II transcription. Genes Dev *28*, 1999-2012.

Borghouts, C., Benguria, A., Wawryn, J., and Jazwinski, S.M. (2004). Rtg2 protein links metabolism and genome stability in yeast longevity. Genetics *166*, 765-777.

Brownell, J.E., Zhou, J., Ranalli, T., Kobayashi, R., Edmondson, D.G., Roth, S.Y., and Allis, C.D. (1996). Tetrahymena histone acetyltransferase A: a homolog to yeast Gcn5p linking histone acetylation to gene activation. Cell *84*, 843-851.

Bufalino, M.R., DeVeale, B., and van der Kooy, D. (2013). The asymmetric segregation of damaged proteins is stem cell-type dependent. J Cell Biol *201*, 523-530.

Bupp, J.M., Martin, A.E., Stensrud, E.S., and Jaspersen, S.L. (2007). Telomere anchoring at the nuclear periphery requires the budding yeast Sad1-UNC-84 domain protein Mps3. J Cell Biol *179*, 845-854.

Burtner, C.R., and Kennedy, B.K. (2010). Progeria syndromes and ageing: what is the connection? Nat Rev Mol Cell Biol *11*, 567-578.

Butow, R.A., and Avadhani, N.G. (2004). Mitochondrial signaling: the retrograde response. Mol Cell *14*, 1-15.

Carr, L.L., and Gottschling, D.E. (2008). Does age influence loss of heterozygosity? Exp Gerontol *43*, 123-129.

Chadrin, A., Hess, B., San Roman, M., Gatti, X., Lombard, B., Loew, D., Barral, Y., Palancade, B., and Doye, V. (2010). Pom33, a novel transmembrane nucleoporin required for proper nuclear pore complex distribution. J Cell Biol *189*, 795-811.

Chao, J.T., Wong, A.K., Tavassoli, S., Young, B.P., Chruscicki, A., Fang, N.N., Howe, L.J., Mayor, T., Foster, L.J., and Loewen, C.J. (2014). Polarization of the Endoplasmic Reticulum by ER-Septin Tethering. Cell *158*, 620-632.

Chymkowitch, P., Eldholm, V., Lorenz, S., Zimmermann, C., Lindvall, J.M., Bjoras, M., Meza-Zepeda, L.A., and Enserink, J.M. (2012). Cdc28 kinase activity regulates the basal transcription machinery at a subset of genes. Proc Natl Acad Sci U S A *109*, 10450-10455.

Clay, L., Caudron, F., Denoth-Lippuner, A., Boettcher, B., Buvelot Frei, S., Snapp, E.L., and Barral, Y. (2014). A sphingolipid-dependent diffusion barrier confines ER stress to the yeast mother cell. Elife *3*, e01883.

Cohen, S., Agmon, N., Sobol, O., and Segal, D. (2010). Extrachromosomal circles of satellite repeats and 5S ribosomal DNA in human cells. Mob DNA *1*, 11.

Colombi, P., Webster, B.M., Frohlich, F., and Lusk, C.P. (2013). The transmission of nuclear pore complexes to daughter cells requires a cytoplasmic pool of Nsp1. J Cell Biol *203*, 215-232.

Conrad-Webb, H., and Butow, R.A. (1995). A polymerase switch in the synthesis of rRNA in Saccharomyces cerevisiae. Mol Cell Biol *15*, 2420-2428.

Cook, C.E., Hochstrasser, M., and Kerscher, O. (2009). The SUMO-targeted ubiquitin ligase subunit Slx5 resides in nuclear foci and at sites of DNA breaks. Cell Cycle *8*, 1080-1089.

D'Mello, N.P., and Jazwinski, S.M. (1991). Telomere length constancy during aging of Saccharomyces cerevisiae. J Bacteriol *173*, 6709-6713.

Dang, W., Steffen, K.K., Perry, R., Dorsey, J.A., Johnson, F.B., Shilatifard, A., Kaeberlein, M., Kennedy, B.K., and Berger, S.L. (2009). Histone H4 lysine 16 acetylation regulates cellular lifespan. Nature *459*, 802-807.

Dechat, T., Pfleghaar, K., Sengupta, K., Shimi, T., Shumaker, D.K., Solimando, L., and Goldman, R.D. (2008). Nuclear lamins: major factors in the structural organization and function of the nucleus and chromatin. Genes Dev *22*, 832-853.

Defossez, P.A., Prusty, R., Kaeberlein, M., Lin, S.J., Ferrigno, P., Silver, P.A., Keil, R.L., and Guarente, L. (1999). Elimination of replication block protein Fob1 extends the life span of yeast mother cells. Mol Cell *3*, 447-455.

Dieppois, G., and Stutz, F. (2010). Connecting the transcription site to the nuclear pore: a multi-tether process that regulates gene expression. J Cell Sci *123*, 1989-1999.

Dilworth, D.J., Suprapto, A., Padovan, J.C., Chait, B.T., Wozniak, R.W., Rout, M.P., and Aitchison, J.D. (2001). Nup2p dynamically associates with the distal regions of the yeast nuclear pore complex. J Cell Biol *153*, 1465-1478.

Egilmez, N.K., and Jazwinski, S.M. (1989). Evidence for the involvement of a cytoplasmic factor in the aging of the yeast Saccharomyces cerevisiae. J Bacteriol *171*, 37-42.

Eisenberg, T., Knauer, H., Schauer, A., Buttner, S., Ruckenstuhl, C., Carmona-Gutierrez, D., Ring, J., Schroeder, S., Magnes, C., Antonacci, L.*, et al.* (2009). Induction of autophagy by spermidine promotes longevity. Nat Cell Biol *11*, 1305-1314.

Eldakak, A., Rancati, G., Rubinstein, B., Paul, P., Conaway, V., and Li, R. (2010). Asymmetrically inherited multidrug resistance transporters are recessive determinants in cellular replicative ageing. Nat Cell Biol *12*, 799-805.

Enomoto, S., Longtine, M.S., and Berman, J. (1994). Enhancement of telomere-plasmid segregation by the X-telomere associated sequence in Saccharomyces cerevisiae involves SIR2, SIR3, SIR4 and ABF1. Genetics *136*, 757-767.

Erjavec, N., Larsson, L., Grantham, J., and Nystrom, T. (2007). Accelerated aging and failure to segregate damaged proteins in Sir2 mutants can be suppressed by overproducing the protein aggregation-remodeling factor Hsp104p. Genes Dev *21*, 2410-2421.

Erjavec, N., and Nystrom, T. (2007). Sir2p-dependent protein segregation gives rise to a superior reactive oxygen species management in the progeny of Saccharomyces cerevisiae. Proc Natl Acad Sci U S A *104*, 10877-10881.

Fabrizio, P., Hoon, S., Shamalnasab, M., Galbani, A., Wei, M., Giaever, G., Nislow, C., and Longo, V.D. (2010). Genome-wide screen in Saccharomyces cerevisiae identifies vacuolar protein sorting, autophagy, biosynthetic, and tRNA methylation genes involved in life span regulation. PLoS Genet *6*, e1001024.

Feser, J., Truong, D., Das, C., Carson, J.J., Kieft, J., Harkness, T., and Tyler, J.K. (2010). Elevated histone expression promotes life span extension. Mol Cell *39*, 724-735.

Fuentealba, L.C., Eivers, E., Geissert, D., Taelman, V., and De Robertis, E.M. (2008). Asymmetric mitosis: Unequal segregation of proteins destined for degradation. Proc Natl Acad Sci U S A *105*, 7732-7737.

Futcher, A.B., and Cox, B.S. (1984). Copy number and the stability of 2-micron circle-based artificial plasmids of Saccharomyces cerevisiae. J Bacteriol *157*, 283-290.

Ganley, A.R., Ide, S., Saka, K., and Kobayashi, T. (2009). The effect of replication initiation on gene amplification in the rDNA and its relationship to aging. Mol Cell *35*, 683-693.

Gebre, S., Connor, R., Xia, Y., Jawed, S., Bush, J.M., Bard, M., Elsalloukh, H., and Tang, F. (2012). Osh6 overexpression extends the lifespan of yeast by increasing vacuole fusion. Cell Cycle *11*, 2176-2188.

Gehlen, L.R., Nagai, S., Shimada, K., Meister, P., Taddei, A., and Gasser, S.M. (2011). Nuclear geometry and rapid mitosis ensure asymmetric episome segregation in yeast. Curr Biol *21*, 25-33.

Gillespie, C.S., Proctor, C.J., Boys, R.J., Shanley, D.P., Wilkinson, D.J., and Kirkwood, T.B. (2004). A mathematical model of ageing in yeast. J Theor Biol *229*, 189-196.

Gotta, M., Laroche, T., Formenton, A., Maillet, L., Scherthan, H., and Gasser, S.M. (1996). The clustering of telomeres and colocalization with Rap1, Sir3, and Sir4 proteins in wild-type Saccharomyces cerevisiae. J Cell Biol *134*, 1349-1363.

Gottlieb, S., and Esposito, R.E. (1989). A new role for a yeast transcriptional silencer gene, SIR2, in regulation of recombination in ribosomal DNA. Cell *56*, 771-776.

Grant, P.A., Duggan, L., Cote, J., Roberts, S.M., Brownell, J.E., Candau, R., Ohba, R., Owen-Hughes, T., Allis, C.D., Winston, F.*, et al.* (1997). Yeast Gcn5 functions in two multisubunit complexes to acetylate nucleosomal histones: characterization of an Ada complex and the SAGA (Spt/Ada) complex. Genes Dev *11*, 1640-1650.

Green, E.M., Jiang, Y., Joyner, R., and Weis, K. (2012). A negative feedback loop at the nuclear periphery regulates GAL gene expression. Mol Biol Cell *23*, 1367-1375.

Gruber, S., Arumugam, P., Katou, Y., Kuglitsch, D., Helmhart, W., Shirahige, K., and Nasmyth, K. (2006). Evidence that loading of cohesin onto chromosomes involves opening of its SMC hinge. Cell *127*, 523-537.

Grund, S.E., Fischer, T., Cabal, G.G., Antunez, O., Perez-Ortin, J.E., and Hurt, E. (2008). The inner nuclear membrane protein Src1 associates with subtelomeric genes and alters their regulated gene expression. J Cell Biol *182*, 897-910.

Guttinger, S., Laurell, E., and Kutay, U. (2009). Orchestrating nuclear envelope disassembly and reassembly during mitosis. Nat Rev Mol Cell Biol *10*, 178-191.

Harman, D. (1956). Aging: a theory based on free radical and radiation chemistry. J Gerontol *11*, 298-300.

Hatch, E.M., Fischer, A.H., Deerinck, T.J., and Hetzer, M.W. (2013). Catastrophic nuclear envelope collapse in cancer cell micronuclei. Cell *154*, 47-60.

Hediger, F., Neumann, F.R., Van Houwe, G., Dubrana, K., and Gasser, S.M. (2002). Live imaging of telomeres: yKu and Sir proteins define redundant telomere-anchoring pathways in yeast. Curr Biol *12*, 2076-2089.

Henderson, K.A., and Gottschling, D.E. (2008). A mother's sacrifice: what is she keeping for herself? Curr Opin Cell Biol *20*, 723-728.

Hoffelder, D.R., Luo, L., Burke, N.A., Watkins, S.C., Gollin, S.M., and Saunders, W.S. (2004). Resolution of anaphase bridges in cancer cells. Chromosoma *112*, 389-397.

Hornsby, P.J. (2007). Telomerase and the aging process. Exp Gerontol *42*, 575-581.

Huberts, D.H., Sik Lee, S., Gonzales, J., Janssens, G.E., Vizcarra, I.A., and Heinemann, M. (2013). Construction and use of a microfluidic dissection platform for long-term imaging of cellular processes in budding yeast. Nat Protoc *8*, 1019-1027.

Hughes, A.L., and Gottschling, D.E. (2012). An early age increase in vacuolar pH limits mitochondrial function and lifespan in yeast. Nature *492*, 261-265.

Huisinga, K.L., and Pugh, B.F. (2004). A genome-wide housekeeping role for TFIID and a highly regulated stress-related role for SAGA in Saccharomyces cerevisiae. Mol Cell *13*, 573-585.

Hyman, B.C., Cramer, J.H., and Rownd, R.H. (1982). Properties of a Saccharomyces cerevisiae mtDNA segment conferring high-frequency yeast transformation. Proc Natl Acad Sci U S A *79*, 1578-1582.

Itoh, N., and Shimizu, N. (1998). DNA replication-dependent intranuclear relocation of double minute chromatin. J Cell Sci *111 (Pt 22)*, 3275-3285.

Janke, C., Magiera, M.M., Rathfelder, N., Taxis, C., Reber, S., Maekawa, H., Moreno-Borchart, A., Doenges, G., Schwob, E., Schiebel, E.*, et al.* (2004). A versatile toolbox for PCR-based tagging of yeast genes: new fluorescent proteins, more markers and promoter substitution cassettes. Yeast *21*, 947-962.

Jaspersen, S.L., and Ghosh, S. (2012). Nuclear envelope insertion of spindle pole bodies and nuclear pore complexes. Nucleus *3*, 226-236.

Jazwinski, S.M. (2005). Rtg2 protein: at the nexus of yeast longevity and aging. FEMS Yeast Res *5*, 1253-1259.

Johnston, J.R. (1966). Reproductive capacity and mode of death of yeast cells. Antonie Van Leeuwenhoek *32*, 94-98.

Kaeberlein, M., and Kennedy, B.K. (2005). Large-scale identification in yeast of conserved ageing genes. Mech Ageing Dev *126*, 17-21.

Kaeberlein, M., McVey, M., and Guarente, L. (1999). The SIR2/3/4 complex and SIR2 alone promote longevity in Saccharomyces cerevisiae by two different mechanisms. Genes Dev *13*, 2570-2580.

Kaganovich, D., Kopito, R., and Frydman, J. (2008). Misfolded proteins partition between two distinct quality control compartments. Nature *454*, 1088-1095.

Kennedy, B.K., Austriaco, N.R., Jr., and Guarente, L. (1994). Daughter cells of Saccharomyces cerevisiae from old mothers display a reduced life span. J Cell Biol *127*, 1985-1993.

Khmelinskii, A., Keller, P.J., Lorenz, H., Schiebel, E., and Knop, M. (2010). Segregation of yeast nuclear pores. Nature *466*, E1.

Khmelinskii, A., Meurer, M., Knop, M., and Schiebel, E. (2011). Artificial tethering to nuclear pores promotes partitioning of extrachromosomal DNA during yeast asymmetric cell division. Curr Biol *21*, R17-18.

Kimmerly, W.J., and Rine, J. (1987). Replication and segregation of plasmids containing cis-acting regulatory sites of silent mating-type genes in Saccharomyces cerevisiae are controlled by the SIR genes. Mol Cell Biol *7*, 4225-4237.

Kirchman, P.A., Kim, S., Lai, C.Y., and Jazwinski, S.M. (1999). Interorganelle signaling is a determinant of longevity in Saccharomyces cerevisiae. Genetics *152*, 179-190.

Kirkwood, T.B., and Melov, S. (2011). On the programmed/non-programmed nature of ageing within the life history. Curr Biol *21*, R701-707.

Kitagawa, K., and Hieter, P. (2001). Evolutionary conservation between budding yeast and human kinetochores. Nat Rev Mol Cell Biol *2*, 678-687.

Klinger, H., Rinnerthaler, M., Lam, Y.T., Laun, P., Heeren, G., Klocker, A., Simon-Nobbe, B., Dickinson, J.R., Dawes, I.W., and Breitenbach, M. (2010). Quantitation of (a)symmetric inheritance of functional and of oxidatively damaged mitochondrial aconitase in the cell division of old yeast mother cells. Exp Gerontol *45*, 533-542.

Kobayashi, T., and Horiuchi, T. (1996). A yeast gene product, Fob1 protein, required for both replication fork blocking and recombinational hotspot activities. Genes Cells *1*, 465-474.

Kobayashi, T., Horiuchi, T., Tongaonkar, P., Vu, L., and Nomura, M. (2004). SIR2 regulates recombination between different rDNA repeats, but not recombination within individual rRNA genes in yeast. Cell *117*, 441-453.

Kohler, A., Schneider, M., Cabal, G.G., Nehrbass, U., and Hurt, E. (2008). Yeast Ataxin-7 links histone deubiquitination with gene gating and mRNA export. Nat Cell Biol *10*, 707-715.

Kowaltowski, A.J., de Souza-Pinto, N.C., Castilho, R.F., and Vercesi, A.E. (2009). Mitochondria and reactive oxygen species. Free Radic Biol Med *47*, 333-343.

Kumaran, R.I., and Spector, D.L. (2008). A genetic locus targeted to the nuclear periphery in living cells maintains its transcriptional competence. J Cell Biol *180*, 51-65.

Kuo, M.H., Brownell, J.E., Sobel, R.E., Ranalli, T.A., Cook, R.G., Edmondson, D.G., Roth, S.Y., and Allis, C.D. (1996). Transcription-linked acetylation by Gcn5p of histones H3 and H4 at specific lysines. Nature *383*, 269-272.

Lai, C.Y., Jaruga, E., Borghouts, C., and Jazwinski, S.M. (2002). A mutation in the ATP2 gene abrogates the age asymmetry between mother and daughter cells of the yeast Saccharomyces cerevisiae. Genetics *162*, 73-87.

Larionov, V.L., Grishin, A.V., and Smirnov, M.N. (1980). 3 micron DNA - an extrachromosomal ribosomal DNA in the yeast Saccharomyces cerevisiae. Gene *12*, 41-49.

Larschan, E., and Winston, F. (2001). The S. cerevisiae SAGA complex functions in vivo as a coactivator for transcriptional activation by Gal4. Genes Dev *15*, 1946-1956.

Laun, P., Pichova, A., Madeo, F., Fuchs, J., Ellinger, A., Kohlwein, S., Dawes, I., Frohlich, K.U., and Breitenbach, M. (2001). Aged mother cells of Saccharomyces cerevisiae show markers of oxidative stress and apoptosis. Mol Microbiol *39*, 1166-1173.

Lee, S.S., Avalos Vizcarra, I., Huberts, D.H., Lee, L.P., and Heinemann, M. (2012). Whole lifespan microscopic observation of budding yeast aging through a microfluidic dissection platform. Proc Natl Acad Sci U S A *109*, 4916-4920.

Li, S.C., and Kane, P.M. (2009). The yeast lysosome-like vacuole: endpoint and crossroads. Biochim Biophys Acta *1793*, 650-663.

Li, Z., Zhu, Y., Zhai, Y., M, R.C., Bao, Y., White, T.E., and Glavy, J.S. (2013). Werner complex deficiency in cells disrupts the Nuclear Pore Complex and the distribution of lamin B1. Biochim Biophys Acta *1833*, 3338-3345.

Lin, S.J., Defossez, P.A., and Guarente, L. (2000). Requirement of NAD and SIR2 for life-span extension by calorie restriction in Saccharomyces cerevisiae. Science *289*, 2126-2128.

Lindstrom, D.L., and Gottschling, D.E. (2009). The mother enrichment program: a genetic system for facile replicative life span analysis in Saccharomyces cerevisiae. Genetics *183*, 413-422, 411SI-413SI.

Lindstrom, D.L., Leverich, C.K., Henderson, K.A., and Gottschling, D.E. (2011). Replicative age induces mitotic recombination in the ribosomal RNA gene cluster of Saccharomyces cerevisiae. PLoS Genet *7*, e1002015.

Liu, B., Larsson, L., Caballero, A., Hao, X., Oling, D., Grantham, J., and Nystrom, T. (2010). The polarisome is required for segregation and retrograde transport of protein aggregates. Cell *140*, 257-267.

Longo, V.D., Shadel, G.S., Kaeberlein, M., and Kennedy, B. (2012). Replicative and chronological aging in Saccharomyces cerevisiae. Cell Metab *16*, 18-31.

Luedeke, C., Frei, S.B., Sbalzarini, I., Schwarz, H., Spang, A., and Barral, Y. (2005). Septin-dependent compartmentalization of the endoplasmic reticulum during yeast polarized growth. J Cell Biol *169*, 897-908.

Lundblad, V., and Szostak, J.W. (1989). A mutant with a defect in telomere elongation leads to senescence in yeast. Cell *57*, 633-643.

Luthra, R., Kerr, S.C., Harreman, M.T., Apponi, L.H., Fasken, M.B., Ramineni, S., Chaurasia, S., Valentini, S.R., and Corbett, A.H. (2007). Actively transcribed GAL genes can be physically linked to the nuclear pore by the SAGA chromatin modifying complex. J Biol Chem *282*, 3042-3049.

Makio, T., Lapetina, D.L., and Wozniak, R.W. (2013). Inheritance of yeast nuclear pore complexes requires the Nsp1p subcomplex. J Cell Biol *203*, 187-196.

Managbanag, J.R., Witten, T.M., Bonchev, D., Fox, L.A., Tsuchiya, M., Kennedy, B.K., and Kaeberlein, M. (2008). Shortest-path network analysis is a useful approach toward identifying genetic determinants of longevity. PLoS One *3*, e3802.

Market, E., and Papavasiliou, F.N. (2003). V(D)J recombination and the evolution of the adaptive immune system. PLoS Biol *1*, E16.

Martin, G.M., and Oshima, J. (2000). Lessons from human progeroid syndromes. Nature *408*, 263-266.

Matecic, M., Smith, D.L., Pan, X., Maqani, N., Bekiranov, S., Boeke, J.D., and Smith, J.S. (2010). A microarray-based genetic screen for yeast chronological aging factors. PLoS Genet *6*, e1000921.

McCormick, M.A., Mason, A.G., Guyenet, S.J., Dang, W., Garza, R.M., Ting, M.K., Moller, R.M., Berger, S.L., Kaeberlein, M., Pillus, L.*, et al.* (2014). The SAGA Histone Deubiquitinase Module Controls Yeast Replicative Lifespan via Sir2 Interaction. Cell Rep *8*, 477-486.

McCullough, S.D., and Grant, P.A. (2010). Histone acetylation, acetyltransferases, and ataxia--alteration of histone acetylation and chromatin dynamics is implicated in the pathogenesis of polyglutamine-expansion disorders. Adv Protein Chem Struct Biol *79*, 165-203.

McFaline-Figueroa, J.R., Vevea, J., Swayne, T.C., Zhou, C., Liu, C., Leung, G., Boldogh, I.R., and Pon, L.A. (2011). Mitochondrial quality control during inheritance is associated with lifespan and mother-daughter age asymmetry in budding yeast. Aging Cell *10*, 885-895.

McMurray, M.A., and Gottschling, D.E. (2003). An age-induced switch to a hyper-recombinational state. Science *301*, 1908-1911.

Mearini, G., Nielsen, P.E., and Fackelmayer, F.O. (2004). Localization and dynamics of small circular DNA in live mammalian nuclei. Nucleic Acids Res *32*, 2642-2651.

Megee, P.C., and Koshland, D. (1999). A functional assay for centromere-associated sister chromatid cohesion. Science *285*, 254-257.

Meinema, A.C., Laba, J.K., Hapsari, R.A., Otten, R., Mulder, F.A., Kralt, A., van den Bogaart, G., Lusk, C.P., Poolman, B., and Veenhoff, L.M. (2011). Long unfolded linkers facilitate membrane protein import through the nuclear pore complex. Science *333*, 90-93.

Menendez-Benito, V., van Deventer, S.J., Jimenez-Garcia, V., Roy-Luzarraga, M., van Leeuwen, F., and Neefjes, J. (2013). Spatiotemporal analysis of organelle and macromolecular complex inheritance. Proc Natl Acad Sci U S A *110*, 175-180.

Merker, R.J., and Klein, H.L. (2002). hpr1Delta affects ribosomal DNA recombination and cell life span in Saccharomyces cerevisiae. Mol Cell Biol *22*, 421-429.

Mortimer, R.K., and Johnston, J.R. (1959). Life span of individual yeast cells. Nature *183*, 1751-1752.

Mullen, J.R., Kaliraman, V., Ibrahim, S.S., and Brill, S.J. (2001). Requirement for three novel protein complexes in the absence of the Sgs1 DNA helicase in Saccharomyces cerevisiae. Genetics *157*, 103-118.

Muller, I. (1985). Parental age and the life-span of zygotes of Saccharomyces cerevisiae. Antonie Van Leeuwenhoek *51*, 1-10.

Ohtsuki, K., Kasahara, K., Shirahige, K., and Kokubo, T. (2010). Genome-wide localization analysis of a complete set of Tafs reveals a specific effect of the taf1 mutation on Taf2 occupancy and provides indirect evidence for different TFIID conformations at different promoters. Nucleic Acids Res *38*, 1805-1820.

Palmer, E. (2003). Negative selection--clearing out the bad apples from the T-cell repertoire. Nat Rev Immunol *3*, 383-391.

Parikh, V.S., Morgan, M.M., Scott, R., Clements, L.S., and Butow, R.A. (1987). The mitochondrial genotype can influence nuclear gene expression in yeast. Science *235*, 576-580.

Parsell, D.A., Kowal, A.S., Singer, M.A., and Lindquist, S. (1994). Protein disaggregation mediated by heat-shock protein Hsp104. Nature *372*, 475-478.

Pascual-Garcia, P., and Rodriguez-Navarro, S. (2009). A tale of coupling, Sus1 function in transcription and mRNA export. RNA Biol *6*, 141-144.

Petes, T.D., and Botstein, D. (1977). Simple Mendelian inheritance of the reiterated ribosomal DNA of yeast. Proc Natl Acad Sci U S A *74*, 5091-5095.

Poole, A.M., Kobayashi, T., and Ganley, A.R. (2012). A positive role for yeast extrachromosomal rDNA circles? Extrachromosomal ribosomal DNA circle accumulation during the retrograde response may suppress mitochondrial cheats in yeast through the action of TAR1. Bioessays *34*, 725-729.

Pray-Grant, M.G., Daniel, J.A., Schieltz, D., Yates, J.R., 3rd, and Grant, P.A. (2005). Chd1 chromodomain links histone H3 methylation with SAGA- and SLIK-dependent acetylation. Nature *433*, 434-438.

Rao, X., Zhang, Y., Yi, Q., Hou, H., Xu, B., Chu, L., Huang, Y., Zhang, W., Fenech, M., and Shi, Q. (2008). Multiple origins of spontaneously arising micronuclei in HeLa cells: direct evidence from long-term live cell imaging. Mutat Res *646*, 41-49.

Reznick, D.N., Bryant, M.J., Roff, D., Ghalambor, C.K., and Ghalambor, D.E. (2004). Effect of extrinsic mortality on the evolution of senescence in guppies. Nature *431*, 1095-1099.

Ristow, M., and Schmeisser, S. (2011). Extending life span by increasing oxidative stress. Free Radic Biol Med *51*, 327-336.

Ristow, M., and Zarse, K. (2010). How increased oxidative stress promotes longevity and metabolic health: The concept of mitochondrial hormesis (mitohormesis). Exp Gerontol *45*, 410-418.

Rodriguez-Navarro, S., Fischer, T., Luo, M.J., Antunez, O., Brettschneider, S., Lechner, J., Perez-Ortin, J.E., Reed, R., and Hurt, E. (2004). Sus1, a functional component of the SAGA histone acetylase complex and the nuclear pore-associated mRNA export machinery. Cell *116*, 75-86.

Rohner, S., Gasser, S.M., and Meister, P. (2008). Modules for cloning-free chromatin tagging in Saccharomyces cerevisae. Yeast *25*, 235-239.

Rubinsztein, D.C., Marino, G., and Kroemer, G. (2011). Autophagy and aging. Cell *146*, 682-695.

Rudolph, K.L., Chang, S., Lee, H.W., Blasco, M., Gottlieb, G.J., Greider, C., and DePinho, R.A. (1999). Longevity, stress response, and cancer in aging telomerase-deficient mice. Cell *96*, 701-712.

Saka, K., Ide, S., Ganley, A.R., and Kobayashi, T. (2013). Cellular senescence in yeast is regulated by rDNA noncoding transcription. Curr Biol *23*, 1794-1798.

Schleit, J., Johnson, S.C., Bennett, C.F., Simko, M., Trongtham, N., Castanza, A., Hsieh, E.J., Moller, R.M., Wasko, B.M., Delaney, J.R.*, et al.* (2013). Molecular mechanisms underlying genotype-dependent responses to dietary restriction. Aging Cell *12*, 1050-1061.

Sharma, P.K., Agrawal, V., and Roy, N. (2011). Mitochondria-mediated hormetic response in life span extension of calorie-restricted Saccharomyces cerevisiae. Age (Dordr) *33*, 143-154.

Shcheprova, Z., Baldi, S., Frei, S.B., Gonnet, G., and Barral, Y. (2008). A mechanism for asymmetric segregation of age during yeast budding. Nature *454*, 728-734.

Shibata, Y., Kumar, P., Layer, R., Willcox, S., Gagan, J.R., Griffith, J.D., and Dutta, A. (2012). Extrachromosomal microDNAs and chromosomal microdeletions in normal tissues. Science *336*, 82-86.

Shimizu, N. (2011). Molecular mechanisms of the origin of micronuclei from extrachromosomal elements. Mutagenesis *26*, 119-123.

Shimizu, N., Kamezaki, F., and Shigematsu, S. (2005). Tracking of microinjected DNA in live cells reveals the intracellular behavior and elimination of extrachromosomal genetic material. Nucleic Acids Res *33*, 6296-6307.

Shimizu, N., Misaka, N., and Utani, K. (2007). Nonselective DNA damage induced by a replication inhibitor results in the selective elimination of extrachromosomal double minutes from human cancer cells. Genes Chromosomes Cancer *46*, 865-874.

Shimizu, N., Shimura, T., and Tanaka, T. (2000). Selective elimination of acentric double minutes from cancer cells through the extrusion of micronuclei. Mutat Res *448*, 81-90.

Sinclair, D.A., and Guarente, L. (1997). Extrachromosomal rDNA circles--a cause of aging in yeast. Cell *91*, 1033-1042.

Sinclair, D.A., Mills, K., and Guarente, L. (1997). Accelerated aging and nucleolar fragmentation in yeast sgs1 mutants. Science *277*, 1313-1316.

Singer, M.S., and Gottschling, D.E. (1994). TLC1: template RNA component of Saccharomyces cerevisiae telomerase. Science *266*, 404-409.

Spokoini, R., Moldavski, O., Nahmias, Y., England, J.L., Schuldiner, M., and Kaganovich, D. (2012). Confinement to organelle-associated inclusion structures mediates asymmetric inheritance of aggregated protein in budding yeast. Cell Rep *2*, 738-747.

Stadtman, E.R. (2006). Protein oxidation and aging. Free Radic Res *40*, 1250-1258.

Suka, N., Luo, K., and Grunstein, M. (2002). Sir2p and Sas2p opposingly regulate acetylation of yeast histone H4 lysine16 and spreading of heterochromatin. Nat Genet *32*, 378-383.

Swiecilo, A., Krawiec, Z., Wawryn, J., Bartosz, G., and Bilinski, T. (2000). Effect of stress on the life span of the yeast Saccharomyces cerevisiae. Acta Biochim Pol *47*, 355-364.

Taddei, A., Van Houwe, G., Hediger, F., Kalck, V., Cubizolles, F., Schober, H., and Gasser, S.M. (2006). Nuclear pore association confers optimal expression levels for an inducible yeast gene. Nature *441*, 774-778.

Takeuchi, Y., Horiuchi, T., and Kobayashi, T. (2003). Transcription-dependent recombination and the role of fork collision in yeast rDNA. Genes Dev *17*, 1497-1506.

Tang, F., Watkins, J.W., Bermudez, M., Gray, R., Gaban, A., Portie, K., Grace, S., Kleve, M., and Craciun, G. (2008). A life-span extending form of autophagy employs the vacuole-vacuole fusion machinery. Autophagy *4*, 874-886.

Terradas, M., Martin, M., Tusell, L., and Genesca, A. (2010). Genetic activities in micronuclei: is the DNA entrapped in micronuclei lost for the cell? Mutat Res *705*, 60-67.

Terweij, M., van Welsem, T., van Deventer, S., Verzijlbergen, K.F., Menendez-Benito, V., Ontoso, D., San-Segundo, P., Neefjes, J., and van Leeuwen, F. (2013). Recombination-induced tag exchange (RITE) cassette series to monitor protein dynamics in Saccharomyces cerevisiae. G3 (Bethesda) *3*, 1261-1272.

Texari, L., Dieppois, G., Vinciguerra, P., Contreras, M.P., Groner, A., Letourneau, A., and Stutz, F. (2013). The nuclear pore regulates GAL1 gene transcription by controlling the localization of the SUMO protease Ulp1. Mol Cell *51*, 807-818.

Timmers, H.T., and Tora, L. (2005). SAGA unveiled. Trends Biochem Sci *30*, 7-10.

Tomaska, L., McEachern, M.J., and Nosek, J. (2004). Alternatives to telomerase: keeping linear chromosomes via telomeric circles. FEBS Lett *567*, 142-146.

Tuna, M., Knuutila, S., and Mills, G.B. (2009). Uniparental disomy in cancer. Trends Mol Med *15*, 120-128.

Utani, K., Kawamoto, J.K., and Shimizu, N. (2007). Micronuclei bearing acentric extrachromosomal chromatin are transcriptionally competent and may perturb the cancer cell phenotype. Mol Cancer Res *5*, 695-704.

Vas, A.C., Andrews, C.A., Kirkland Matesky, K., and Clarke, D.J. (2007). In vivo analysis of chromosome condensation in Saccharomyces cerevisiae. Mol Biol Cell *18*, 557-568.

Veatch, J.R., McMurray, M.A., Nelson, Z.W., and Gottschling, D.E. (2009). Mitochondrial dysfunction leads to nuclear genome instability via an iron-sulfur cluster defect. Cell *137*, 1247-1258.

Vinciguerra, P., and Stutz, F. (2004). mRNA export: an assembly line from genes to nuclear pores. Curr Opin Cell Biol *16*, 285-292.

Wang, L., Liu, L., and Berger, S.L. (1998). Critical residues for histone acetylation by Gcn5, functioning in Ada and SAGA complexes, are also required for transcriptional function in vivo. Genes Dev *12*, 640-653.

Warsi, T.H., Navarro, M.S., and Bachant, J. (2008). DNA topoisomerase II is a determinant of the tensile properties of yeast centromeric chromatin and the tension checkpoint. Mol Biol Cell *19*, 4421-4433.

White, M.F., and Dillingham, M.S. (2012). Iron-sulphur clusters in nucleic acid processing enzymes. Curr Opin Struct Biol *22*, 94-100.

Wigley, W.C., Fabunmi, R.P., Lee, M.G., Marino, C.R., Muallem, S., DeMartino, G.N., and Thomas, P.J. (1999). Dynamic association of proteasomal machinery with the centrosome. J Cell Biol *145*, 481-490.

Wilkins, B.J., Rall, N.A., Ostwal, Y., Kruitwagen, T., Hiragami-Hamada, K., Winkler, M., Barral, Y., Fischle, W., and Neumann, H. (2014). A cascade of histone modifications induces chromatin condensation in mitosis. Science *343*, 77-80.

Winkler, J., Tyedmers, J., Bukau, B., and Mogk, A. (2012). Chaperone networks in protein disaggregation and prion propagation. J Struct Biol *179*, 152-160.

Xie, Z., Zhang, Y., Zou, K., Brandman, O., Luo, C., Ouyang, Q., and Li, H. (2012). Molecular phenotyping of aging in single yeast cells using a novel microfluidic device. Aging Cell *11*, 599-606.

Yam, C., Gu, Y., and Oliferenko, S. (2013). Partitioning and remodeling of the Schizosaccharomyces japonicus mitotic nucleus require chromosome tethers. Curr Biol *23*, 2303-2310.

Yankiwski, V., Marciniak, R.A., Guarente, L., and Neff, N.F. (2000). Nuclear structure in normal and Bloom syndrome cells. Proc Natl Acad Sci U S A *97*, 5214-5219.

Zhang, Q., Chakravarty, S., Ghersi, D., Zeng, L., Plotnikov, A.N., Sanchez, R., and Zhou, M.M. (2010). Biochemical profiling of histone binding selectivity of the yeast bromodomain family. PLoS One *5*, e8903.

Zhou, C., Slaughter, B.D., Unruh, J.R., Eldakak, A., Rubinstein, B., and Li, R. (2011). Motility and segregation of Hsp104-associated protein aggregates in budding yeast. Cell *147*, 1186-1196.

6. Strain list

yYB number		genotype
6637	a	*nup82::NUP82-3sfGFP:kanMX4;* pPCM14 *(224 tetO-REC-URA3-CEN-REC-LEU2); P_{URA3}-TETR-mCherry:kanMX4; his3::P_{GAL}-REC:HIS3; trp1::GAL4-EBD:TRP1; ade2-101*
10071, 10072, 10073	a	*fob1::FOB1-yeGFP:hphNT1;* pPCM14 *(224 tetO-REC-URA3-CEN-REC-LEU2); P_{URA3}-TETR-mCherry:kanMX4; his3::P_{GAL}-REC:HIS3; trp1::GAL4-EBD:TRP1; ade2-101;* clones 1-3
6271	a	*nup82::NUP82-yeGFP:natNT2;* pPCM14 *(224 tetO-REC-URA3-CEN-REC-LEU2); P_{URA3}-TETR-mCherry:kanMX4; his3::P_{GAL}-REC:HIS3; trp1::GAL4-EBD:TRP1; ade2-101*
9038	a	*nup49::NUP49-yeGFP:hphNT1;* pPCM14 *(224 tetO-REC-URA3-CEN-REC-LEU2); P_{URA3}-TETR-mCherry:kanMX4; his3::P_{GAL}-REC:HIS3; trp1::GAL4-EBD:TRP1; ade2-101*
9415,9416, 10454	a	*nup49::NUP49-yeGFP:hphNT1; bud6::natNT2;* pPCM14 *(224 tetO-REC-URA3-CEN-REC-LEU2); P_{URA3}-TETR-mCherry:kanMX4; his3::P_{GAL}-REC:HIS3; trp1::GAL4-EBD:TRP1; ade2-101* clones 1-3
4221	a	pPCM14 *(224 tetO-REC-URA3-CEN-REC-LEU2); spc42::SPC42-CFP:kanMX4; leu2::TETR-GFP:LEU2; his3::P_{GAL}-REC:HIS3; trp1::GAL4-EBD:TRP1; ade2-101*
4222,5547, 6521	a	*bud6::natNT2;* pPCM14 *(224 tetO-REC-URA3-CEN-REC-LEU2); spc42::SPC42-CFP:kanMX4; leu2::TETR-GFP:LEU2; his3::P_{GAL}-REC:HIS3; trp1::GAL4-EBD:TRP1; ade2-101;* clones 1-3
5516,5517, 8099	a	*yku70::hphNT1;* pPCM14 *(224 tetO-REC-URA3-CEN-REC-LEU2); spc42::SPC42-CFP:kanMX4; leu2::TETR-GFP:LEU2; his3::P_{GAL}-REC:HIS3; trp1::GAL4-EBD:TRP1; ade2-101;* clones 1-3
4124,4161, 7237	a	*sir1::natNT2;* pPCM14 *(224 tetO-REC-URA3-CEN-REC-LEU2); spc42::SPC42-CFP:kanMX4; leu2::TETR-GFP:LEU2; his3::P_{GAL}-REC:HIS3; trp1::GAL4-EBD:TRP1; ade2-101;* clones 1-3
4165,4260, 4261	a	*sir2::natNT2;* pPCM14 *(224 tetO-REC-URA3-CEN-REC-LEU2); spc42::SPC42-CFP:kanMX4; leu2::TETR-GFP:LEU2; his3::P_{GAL}-REC:HIS3; trp1::GAL4-EBD:TRP1; ade2-101;* clones 1-3
4121,7239, 7240	a	*sir3::natNT2;* pPCM14 *(224 tetO-REC-URA3-CEN-REC-LEU2); spc42::SPC42-CFP:kanMX4; leu2::TETR-GFP:LEU2; his3::P_{GAL}-REC:HIS3; trp1::GAL4-EBD:TRP1; ade2-101;* clones 1-3
4235,4236, 7243	a	*sir4::natNT2;* pPCM14 *(224 tetO-REC-URA3-CEN-REC-LEU2); spc42::SPC42-CFP:kanMX4; leu2::TETR-GFP:LEU2; his3::P_{GAL}-REC:HIS3; trp1::GAL4-EBD:TRP1; ade2-101;* clones 1-3
8100,8101, 8102	a	*mps3::mps3-aa75-100Δ:hphNT1;* pPCM14 *(224 tetO-REC-URA3-CEN-REC-LEU2); spc42::SPC42-CFP:kanMX4; leu2::TETR-GFP:LEU2; his3::P_{GAL}-REC:HIS3; trp1::GAL4-EBD:TRP1; ade2-101;* clones 1-3
6524,6652, 8059	a	*src1::natNT2;* pPCM14 *(224 tetO-REC-URA3-CEN-REC-LEU2); spc42::SPC42-CFP:kanMX4; leu2::TETR-GFP:LEU2; his3::P_{GAL}-REC:HIS3; trp1::GAL4-EBD:TRP1; ade2-101;* clones 1-3
7957,7958, 7960	a	*heh2::hphNT1;* pPCM14 *(224 tetO-REC-URA3-CEN-REC-LEU2); spc42::SPC42-CFP:kanMX4; leu2::TETR-GFP:LEU2; his3::P_{GAL}-REC:HIS3; trp1::GAL4-EBD:TRP1; ade2-101;* clones 1-3
7954,7955, 7956	a	*slx5::hphNT1;* pPCM14 *(224 tetO-REC-URA3-CEN-REC-LEU2); spc42::SPC42-CFP:kanMX4; leu2::TETR-GFP:LEU2; his3::P_{GAL}-REC:HIS3; trp1::GAL4-EBD:TRP1; ade2-101;* clones 1-3

4120,4263, 4264	a	*gcn5::natNT2;* pPCM14 *(224 tetO-REC-URA3-CEN-REC-LEU2); spc42::SPC42-CFP:kanMX4; leu2::TETR-GFP:LEU2; his3::P_{GAL}-REC:HIS3; trp1::GAL4-EBD:TRP1; ade2-101;* clones 1-3
4118,4119, 4262	a	*spt3::natNT2;* pPCM14 *(224 tetO-REC-URA3-CEN-REC-LEU2); spc42::SPC42-CFP:kanMX4; leu2::TETR-GFP:LEU2; his3::P_{GAL}-REC:HIS3; trp1::GAL4-EBD:TRP1; ade2-101;* clones 1-3
4287,4577, 5518	a	*sgf73::natNT2;* pPCM14 *(224 tetO-REC-URA3-CEN-REC-LEU2); spc42::SPC42-CFP:kanMX4; leu2::TETR-GFP:LEU2; his3::P_{GAL}-REC:HIS3; trp1::GAL4-EBD:TRP1; ade2-101;* clones 1-3
5319,5320, 5321	a	*gcn5::gcn5E173A:hphNT1;* pPCM14 *(224 tetO-REC-URA3-CEN-REC-LEU2); spc42::SPC42-CFP:kanMX4; leu2::TETR-GFP:LEU2; his3::P_{GAL}-REC:HIS3; trp1::GAL4-EBD:TRP1; ade2-101;* clones 1-3
4166,4237, 4238	a	*sac3::natNT2;* pPCM14 *(224 tetO-REC-URA3-CEN-REC-LEU2); spc42::SPC42-CFP:kanMX4; leu2::TETR-GFP:LEU2; his3::P_{GAL}-REC:HIS3; trp1::GAL4-EBD:TRP1; ade2-101;* clones 1-3
4122,4573, 8103	a	*sus1::natNT2;* pPCM14 *(224 tetO-REC-URA3-CEN-REC-LEU2); spc42::SPC42-CFP:kanMX4; leu2::TETR-GFP:LEU2; his3::P_{GAL}-REC:HIS3; trp1::GAL4-EBD:TRP1; ade2-101;* clones 1-3
384	a	*ura3-52; his3Δ200; leu2; lys2-801; ade2-101; trp1Δ63*
3870	a	*gcn5::natNT2; ura3-52; his3Δ200; leu2; lys2-801; ade2-101; trp1Δ63*
4287	a	*sgf73::natNT2; ura3-52; his3Δ200; leu2; lys2-801; ade2-101; trp1Δ63*
3415	a	*hoD::P_{SCW11}-Cre-EBD78:natMX; ubc9::loxP-UBC9-loxP:LEU2; cdc20::loxP-CDC20-intron-loxP:hphMX; ade2::hisG; his3; lys2; ura3; trp1Δ63*
6580	a	*gcn5::kanMX4; hoD::P_{SCW11}-Cre-EBD78:natMX; ubc9::loxP-UBC9-loxP:LEU2; cdc20::loxP-CDC20-intron-loxP:hphMX; ade2::hisG; his3; lys2; ura3; trp1Δ63*
6195	a	*sgf73::kanMX4; hoD::P_{SCW11}-Cre-EBD78:natMX; ubc9::loxP-UBC9-loxP:LEU2; cdc20::loxP-CDC20-intron-loxP:hphMX; ade2::hisG; his3; lys2; ura3; trp1Δ63*
5457	a	pPCM14 *(224 tetO-REC-URA3-CEN-REC-LEU2); spc42::SPC42-redStar:natNT2; nup170::NUP170-mCherry:kanMX4; leu2::TETR-GFP:LEU2; his3::P_{GAL}-REC:HIS3; trp1::GAL4-EBD:TRP1; ade2-101;*
5502,5503, 5504	a	*gcn5::hphNT1;* pPCM14 *(224 tetO-REC-URA3-CEN-REC-LEU2); spc42::SPC42-redStar:natNT2; nup170::NUP170-mCherry:kanMX4; leu2::TETR-GFP:LEU2; his3::P_{GAL}-REC:HIS3; trp1::GAL4-EBD:TRP1; ade2-101;* clones 1-3
8115,8116, 8117	a	*sus1::hphNT1;* pPCM14 *(224 tetO-REC-URA3-CEN-REC-LEU2); spc42::SPC42-redStar:natNT2; nup170::NUP170-mCherry:kanMX4; leu2::TETR-GFP:LEU2; his3::P_{GAL}-REC:HIS3; trp1::GAL4-EBD:TRP1; ade2-101;* clones 1-3
6648	a	pPCM14 *(224 tetO-REC-URA3-CEN-REC-LEU2); nup82::NUP82-3sfGFP:kanMX4; P_{URA3}-TETR-mCherry:kanMX4; spc42::SPC42-yeGFP:hphNT1; his3::P_{GAL}-REC:HIS3; trp1::GAL4-EBD:TRP1; ade2-101*
6752,6765, 6895	a	*gcn5::natNT2;* pPCM14 *(224 tetO-REC-URA3-CEN-REC-LEU2); nup82::NUP82-3sfGFP:kanMX4; P_{URA3}-TETR-mCherry:kanMX4; spc42::SPC42-yeGFP:hphNT1; his3::P_{GAL}-REC:HIS3; trp1::GAL4-EBD:TRP1; ade2-101;* clones 1-3

8093,8094, 8095	a	*sus1::natNT2;* pPCM14 *(224 tetO-REC-URA3-CEN-REC-LEU2); nup82::NUP82-3sfGFP:kanMX4; P_{URA3}-TETR-mCherry:kanMX4; spc42::SPC42-yeGFP:hphNT1; his3::P_{GAL}-REC:HIS3; trp1::GAL4-EBD:TRP1; ade2-101;* clones 1-3
5881,5882, 5883	a	*nup170::NUP170-linker-TETR-mCherry:hphNT1;* pPCM14 *(224 tetO-REC-URA3-CEN-REC-LEU2); spc42::SPC42-CFP:kanMX4; leu2::TETR-GFP:LEU2; his3::P_{GAL}-REC:HIS3; trp1::GAL4-EBD:TRP1; ade2-101;* clones 1-3
5886,7253, 7254	a	*nup170::NUP170-linker-TETR-mCherry:hphNT1; gcn5::natNT2;* pPCM14 *(224 tetO-REC-URA3-CEN-REC-LEU2); spc42::SPC42-CFP:kanMX4; leu2::TETR-GFP:LEU2; his3::P_{GAL}-REC:HIS3; trp1::GAL4-EBD:TRP1; ade2-101;* clones 1-3
5962,5973, 7863	a	*nup170::NUP170-linker-TETR-mCherry:hphNT1; sus1::natNT2;* pPCM14 *(224 tetO-REC-URA3-CEN-REC-LEU2); spc42::SPC42-CFP:kanMX4; leu2::TETR-GFP:LEU2; his3::P_{GAL}-REC:HIS3; trp1::GAL4-EBD:TRP1; ade2-101;* clones 1-3
5933,5934, 5935	a	*nup49::NUP49-linker-TETR-mCherry:hphNT1;* pPCM14 *(224 tetO-REC-URA3-CEN-REC-LEU2); spc42::SPC42-CFP:kanMX4; leu2::TETR-GFP:LEU2; his3::P_{GAL}-REC:HIS3; trp1::GAL4-EBD:TRP1; ade2-101;* clones 1-3
7959,8032, 8033	a	*nup49::NUP49-linker-TETR-mCherry:hphNT1; gcn5::natNT2;* pPCM14 *(224 tetO-REC-URA3-CEN-REC-LEU2); spc42::SPC42-CFP:kanMX4; leu2::TETR-GFP:LEU2; his3::P_{GAL}-REC:HIS3; trp1::GAL4-EBD:TRP1; ade2-101;* clones 1-3
7865,7866, 7867	a	*nup49::NUP49-linker-TETR-mCherry:hphNT1; sgf73::natNT2;* pPCM14 *(224 tetO-REC-URA3-CEN-REC-LEU2); spc42::SPC42-CFP:kanMX4; leu2::TETR-GFP:LEU2; his3::P_{GAL}-REC:HIS3; trp1::GAL4-EBD:TRP1; ade2-101;* clones 1-3
5884,5885, 5961	a	*nup170::NUP170-linker-TETR-mCherry:hphNT1; sgf73::natNT2;* pPCM14 *(224 tetO-REC-URA3-CEN-REC-LEU2); spc42::SPC42-CFP:kanMX4; leu2::TETR-GFP:LEU2; his3::P_{GAL}-REC:HIS3; trp1::GAL4-EBD:TRP1; ade2-101;* clones 1-3
5966,5967, 7864	a	*nup49::NUP49-linker-TETR-mCherry:hphNT1; sus1::natNT2;* pPCM14 *(224 tetO-REC-URA3-CEN-REC-LEU2); spc42::SPC42-CFP:kanMX4; leu2::TETR-GFP:LEU2; his3::P_{GAL}-REC:HIS3; trp1::GAL4-EBD:TRP1; ade2-101;* clones 1-3
5968,5969, 5970	a	*nup49::NUP49-linker-TETR-mCherry:hphNT1; bud6::natNT2;* pPCM14 *(224 tetO-REC-URA3-CEN-REC-LEU2); spc42::SPC42-CFP:kanMX4; leu2::TETR-GFP:LEU2; his3::P_{GAL}-REC:HIS3; trp1::GAL4-EBD:TRP1; ade2-101;* clones 1-3
5963,5964, 5965	a	*nup170::NUP170-linker-TETR-mCherry:hphNT1; bud6::natNT2;* pPCM14 *(224 tetO-REC-URA3-CEN-REC-LEU2); spc42::SPC42-CFP:kanMX4; leu2::TETR-GFP:LEU2; his3::P_{GAL}-REC:HIS3; trp1::GAL4-EBD:TRP1; ade2-101;* clones 1-3
5852,5853, 5854	a	*gcn5::GCN5-linker-SAC3:hphNT1;* pPCM14 *(224 tetO-REC-URA3-CEN-REC-LEU2); spc42::SPC42-CFP:kanMX4; leu2::TETR-GFP:LEU2; his3::P_{GAL}-REC:HIS3; trp1::GAL4-EBD:TRP1; ade2-101;* clones 1-3
7141,7142, 7143	a	*spt7::SPT7-linker-NUP49:hphNT1;* pPCM14 *(224 tetO-REC-URA3-CEN-REC-LEU2); spc42::SPC42-CFP:kanMX4; leu2::TETR-GFP:LEU2; his3::P_{GAL}-REC:HIS3; trp1::GAL4-EBD:TRP1; ade2-101;* clones 1-3

5888,5889, 7856	a	*gcn5::GCN5-linker-SAC3:hphNT1; sus1::natNT2;* pPCM14 *(224 tetO-REC-URA3-CEN-REC-LEU2); spc42::SPC42-CFP:kanMX4; leu2::TETR-GFP:LEU2; his3::P_{GAL}-REC:HIS3; trp1::GAL4-EBD:TRP1; ade2-101;* clones 1-3
7859,7869, 7870	a	*spt7::SPT7-linker-NUP49:hphNT1; sus1::natNT2;* pPCM14 *(224 tetO-REC-URA3-CEN-REC-LEU2); spc42::SPC42-CFP:kanMX4; leu2::TETR-GFP:LEU2; his3::P_{GAL}-REC:HIS3; trp1::GAL4-EBD:TRP1; ade2-101;* clones 1-3
6048,7858, 7868	a	*gcn5::GCN5-linker-SAC3:hphNT1; sgf73::natNT2;* pPCM14 *(224 tetO-REC-URA3-CEN-REC-LEU2); spc42::SPC42-CFP:kanMX4; leu2::TETR-GFP:LEU2; his3::P_{GAL}-REC:HIS3; trp1::GAL4-EBD:TRP1; ade2-101; clones 1-3*
7557,7860, 7861	a	*spt7::SPT7-linker-NUP49:hphNT1; sgf73::natNT2;* pPCM14 *(224 tetO-REC-URA3-CEN-REC-LEU2); spc42::SPC42-CFP:kanMX4; leu2::TETR-GFP:LEU2; his3::P_{GAL}-REC:HIS3; trp1::GAL4-EBD:TRP1; ade2-101;* clones 1-3
9520,9521, 9522	a	*gcn5::GCN5-yeGFP:hphNT1;* pPCM14 *(224 tetO-REC-URA3-CEN-REC-LEU2); P_{URA3}-TETR-mCherry:kanMX4; his3::P_{GAL}-REC:HIS3; trp1::GAL4-EBD:TRP1; ade2-101;* clones 1-3
9523,9524, 9525	a	*sgf73::SGF73-yeGFP:hphNT1;* pPCM14 *(224 tetO-REC-URA3-CEN-REC-LEU2); P_{URA3}-TETR-mCherry:kanMX4; his3::P_{GAL}-REC:HIS3; trp1::GAL4-EBD:TRP1; ade2-101;* clones 1-3
7311	α	pYB1670 *(REC-URA3-CEN-REC-ARS1-LEU2-AmpR); his3::P_{GAL}-REC:HIS3; trp1::GAL4-EBD:TRP1; leu2Δ0; ura3Δ0; met15Δ0*
7555	a	*gcn5::GCN5-yeGFP:HIS3;* pYB1670 *(REC-URA3-CEN-REC-ARS1-LEU2-AmpR); his3::P_{GAL}-REC:HIS3; trp1::GAL4-EBD:TRP1; leu2Δ0; ura3Δ0; met15Δ0*
7524	α	*spt20::SPT20-yeGFP:HIS3;* pYB1670 *(REC-URA3-CEN-REC-ARS1-LEU2-AmpR); his3::P_{GAL}-REC:HIS3; trp1::GAL4-EBD:TRP1; leu2Δ0; ura3Δ0; met15Δ0*
8831,8832, 8833	a	*nup82::NUP82-3sfGFP:kanMX4; gcn5::hphNT1;* pPCM14 *(224 tetO-REC-URA3-CEN-REC-LEU2); P_{URA3}-TETR-mCherry:kanMX4; his3::P_{GAL}-REC:HIS3; trp1::GAL4-EBD:TRP1; ade2-101;* clones 1-3
9002,9003, 10455	a	*nup82::NUP82-3sfGFP:kanMX4; sgf73::hphNT1;* pPCM14 *(224 tetO-REC-URA3-CEN-REC-LEU2); P_{URA3}-TETR-mCherry:kanMX4; his3::P_{GAL}-REC:HIS3; trp1::GAL4-EBD:TRP1; ade2-101;* clones 1&2
9039	a	*nup170::NUP170-yeGFP:hphNT1;* pPCM14 *(224 tetO-REC-URA3-CEN-REC-LEU2); P_{URA3}-TETR-mCherry:kanMX4; his3::P_{GAL}-REC:HIS3; trp1::GAL4-EBD:TRP1; ade2-101;* clones 1-3
9392	a	*nup170::NUP170-yeGFP:hphNT1; gcn5::natNT2;* pPCM14 *(224 tetO-REC-URA3-CEN-REC-LEU2); P_{URA3}-TETR-mCherry:kanMX4; his3::P_{GAL}-REC:HIS3; trp1::GAL4-EBD:TRP1; ade2-101*
7828	a	*nup49::NUP49-yeGFP:HIS3; leu2Δ0; ura3Δ0; met15Δ0*
8112	a	*nup170::NUP170-yeGFP:HIS3; leu2Δ0; ura3Δ0; met15Δ0*
8182	a	*nup82::NUP82-yeGFP:HIS3; leu2Δ0; ura3Δ0; met15Δ0*
9337,9338, 9339	a	*nup170::NUP170-yeGFP:HIS3; bud6::kanMX4; leu2Δ0; ura3Δ0; met15Δ0;* clones 1-3
9612,9613, 9614	a	*nup170::NUP170-yeGFP:HIS3; fob1::kanMX4; leu2Δ0; ura3Δ0; met15Δ0;* clones 1-3

9616,9617, 9618	a	*nup170::NUP170-yeGFP:HIS3; sir2::kanMX4; leu2Δ0; ura3Δ0; met15Δ0;* clones 1-3
9372,9373, 9374	a	*nup170::NUP170-yeGFP:HIS3; sgf73::hphNT1; leu2Δ0; ura3Δ0; met15Δ0;* clones 1-3
9171,9173, 9174	a	*nup49::NUP49-yeGFP:HIS3; fob1::kanMX4; leu2Δ0; ura3Δ0; met15Δ0;* clones 1-3
9181,9182, 9183	a	*nup49::NUP49-yeGFP:HIS3; sir2::kanMX4; leu2Δ0; ura3Δ0; met15Δ0;* clones 1-3
4499,4500, 4501	a	*nup49::NUP49-yeGFP:HIS3; sgf73::kanMX4; leu2Δ0; ura3Δ0; met15Δ0;* clones 1-3
9360,9361, 9362	a	*nup170::NUP170-yeGFP:HIS3; sgf73::kanMX4; spt7::SPT7-linker-NUP49:hphNT1; leu2Δ0; ura3Δ0; met15Δ0;* clones 1-3
9340,9341, 9342	a	*nup170::NUP170-yeGFP:HIS3; sgf73::kanMX4; gcn5::GCN5-linker-SAC3:hphNT1; leu2Δ0; ura3Δ0; met15Δ0;* clones 1-3
5520	a	*his3Δ1; leu2Δ0; ura3Δ0; met15Δ0 (EUROSCARF wt)*
5142	a	*gcn5::kanMX4; his3Δ1; leu2Δ0; ura3Δ0; met15Δ0*
8108	a	*sgf73::kanMX4; his3Δ1; leu2Δ0; ura3Δ0; met15Δ0*
10453	a	*fob1::kanMX4; his3Δ1; leu2Δ0; ura3Δ0; met15Δ0*
9915,9916, 9917	a	*fob1::kanMX4; gcn5::hphNT1; his3Δ1; leu2Δ0; ura3Δ0; met15Δ0;* clones 1-3
6626	a	*gcn5::GCN5-linker-SAC3:hphNT1; his3Δ1; leu2Δ0; ura3Δ0; met15Δ0*
7252	a	*spt7::SPT7-linker-NUP49:hphNT1; his3Δ1; leu2Δ0; ura3Δ0; met15Δ0*
6632,6633, 6634	a	*gcn5::GCN5-linker-SAC3:hphNT1; sgf73::kanMX4; his3Δ1; leu2Δ0; ura3Δ0; met15Δ0;* clones 1-3
7540,7541, 7542	a	*spt7::SPT7-linker-NUP49:hphNT1; sgf73::kanMX4; his3Δ1; leu2Δ0; ura3Δ0; met15Δ0;* clones 1-3
5532	a	*nsg1::NSG1-yeGFP:HIS3; leu2Δ0; ura3Δ0; met15Δ0*
4233,7303, 7304	a	*bud6::natNT2; nsg1::NSG1-yeGFP:HIS3; leu2Δ0; ura3Δ0; met15Δ0;* clones 1-3
6897,8105, 8106	a	*yku70::hphNT1; nsg1::NSG1-yeGFP:HIS3; leu2Δ0; ura3Δ0; met15Δ0;* clones 1-3
6766,6767, 8104	a	*gcn5::natNT2; nsg1::NSG1-yeGFP:HIS3; leu2Δ0; ura3Δ0; met15Δ0;* clones 1-3
4601,4615, 4616	a	*sgf73::kanMX4; nsg1::NSG1-yeGFP:HIS3; leu2Δ0; ura3Δ0; met15Δ0;* clones 1-3
2177	α	*nup49::NUP49-yeGFP:HIS3; leu2Δ0; ura3Δ0; met15Δ0*

3403,3583, 4223	α	*bud6::kanMX4; nup49::NUP49-yeGFP:HIS3; leu2Δ0; ura3Δ0; met15Δ0;* clones 1-3
4094,4095, 4096	α	*gcn5::natNT2; nup49::NUP49-yeGFP:HIS3; leu2Δ0; ura3Δ0; met15Δ0;* clones 1-3
8109	a	*nup2::NUP2-yeGFP:HIS3; leu2Δ0; ura3Δ0; met15Δ0*
8110	a	*nup60::NUP60-yeGFP:HIS3; leu2Δ0; ura3Δ0; met15Δ0*
8111	a	*mlp1::MLP1-yeGFP:HIS3; leu2Δ0; ura3Δ0; met15Δ0*
8112	a	*nup170::NUP170-yeGFP:HIS3; leu2Δ0; ura3Δ0; met15Δ0*
7828	a	*nup49::NUP49-yeGFP:HIS3; leu2Δ0; ura3Δ0; met15Δ0*
7336	a	*nup1::NUP1-yeGFP:HIS3; leu2Δ0; ura3Δ0; met15Δ0*
7503,8113, 8114	a	*nup1::NUP1-linker-TETR-mCherry:hphNT1;* pPCM14 *(224 tetO-REC-URA3-CEN-REC-LEU2); spc42::SPC42-CFP:kanMX4; leu2::TETR-GFP:LEU2; his3::P_{GAL}-REC:HIS3; trp1::GAL4-EBD:TRP1; ade2-101;* clones 1-3
5933,5934, 5935	a	*nup49::NUP49-linker-TETR-mCherry:hphNT1;* pPCM14 *(224 tetO-REC-URA3-CEN-REC-LEU2); spc42::SPC42-CFP:kanMX4; leu2::TETR-GFP:LEU2; his3::P_{GAL}-REC:HIS3; trp1::GAL4-EBD:TRP1; ade2-101;* clones 1-3
5881,5882, 5883	a	*nup170::NUP170-linker-TETR-mCherry:hphNT1;* pPCM14 *(224 tetO-REC-URA3-CEN-REC-LEU2); spc42::SPC42-CFP:kanMX4; leu2::TETR-GFP:LEU2; his3::P_{GAL}-REC:HIS3; trp1::GAL4-EBD:TRP1; ade2-101;* clones 1-3
5930,5931, 5932	a	*mlp1::MLP1-linker-TETR-mCherry:hphNT1;* pPCM14 *(224 tetO-REC-URA3-CEN-REC-LEU2); spc42::SPC42-CFP:kanMX4; leu2::TETR-GFP:LEU2; his3::P_{GAL}-REC:HIS3; trp1::GAL4-EBD:TRP1; ade2-101;* clones 1-3
5843,5844, 5845	a	*nup60::NUP60-linker-TETR-mCherry:hphNT1;* pPCM14 *(224 tetO-REC-URA3-CEN-REC-LEU2); spc42::SPC42-CFP:kanMX4; leu2::TETR-GFP:LEU2; his3::P_{GAL}-REC:HIS3; trp1::GAL4-EBD:TRP1; ade2-101;* clones 1-3

7. *Curriculum vitae*

Personal informations

Name : Annina Denoth Lippuner
Adress : Ackersteinstrasse 93, 8049 Zurich, Switzerland
Email : anninadenoth@hotmail.com
Birth: 29. April 1982
Place of citizenship: Vnà, Valsot (GR), Switzerland
Nationality: Swiss

Education

2008-present :	PhD studies in the group of Professor Yves Barral, Institute of Biochemistry, ETH Zurich, Switzerland
2007-2008:	Studies and Master in higher education, ETH Zurich, Switzerland
2002-2007:	Studies in biology, Master in biology, ETH Zurich, Switzerland
1997-2001 :	College, Sargans, Switzerland
1989-1997 :	Primary and high school, Buchs, Switzerland

List of publications

Clay, L.*, Caudron, F.*, Denoth-Lippuner, A., Boettcher, B., Buvelot Frei, S., Snapp, E.L., and Barral, Y. (2014). A sphingolipid-dependent diffusion barrier confines ER stress to the yeast mother cell. Elife *3*, e01883.

Denoth Lippuner, A.*, Julou, T.*, and Barral, Y. (2014). Budding yeast as a model organism to study the effects of age. FEMS Microbiol Rev.

Leisner, C.*, Kammerer, D.*, Denoth, A.*, Britschi, M., Barral, Y., and Liakopoulos, D. (2008). Regulation of mitotic spindle asymmetry by SUMO and the spindle-assembly checkpoint in yeast. Curr Biol *18*, 1249-1255.

* Authors contributed equally to this work

Oral communications

Molecular Genetics of Aging, 28.9.- 2.10. 2010, Cold Spring Harbor, New York, USA
Retention of Aging Factors in Yeast Mother Cells is SAGA dependent. Annina Denoth and Yves Barral.

Nuclear Organization and Function, 18. 8. – 23. 8. 2014, Cold Spring Harbor, New York, USA
SAGA-dependent attachment of DNA circles to nuclear pores mediates the concomitant accumulation of pores and circles in aging yeast cells. Annina Denoth, Marek Konrad Krzyzanowski, Yves Barral.

8. Acknowledgments

First of all I would like to thank Yves Barral for being an absolutely great mentor throughout all these years. I would like to thank him not only for his great advice, novel and unique ideas, inspiring discussions and helpful guidance, but also for giving me the freedom to come up and implement my own ideas and hypotheses. It always felt like having someone in the back supporting me. Thanks to him, I not only grasped how to do research in a passionate way, but I also learned to ask big questions and to enjoy science.

Furthermore, I would like to thank my thesis committee Ulrike Kutay, Françoise Stutz and Claudio Sunkel for their constant help throughout this time.

I would like to thank Christian Leisner, who was my supervisor during my diploma work and who sparked my fascination for science. I would also like to thank Sandro Baldi, who helped me a lot during the first years of my PhD by giving important advice, providing many ideas and endless scientific discussions. A big thanks also goes to Tom Kruitwagen, who corrected my thesis and manuscripts meticulously, who always shared his opinion with me and with whom it is great fun to work with. I would also like to thank Mathias Bayer, for being a great friend in the lab throughout the highs and lows of a PhD.

I would also like to thank Catherine Stober, who performed the ChIP experiments and Marek Krzyzanowski, who contributed a lot to the investigations of NPCs in old cells. Without their help we could not have completed our nice manuscript. I also thank Thomas Julou for the interesting discussions during the writing of our review.

Further thanks goes to Lori Clay for helping me getting acquainted with the work with mammalian cells, Barbara Böttcher for showing me how to FLIP, Benjamin Farnung and Nana Farcas for teaching me how to do Southern blots and Emmanuelle Fabre for working on the plasmid localization. I also thank the people from the LMC for helping me with all these different microscopes and accompanying problems.

I would like to thank all my colleagues from the current and past Barral lab. Especially Fabrice Caudron, Manuel Hotz, Alex Rauch, Jette Lengefeld, Juha Saarikangas, Andrzej Sliwa-Gonzalez and many more for creating a great working place, for endless discussions about scientific and non-scientific issues, for sharing great times together, for memorable parties and for refreshing (but always short) detours to the Töggelichaschte. I'd like to also thank the whole plasmid crew and the Kroschewski lab for the fruitful discussions and new ideas.

I also thank the two students I was teaching during my PhD: Mauro Pellanda and Melissa Amrein. I wish them both great success and lots of fun with their future projects.

Finally, I would like to thank my parents for supporting me throughout all these years and for their great assistance in the back. And of course, I would like to thank my husband Florian Lippuner, not only for his great patience and understanding during quite some night and weekend shifts, but also for his unconditional support and his amazing ability to encourage me in whatever I'm doing.